

# Time-Dependent Kondo Model with a Factorized Initial State

Von der Mathematisch-Naturwissenschaftlichen Fakultät  
der Universität Augsburg  
zur Erlangung eines Doktorgrades der Naturwissenschaften  
genehmigte Dissertation

von  
M.S. Dmitry Lobaskin  
aus  
Russland



## CONTENTS

<b>1. Introduction</b> . . . . .	1
1.1 Non-Equilibrium Kondo Effect . . . . .	1
1.2 Theoretical Motivation . . . . .	4
1.3 Experimental Motivation . . . . .	7
1.4 Goals of This Work . . . . .	12
<b>2. Time-dependent Kondo Model</b> . . . . .	17
2.1 Equilibrium Kondo Problem . . . . .	17
2.2 Time-dependent Kondo Hamiltonian . . . . .	21
<b>3. Non-Equilibrium Kondo Model at the Toulouse point</b> . . . . .	27
3.1 Diagonalization of the Effective Hamiltonian . . . . .	31
3.2 Magnetization . . . . .	34
3.3 Spin-spin Correlation Function . . . . .	36
3.4 Conclusion . . . . .	44
<b>4. Non-Equilibrium Kondo Model in the Kondo Limit</b> . . . . .	45
4.1 Flow Equation Approach . . . . .	46
4.2 Effective Hamiltonian . . . . .	49
4.3 Numerical Results . . . . .	53
4.4 Analytical Estimations of the Asymptotics . . . . .	54
4.5 Conclusion . . . . .	59

---

<b>5. Violation of the Fluctuation-Dissipation Theorem in the Non-Equilibrium Kondo Model</b> . . . . .	61
5.1 Fluctuation-Dissipation Theorem . . . . .	61
5.2 FDT Violation in Nonequilibrium . . . . .	64
5.3 Toulouse Point . . . . .	66
5.4 Kondo Limit . . . . .	74
5.5 Conclusion . . . . .	75
<b>6. Quasiparticle Spectral Function</b> . . . . .	79
6.1 Nonequilibrium Spectral Density . . . . .	79
6.2 Results of the Fermi Liquid Theory . . . . .	81
6.3 Buildup of the Kondo Resonance . . . . .	82
6.4 Conclusion . . . . .	85
<b>7. Summary</b> . . . . .	87
<b>Appendix</b> . . . . .	93
<b>A. Details of non-regular sum calculations</b> . . . . .	95
<b>Publications</b> . . . . .	105
<b>Curriculum Vitae</b> . . . . .	107
<b>Acknowledgements</b> . . . . .	109

## 1. INTRODUCTION

### 1.1 Non–Equilibrium Kondo Effect

Since early 1970s, the microelectronic industry has been rapidly progressing following the Moore's Law to double processing power every 18 months. For many years this has been satisfied largely by scaling devices to even smaller dimensions. Extrapolating the Moore's law into the next 10-15 years, it becomes apparent that the scaling will run into physical limits: limits of material used, but also fundamental limits arising from the laws of quantum mechanics which become increasingly important at very small length scales. Of course, the ultimate goal then is to construct a functional device capable of transporting a single electron.

In 1985 D. Averin and K. Likharev (Averin and Likharev 1986) proposed the idea of a new three-terminal device called a single-electron tunneling (SET) transistor. Two years later Theodore Fulton and Gerald Dolan at Bell Labs in the US fabricated such a device and demonstrated how it operates.

As of August 23 2004, Stanford University has been able to construct a transistor from single-walled carbon nanotubes and organic molecules. These single-walled carbon nanotubes are basically a rolled up sheet of carbon atoms. They have accomplished creating this transistor making it two nanometers wide and able to maintain current three nanometers in length.

Unlike field-effect transistors, single-electron devices are based on an intrinsically quantum phenomenon: the tunnel effect. This is observed when two metallic electrodes are separated by an insulating barrier about 1 nm thick - in other words, just 10 atoms in a row. Electrons at the Fermi energy can "tunnel" through the insulator, even though in classical terms their energy would be too low to overcome the potential barrier.

Due to incredibly small sizes of these devices all kinds of non–equilibrium quantum–correlated processes start play the role. Even small external perturbations comparing to that in the bulk macroscopic samples may drive SET transistor far from equilibrium. Small sizes and low temperatures necessary for operating such a system give rise to wide variety of non–equilibrium quantum many–body correlations.

It is not yet clear whether electronics based on individual molecules and single-

electron effects will replace conventional circuits based on scaled-down versions of field-effect transistors. Only one thing is certain: if the pace of miniaturization continues unabated, the quantum properties of electrons will become crucial in determining the design of electronic devices before the end of the next decade.

Fast development of nanoelectronics is already sufficient motivation to study non-equilibrium quantum many-body physics which however is not confined to it. Actually, non-equilibrium many-body physics is one of the most fascinating and challenging topics in modern physics, due to both the wide variety of observed phenomena and difficulty in theoretical description.

Typical situation of non-equilibrium includes the system subjected to some external generally time-dependent perturbation. If the perturbation is infinitesimally small and, therefore, the state of the system is almost the equilibrium one, the linear response description of an externally driven system dynamics is valid. Within this method deviations of all quantities from their equilibrium values can always be expressed via their fluctuations in equilibrium. In particular, the so-called fluctuation-dissipation theorem is fulfilled in this regime. It connects generalized susceptibility of the system to some external perturbation with the equilibrium correlation functions.

Unfortunately, the linear response formalism is only valid while the perturbation does not drive the system far from equilibrium. For example, during measuring of transport properties (conductivity, thermoresistivity, etc.) an applied bias voltage causes a non-equilibrium current to flow through a sample. After certain relaxation time a stationary current establishes and systems are said to be in the steady state. Although such a state is time-independent and thus seems to be equilibrium, this statement is false since it is a highly excited state with respect to a thermodynamically equilibrium one. Another common example is a non-adiabatically applied external time-dependent electromagnetic field. It can be a monochromatic perturbation if we are interested in measurement of a Fourier component of a specific quantity related to response to such a perturbation. It can be an external constraint changed at some moment, as well. In latter case, for example, the equilibrium state of the system might differ significantly from the initial one and can be even non-analytically related to parameters of the original problem. For such a case standard time-independent perturbation theory does not work. Its non-equilibrium extension (Keldysh diagrammatic technic) is applicable in the case of a small, weakly coupled perturbation, when summation up to some finite order of the perturbation theory is sufficient to get an accurate result. For the strong-coupling problem the series of diagrams are divergent, and the method is only applicable if one can manage to sum up all diagrams which contribute most. Even if it is possible the result is often approximate and might miss some important features of a true solution.

A distinct example of such a problem which incorporates all above mentioned

difficulties of the theoretical description together with the practical importance in nanoelectronics is the non-equilibrium Kondo effect. Study of this one of the paradigm model of the condensed matter physics will inevitably help to achieve much better understanding of the basics of electronic properties of nanoscaled structures, including many-body, collective and spin effects.

The equilibrium Kondo effect, as we have mentioned, is the paradigm model of the condensed matter physics. It describes the interaction between magnetic impurity embedded into a metal and the conduction band Fermi sea. For the antiferromagnetic coupling, at temperatures lower than the so-called Kondo temperature  $T_K$  conduction electrons tend to screen the impurity spin. Since it is not possible to form a bound state from the impurity spin and single conduction electron, interaction leads to a complicated many-body scattering state – screening cloud made of conduction electrons. For the impurity spin equal to one half ground state of the system becomes a singlet. Its energy is proportional to the Kondo temperature and depends non-analytically on the strength of the coupling which demonstrates breakdown of the conventional perturbation theory. The Kondo effect manifests itself in many thermodynamic and transport properties such as specific heat, magnetic susceptibility, conductivity, etc. Because of formation of a quasi-bounded state of conduction electrons in the vicinity of the impurity site, the density of states gets enhancement (so-called Kondo resonance) at the Fermi level. This, in its turn, provides additional contribution to above mentioned properties with the weight proportional to the impurity concentration.

In experiment during the measurement of transport properties an applied finite bias voltage tries to destruct the Kondo cloud. Once the voltage is high enough the physics is no longer described by the equilibrium Kondo effect together with the linear response theory. This is unimportant for a bulk measurements. Due to the macroscopic size of a sample one cannot reach high enough electric fields inside to go far from equilibrium. That is why one is always in the linear response regime there. On the other hand, in miniature devices such fields can be easily reached even for small enough bias voltages (Franceschi, Hanson, van der Wiel, Elzerman, Wijkema, Fujisawa, Tarucha and Kouwenhoven 2002). Similar problem arises while the time-dependent electromagnetic field is applied to the sample (Kogan, Amasha and Kastner 2004). All such perturbations are extremely relevant for a small-sized devices.

Another important example is the equilibration after imposing (or, equivalently, removing) non-adiabatically a constraint to the system. One particular aspect is the general problem of an initial preparation of a system and its subsequent relaxation towards equilibrium with an external reservoir. It is a common case in many experiments that a measurable observable is initially decoupled from the other degrees of freedom. Such a factorized initial state might be even orthogonal to an equilibrium state of the coupled system. Natural characteristic for such

systems will be a speed of the equilibration of observables of interest.

In the non–equilibrium Kondo effect language such a problem takes place when the impurity spin is initially decoupled from the Fermi sea and then at some time the coupling is switched on. Whereas initial state of conduction band electrons is the unperturbed Fermi sea, the switching on the coupling leads to the formation of the Kondo cloud – complicated many–body correlated state. The speed of its buildup defines corresponding relaxation rate of thermodynamic and transport properties.

Next non–equilibrium problem is the equilibration of the initially frozen impurity spin (e.g. by a strong magnetic field) after the constraint is released. In this case the initial state of the conduction band is a polarized potential–scattering state because of absence of spin flip processes.

In the following thesis we are focused on above mentioned non–equilibrium types of the initial preparation, namely:

- I) the impurity spin is initially decoupled from the Fermi sea and then at some time the coupling is switched on;
- II) the impurity spin is frozen for some time (e.g. by a strong magnetic field) and at a certain time constraint is removed.

A special case of interests are calculation of various thermodynamic and transport properties of the impurity spin degree of freedom, and particularly their relaxation laws.

In the next two sections we will discuss why this problem is theoretically and experimentally relevant.

## 1.2 Theoretical Motivation

Theoretical study of the non–equilibrium Kondo effect has a long history. After applying special transformation Kondo problem can be mapped on the spin–boson model – also one of the paradigm model of the condensed matter physics which describes dissipative quantum mechanics of the two–level system. In this formulation the problem was already considered by Leggett, Chakravarty, Dorsey, Fisher, Garg and Zwerger (1987). In spin–boson language the non–equilibrium prepared initial state corresponds to the particle originally situated at one of levels (for Kondo model it means definite impurity spin projection) and then at some time it starts its dynamics with hopping between levels. Using so–called noninteracting–blip approximation Leggett et al. (1987) have derived results for the level occupation (magnetization in the Kondo model language) exactly at the special value of the coupling constant (so–called Toulouse point (Toulouse 1969)),

and approximately in the whole parameter space. Their main result is that occupation of the level (magnetization) goes to zero exponentially fast with time

$$P(t) \stackrel{\text{def}}{=} \langle S_z(t) \rangle \sim \exp\left(-\frac{t}{\text{character. time scale}}\right). \quad (1.1)$$

This result was confirmed later by Lesage and Saleur (1998), who have proven it asymptotically using the form-factor approach. However, there are no exact or numerical results giving behavior of the magnetization in the whole parameter range at all time scales.

Another open question is behavior of the impurity spin-spin correlation function  $C(t, t')$  defined as

$$C(t, t') \stackrel{\text{def}}{=} \langle S_z(t) S_z(t') \rangle. \quad (1.2)$$

This general two-time definition is suitable in and out of equilibrium situations. Times  $t$  and  $t'$  are the times of the first and the second measurements of the impurity spin. While the system is in equilibrium the time-translation invariance is present and all correlation functions depend only on the time difference between two measurements  $\tau = t - t'$ . In our case there is one specific point on the time axis – the time of switching on the coupling. Thus, time-translation invariance is violated immediately and time-dependent correlation functions depend on both times explicitly. One may only expect that when both times are sufficiently far from the switching time correlation functions should become almost equilibrium ones. How fast this process happens depends on the explicit system setup and is one of the most important questions of the non-equilibrium physics. In case of the Kondo model in equilibrium, with the Fermi-liquid theory one can show algebraic long-time decay of this function

$$C(t, t') = C(t - t') \propto 1/(t - t')^2. \quad (1.3)$$

On the other hand,

$$C(t, 0) = \frac{1}{2} P(t) \quad (1.4)$$

and it should decay exponentially out of equilibrium according to (1.1). Particular interest is how such an exponential decay crosses into algebraic long-time behavior when the system observables evolve toward their equilibrium values. One possible scenario was suggested in the work by Nordlander, Pustilnik, Meir, Wingreen, and Langreth (1999). Using as an example the height of the Kondo resonance at the Fermi energy, they have introduced the concept of the *effective temperature* claiming that the relaxation of system observables at zero temperature out of equilibrium happens as if it were *equilibrium time-independent behavior but at some finite effective temperature* which, in its turn, is time-dependent. If above statement is true and applicable to the other observables, one conclusion follows that one will *never realize the algebraic long-time decay of the spin-spin*

*correlation function in experiment* since at any finite temperature the correlator decays exponentially. This is one of the most important issue to be solved. It is also tightly connected with the fluctuation–dissipation theorem since imaginary and real parts of the Fourier transform of (1.2) are connected by this relation. If it is violated then the concept of the effective temperature serves exactly as a measure of its violation. Thus, one may ask the following questions: whether the fluctuation–dissipation theorem is fulfilled or not; how to define the effective temperature if it is violated in specified non–equilibrium case; to what extent this definition is applicable. Finally, one is also interested in calculation of transport properties, such as conductivity, which are most easily measured in experiment.

The Kondo problem is the strong–coupling problem and it is already difficult by itself, without any time–dependence. With non–equilibrium initial conditions it becomes a *time-dependent strong-coupling model* for which no general methods exist.

Results obtained by various approximate analytic technics, such as time–dependent non–crossing approximation (Nordlander et al. 1999, Nordlander, Wingreen, Meir and Langreth 2000, Plihal, Langreth and Nordlander 2000) have confirmed existence of time scale

$$t_K \propto \hbar/k_B T_K \quad (1.5)$$

related to the Kondo temperature  $T_K$  relevant for the buildup of the Kondo resonance. Another line of attack of this problem is to use different numerical methods. Suitable approaches which have been already applied to the equilibrium Kondo model are the numerical renormalization group (Costi 1997), density–matrix renormalization group (Schollwoeck 2005), quantum Monte–Carlo (Egger 2004). In principle, these technics can be applied unchanged for the calculation of the highly excited initial state relaxation. However, technically it is very difficult since the number of eigenstates is limited by calculation time whereas one needs a very high energy resolution while searching for the long–time dynamics. Implementation of these methods to other problems such as non–equilibrium steady state with applied voltage bias is even much harder since all methods need to be generalized and are not directly applicable in their equilibrium versions. There are few exact results in addition to the Leggett’s result for the magnetization which can serve as a benchmark for adjusting of numerical methods. Schiller et al in a number of works (Schiller and Herschfield 2000, Schiller and Herschfield 1995, Schiller and Herschfield 1998, Majumdar, Schiller and Herschfield 1998) got exact solution for the non–equilibrium Kondo model with the finite voltage bias at some specific point of the parameter space. Yet, there is no complete picture of these phenomena as well as any exact results regarding the crossover from non–equilibrium to equilibrium behavior in this one of the most important problems of the solid state physics.

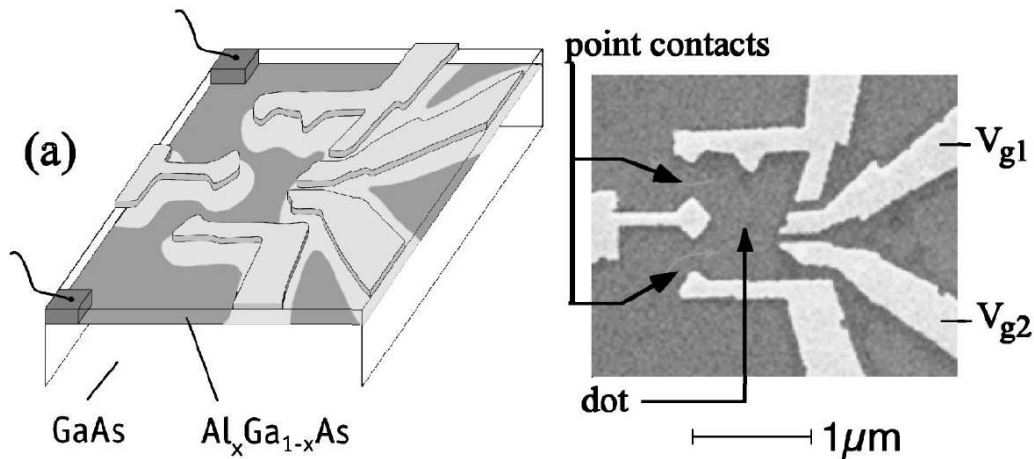


**Figure 1.1:** Picture of a lateral quantum dot used by Folk et al. (1996). Gate and bias voltages provide continuous control of this device, which is not possible in bulk materials.

### 1.3 Experimental Motivation

Equilibrium Kondo effect in bulk materials is known for a long time (de Haas, de Boer and van den Berg 1934). However non-equilibrium realizations with the impurity spin initially decoupled from the conduction band are obviously not possible in a bulk material. Another experimental difficulty is to avoid interaction between impurities since one usually needs substantial impurity concentration for detecting single-impurity effects. Actually, all theories of the Kondo effect depend on several parameters whose values are not independently and continuously tunable in bulk materials.

Non-equilibrium Kondo problem attracted much interest recently when many experimental groups succeeded in fabricating various low-dimensional nanometer-sized systems usually called 'quantum dots' (Kastner 1992). This name refers to the quantum confinement in all three spatial dimensions. Typical quantum dot is made by forming a two-dimensional electron gas in the interface region of a semiconductor heterostructure (usually GaAs) and applying an electrostatic potential to metal gates to confine electrons to a small region in the interface plane. Changing couplings of the central region ("dot") to leads and passing current through the system one measures various transport properties. There are a number of other miniature devices such as metallic nanoparticles, fullerenes, carbon nanotubes whose measured properties exhibit unexpectedly similar behavior to that of the quantum dots. This suggests that quantum dots are generic systems to investigate coherent quantum devices. A typical example of a quantum dot is shown in Fig.1.1.

There are several techniques to produce quantum dots. A typical example on the Fig.1.1 is made by molecular-beam epitaxy when a layer of AlGaAs is grown on the top of a layer of GaAs. Electrons in the interface between two layers form a two-dimensional electron gas, because of the confinement in the vertical direction. Metal gates (lighter regions) are created by electron-beam lithography. Applying a negative bias to the top metal gate restricts electron motion to a small region ("dot"). Dot is coupled to the 2D electron gas by two adjustable point contacts. Gate voltages  $V_{g1}$  and  $V_{g2}$  control the shape of the quantum well. Transport properties of the system are measured by applying a voltage  $V_{sd}$  (s for source and d for drain) and the conductance of the dot can be measured via

$$G = \frac{I}{V_{sd}} \quad (1.6)$$

Typical values for quantum dots produced in experiments are the following: confined electrons are  $\sim 50 - 100$  nm below the surface; effective mass of an electron in GaAs is  $m^* = 0.067m_e$ ; typical sheet density  $n_s \sim 4 \times 10^{11} \text{cm}^{-2}$ , which gives for a Fermi wavelength  $\lambda_F = (2\pi/n_s)^{1/2} \sim 40 \text{nm}$  (two orders of magnitude larger than in a metal) and Fermi energy  $E_F = 14$  meV; mobility of electrons of order  $\mu_e \sim 10^4 - 10^6 \text{cm}^2/\text{V}$ , giving typical mean free path of  $l = v_F m^* \mu_e / e \sim 0.1 - 10 \mu\text{m}$ . In the dots with effective area  $A \sim 0.3 \mu\text{m}^2$  motion of dot electrons is, therefore, ballistic. To observe quantum coherence effect in dots that are weakly coupled to leads, so called "closed" dots,

$$G \ll e^2/h \quad (1.7)$$

one should have a temperature which are smaller than a mean single-particle level spacing  $\delta E$  inside the quantum well. Taking above numbers one gets for the spacing  $\delta E = \pi \hbar^2 / m^* A \sim 11 \mu\text{eV}$  which can be resolved at temperatures of  $\sim 100 \text{mK}$  ( $8.6 \mu\text{eV}$ ). Nowadays, the temperature can be made even lower of order  $20 - 25 \text{mK}$ .

Most interesting phenomenon observed in quantum dots is charge quantization in the dot which is called Coulomb Blockade (Giaever and Zeller 1968, Kulik and Shekhter 1975, Ben-Jacob and Gefen 1985, Likharev and Zorin 1985, Averin and Likharev 1986, Fulton and Dolan 1987, Scott-Thomas, Field, Kastner, Smith and Antonadis 1989). It already takes place at temperatures lower than the charging energy of the dot  $k_B T \ll E_C = e^2/2C$ , where  $C$  is classical capacitance of the charged region. This is the energy one needs to pay to add an extra electron to the dot. At such temperatures the tunneling through the dot is blocked by the Coulomb repulsion. Changing gate voltage  $V_g$  one can compensate that repulsion and cause activationless transport through the dot when the filled energy level of the dot crosses the Fermi energy of the attached leads (see Fig.1.2).

At temperatures lower than single-particle level spacing

$$k_B T \ll \delta E \quad (1.8)$$

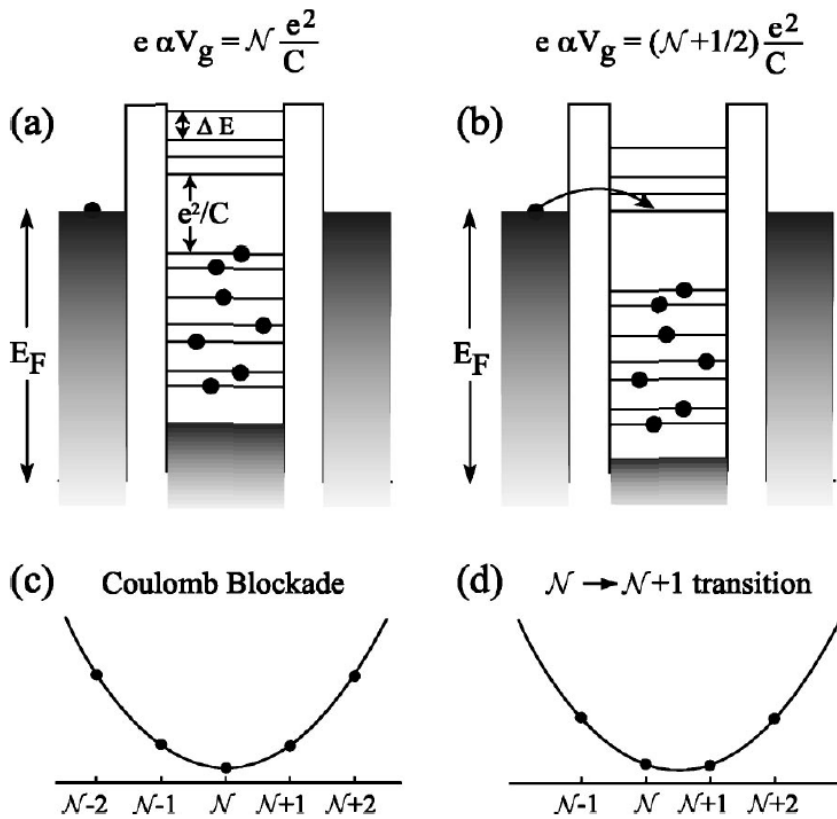


**Figure 1.2:** Explanation of the Coulomb Blockade phenomenon. When the gate voltage makes  $|N\rangle$  and  $|N+1\rangle$  states equally favorable, it causes activationless transport of the electric charge through the dot. Tuning the gate voltage we can switch between various regimes when the top-most level is zero-, single- or double-occupied. (Taken from Alhassid (2000))

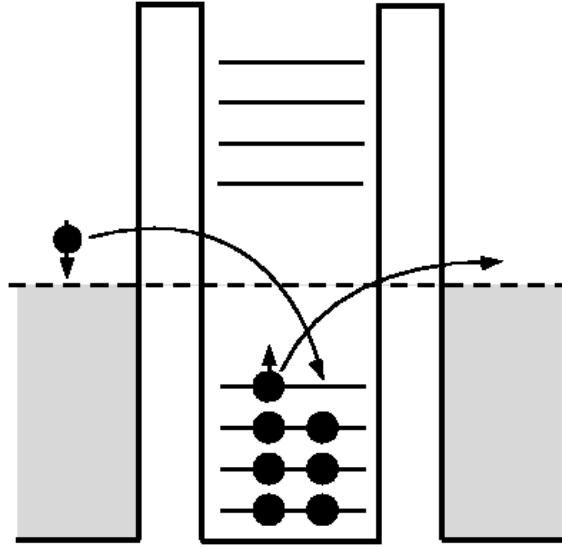


**Figure 1.3:** Elastic co-tunneling with a flip of spin.

one has to take into account whether the top-most level is singly or doubly occupied. When the top-most level is single-particle occupied the dot has a magnetic moment and the level is spin degenerate. Ground state of the dot is described by a certain spin projection and elastic transfer of the electrons from one lead to another lead is accompanied by a spin flip (see Fig.1.3). Resulting effective model is the Kondo model and it is valid for all energies below the threshold  $\delta E$  (see review by Glazman and Pustilnik (2003), for example).

Due to extreme flexibility in control of the quantum dot one can realize all kinds of the non-equilibrium conditions we have discussed before. Starting with the applying constant bias voltage and finishing with the applied time-dependent external electromagnetic fields.

One possible experiment for realization of the non-equilibrium situation when the spin is initially decoupled from the conduction band was proposed by Nordlander et al. (1999). Quantum dot with a singly occupied top-most level well below the Fermi energy of the leads can be considered as effectively decoupled from the Fermi sea of the conduction band electrons. Indeed, if the impurity level is much below the Fermi energy then the coupling between the impurity spin and conduction electrons is too small and the spin is unscreened. One can also think about the Kondo temperature much smaller than the actual temperature of the experiment  $T_K \ll T$ . Applying step-like gate voltage impulse we can push impurity

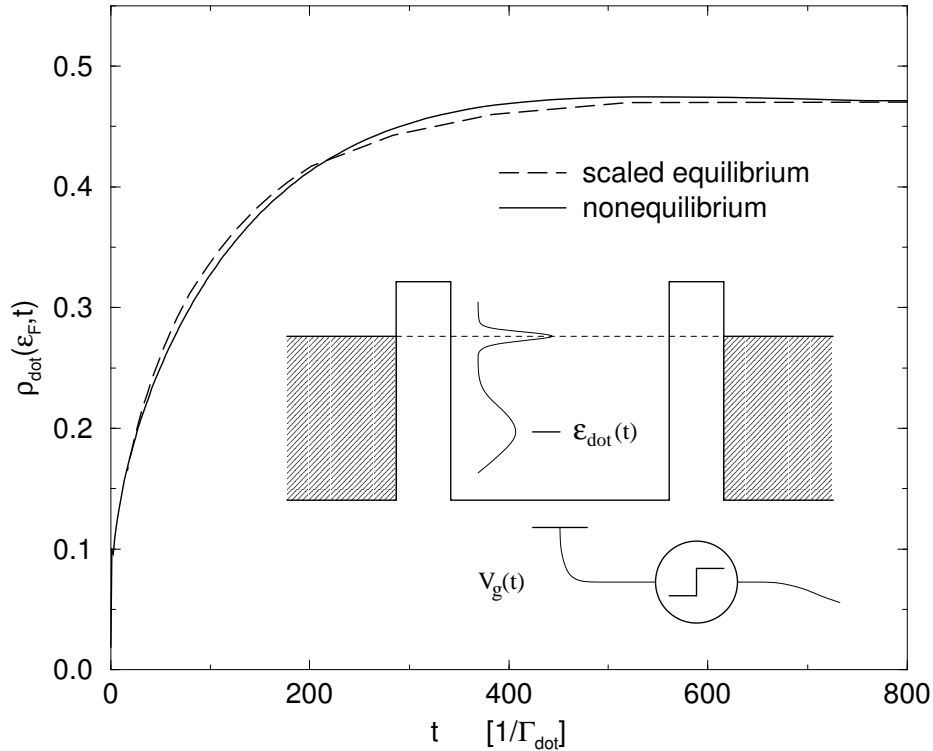


**Figure 1.4:** Quantum dots experiments with time-dependent gate voltages: Time-dependent buildup of many-body correlations (figure from Nordlander et al. (1999))

level up and switch on the Kondo regime when  $T_K \gg T$ . Proposed experiment is plotted in Fig.1.4. Measuring magnetization and magnetic susceptibility one can check deviations of this quantities from their equilibrium analogues.

The main obstacle to observe this phenomenon in experiment is the smallness of the time scale  $t_K$ . For a typical Kondo temperature in quantum dots of order 0.01 – 1K we get the Kondo time scale  $t_K$  which corresponds to the frequencies from several gigahertzes up to terahertz. Hence, to find indications of described non-equilibrium Kondo effect the time of switching on the coupling should be much smaller than this time scale. The lower is the Kondo temperature, the longer is the relaxation of the dot spin and, consequently, the easier is to measure it. On the other hand, the Kondo temperature must be much higher than the actual temperature of the experiment for system still to be in the Kondo regime. We believe that such an experiment can be made in the nearest future.

Experimental importance of such an investigation is tightly connected with an attempt to make a functional qubit, a two-level system, the building block of a possible quantum computer realization made of SET transistors. The most promising candidates are the quantum dots and the Josephson junctions. In reality any such a system is coupled to environment and subjected to energy

dissipation. Thus, to build a qubit capable of performing tens of thousands operations before environmental decoherence sets one should achieve a relaxation time which is much longer than the operation time. Although the coupling to the environment is usually weak and, therefore, described by the different model called the spin–boson model solution for the non–equilibrium Kondo regime of a strongly screened impurity is a very important benchmark in all further study of these systems since both models can be exactly mapped on each other.

## 1.4 Goals of This Work

Summing up all open questions we can formulate goals of the underlined thesis. The main subject is to study the non–equilibrium Kondo effect for two different initial preparations I) when the impurity spin is initially decoupled from the conduction band and II) when it is fixed by the external magnetic field at zero temperature.

We aim at

- 1 Finding full crossover between the exponential non–equilibrium decay and the equilibrium algebraic long–time behavior of the spin–spin correlation functions
  - at the exactly solvable Toulouse point
  - in the physically relevant Kondo limit
- 2 Checking the fulfillment of the fluctuation–dissipation theorem for the real and imaginary parts of the spin–spin correlation function in the quantum limit.
- 3 Deriving analytical asymptotic results for the magnetization  $P(t)$  at large and small times and extend these results for all intermediate time scales.
- 4 Connecting relaxation of the thermodynamic properties with the behavior of the transport properties (e.g. conductivity) by calculation of the quasiparticle spectral function, which is directly related with the non–equilibrium current through a quantum dot.

The central problem is to choose appropriate methods which allow us to solve all posed issues.

We use bosonization and refermionization techniques to calculate the zero temperature spin–spin correlation function of the Kondo model at the Toulouse point. After applying these transformations the strong–coupling time–dependent Kondo

model becomes equivalent to the non-interacting resonant level model which is quadratic and therefore can be solved exactly. We find equations of motion for all observables in the Heisenberg picture and average afterwards with respect to the non-equilibrium initial states I) and II) which are time-independent in this representation. Although calculation is lengthy it is straightforward and the final solution for the correlation functions  $P(t)$  and  $C(t, t')$  can be given in the closed form. The main result following from this solution is that relaxation occurs exponentially fast with a time scale set by the inverse Kondo temperature and independently on the incipient state I) or II) of the system. Result for  $P(t)$  is the confirmation of the Leggett result but obtained by another method. However, result for  $C(t, t')$  is completely new and was not known before. Closed expressions let us trace the crossover from the exponential decay to the algebraic long-time behavior at all intermediate time scales.

Remarkable conclusion which follows immediately from the exact solution is the inapplicability of the effective temperature concept to calculation of correlation functions in the manner proposed by Nordlander et al. (1999). From exact analytical expressions it is clear that the difference between non-equilibrium and equilibrium spin-spin correlators vanishes exponentially for  $t_w \gg t_K$  and one realizes the algebraic long-time decay immediately at both initial preparations I) and II) once the time of the first measurement is larger than zero.

Since the Toulouse point is a very special point of the parameter space, it is interesting in which extent these results are generic for the whole problem. Away from this point the Kondo model is no longer described by a non-interacting Hamiltonian and another approach is needed. For this purpose we use the flow-equation method developed by Wegner (1994) and applied later to a number of problems including the equilibrium Kondo effect as well (Kehrein 2001, Hofstetter and Kehrein 2001, Kehrein and Mielke 1996, Kehrein and Mielke 1997). This approach is the controlled approximation which gives results with a very high accuracy for the Kondo model in the whole parameter region. Flow equations become exact at the Toulouse point, hence, connecting continuously results at all coupling strengths with our exact analytical expressions. Main result one gets after applying the flow-equation approach is the confirmation of the exponential relaxation at large times. At shorter times comparing with  $t_K$  the relaxation is even faster, which is due to unrenormalized coupling constants at large energies that dominate the short-time behavior.

Next issue which we address is the fulfillment of the fluctuation-dissipation theorem which connects real (equilibrium spin fluctuations) and imaginary (magnetic susceptibility) parts of the spin-spin correlation function in equilibrium. We find in our case that the fluctuation-dissipation theorem is maximally violated at intermediate time scales of order the inverse Kondo temperature. At this point we naturally introduce the concept of the effective temperature as a measure of

the fluctuation–dissipation theorem violation, as it is usually done in the widely investigated context of glassy systems (see Fisher and Hertz (1991) for a review). The effective temperature becomes of order the Kondo temperature due to heating of the conduction band electrons by the formation of the Kondo singlet. The system then relaxes towards equilibrium and the fluctuation–dissipation theorem becomes fulfilled exponentially fast at larger times. Again this relaxation is given in the analytical form at the Toulouse point and extended away from it by using the flow–equation method. Although our definition of the effective temperature is not unique its behavior qualitatively grabs the actual thermic effects which happen during the formation of the Kondo cloud and can be measured in experiment. These observations could be relevant for designing time-dependent functional nanostructures with time-dependent gate potentials since they give a quantitative insight into how long one needs to wait after switching for the system to return to effectively zero temperature.

In experiment one typically measures conductance of a given sample. A quantum dot suddenly shifted into the Kondo regime exhibits an increase in the conductance due to a forming of the Kondo resonance at the Fermi energy. Thus, an interesting quantity to evaluate is the non-equilibrium density of states which is proportional to such an increase. Unfortunately, the direct translation of this problem into the language of the effective models, which are the main ingredients of our exact Toulouse point calculation and approximate flow–equation solution, looks impossible. Excitations of the effective models are many–electron soliton–like structures and are not suitable objects for evaluation of the single–particle quantities (like density of states needed for calculation of conductance). It is very hard to re–express them even at the exactly solvable Toulouse point. Thus, another approach is implemented. For calculation of the spectral density, we use the result of the microscopic Fermi liquid theory which states that in equilibrium the density of states at the impurity site  $\rho_{\text{imp}}(\epsilon)$ , in the vicinity of the Fermi energy, is proportional to the quasiparticle density of states of the effective model  $\rho_{\text{eff}}(\epsilon)$  (see Hewson (1993))

$$\rho_{\text{imp}}(\epsilon) = z\rho_{\text{eff}}(\epsilon), \quad (1.9)$$

where  $z$  is known as a wavefunction renormalization factor. In our approach we assume that  $z$  factor remains time-independent in the non-equilibrium situation or, at least, it remains constant on the scale of order of  $t_K = 1/T_K$ . Next step is to calculate the spectral function for the effective model. Resulting spectral densities exhibit exponential relaxation toward their equilibrium values and are in agreement with results obtained by non–crossing approximation (Nordlander et al. 1999) which however is not applicable at temperatures much lower than  $T_K$ . Energy dependence of the non–equilibrium spectral functions demonstrates very peculiar Friedel–type oscillations with the frequency equal to the time distance to switching on the coupling.

All the mentioned results are published in a sequence of papers (Lobaskin and Kehrein 2005a, Lobaskin and Kehrein 2005b, Lobaskin and Kehrein 2005c).

The dissertation is organized as follows:

In the next chapter we discuss the Kondo model in equilibrium and out of equilibrium and describe in details both types of the non-equilibrium situations considered. With the help of bosonization and refermionization technics we derive effective time-dependent Hamiltonian needed for a further study.

In chapter III we give full details of exact calculations of the magnetization  $P(t)$  and the spin-spin correlation functions  $C(t, t')$  at the Toulouse point of the Kondo model out of equilibrium. We show that results are independent on the type of the initial preparation.

In the next chapter details of the flow-equation approach applied to this model are discussed, and numerical results for correlation functions are given along with analytical asymptotics of these functions in small and large time limits. Again we confirm independency of the full solution on the original state I) or II). We also discuss important differences between the full flow-equation solution of the problem and analytical Toulouse point result.

Chapter V contains discussion of the fluctuation-dissipation theorem violation in the quantum case  $T = 0$  out of equilibrium. Concept of the effective temperature is introduced to define the measure of the fluctuation-dissipation theorem violation. These general theoretical results are applied to the non-equilibrium Kondo effect.

In chapter VI the results for the non-equilibrium density of states of the effective model are presented, which is directly related with experimentally measurable conductance of a sample.

In the last chapter we give a summary and an outlook.



## 2. TIME-DEPENDENT KONDO MODEL

### 2.1 Equilibrium Kondo Problem

Recognition of the fundamental role of the magnetic impurities influence on transport and thermodynamic properties of metals got its start from the famous work of J. Kondo (Kondo 1969). It was him who explained the temperature minimum in the electric resistivity observed earlier in several experiments with doped metals, phenomenon which puzzled people for 30 years. In most metals resistivity is mainly caused by scattering of conduction electrons over lattice phonons and decreases very rapidly with temperature as  $T^5$ , whereas in experiments on *Au* by de Haas et al. (1934) and on dilute alloys of *Fe* in a series of *Nb - Mo* alloys as host metals by Sarachik, Corenzvit and Longinotti (1964) resistivity dropped with temperature down to some finite value and unexpectedly increased with further temperature lowering (see Fig.2.1).

Basis for Kondo calculations was provided in earlier contributions by J.Friedel (Friedel 1952, Friedel 1958, Friedel 1956, Blandin and Friedel 1959) and P.W.Anderson (Anderson 1961). In the former work an important concept of the "virtual bound states", almost localized states due to a resonant scattering at the impurity site, was introduced. If a local impurity potential is not attractive enough to form a bound state in 3D it still may localize electrons in the vicinity of an impurity for sufficiently long time. Provided such a resonance is situated near the Fermi energy, it enhances impurity contributions to all thermodynamic properties of metal. In the latter work by Anderson a different approach was formulated within the famous model which now bears his name

$$H_{\text{Anderson}} = \sum_{\sigma} \epsilon_d n_{d\sigma} + U n_{d\uparrow} n_{d\downarrow} + \sum_{k\sigma} \epsilon_k c_{k\sigma}^{\dagger} c_{k\sigma} + \sum_{k\sigma} (V_k c_{d\sigma}^{\dagger} c_{k\sigma} + V_k^* c_{k\sigma}^{\dagger} c_{d\sigma}). \quad (2.1)$$

This Hamiltonian describes the conduction band electrons with a dispersion  $\epsilon_k$  interacting with the localized impurity orbital at an energy  $\epsilon_d$ , which has an on-site interaction  $U$ . Coulomb repulsion  $U$  between localized electrons is essential to explain origination of the localized magnetic moments in host metal. Indeed, considering the case  $V_k = 0$ , which is reasonable assumption for a further perturbation theory expansion since the hybridization parameter is of order  $0.1 - 0.7\text{eV}$  whereas Coulomb repulsion is in range of several eV, we immediately see that for

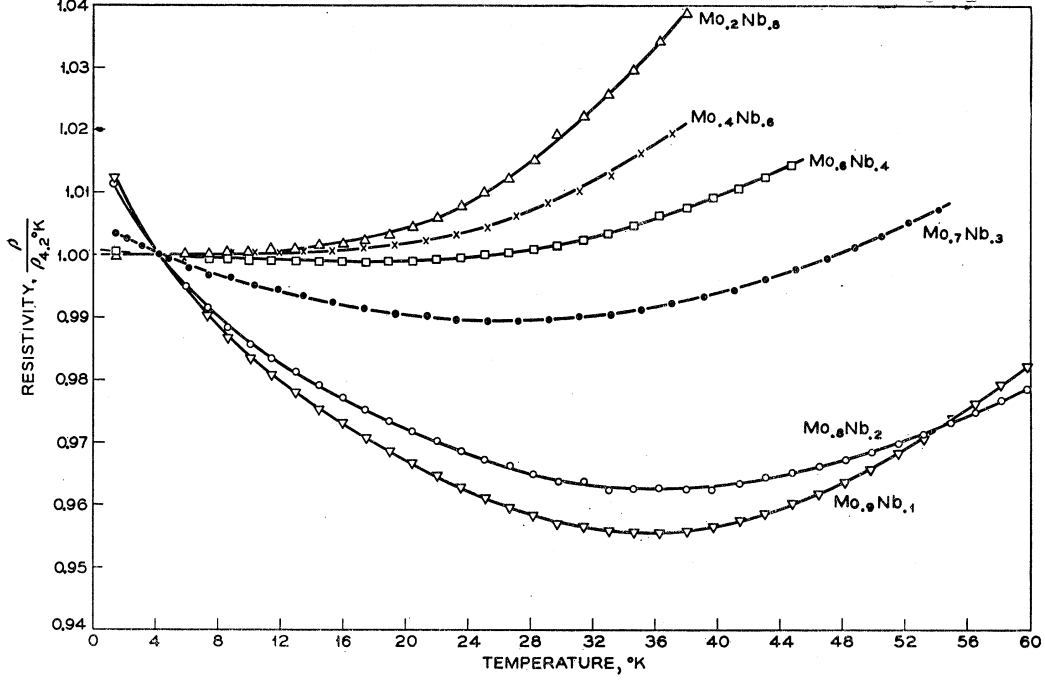


**Figure 2.1:** Resistance minima for Fe in a series of Mo-Nb alloys (taken from Sarachik et al. (1964))

$\epsilon_d < \epsilon_F$  and  $\epsilon_d + U > \epsilon_F$  the most favorable configuration is the singly occupied one. Addition of an extra electron or removing one costs extra energy, hence, the ground state is two-fold degenerate. Taking into account doubly-occupied and empty states as an excited states in lowest order in  $V_k$  and replacing

$$S^+ = c_{d\uparrow}^\dagger c_{d\downarrow} \quad , \quad S_z = \frac{1}{2}(n_{d\uparrow} - n_{d\downarrow}) \quad (2.2)$$

which always hold in the  $n_d = 1$  subspace, one can derive from (2.1) the well-known s-d model or, simply, the Kondo model (Schrieffer and Wolff 1966)

$$H_{\text{Kondo}} = \sum_{k\sigma} \epsilon_k c_{k\sigma}^\dagger c_{k\sigma} + \sum_{kk'} J_{kk'} (S^+ c_{k\downarrow}^\dagger c_{k'\uparrow} + S^- c_{k\uparrow}^\dagger c_{k'\downarrow} + S_z (c_{k\uparrow}^\dagger c_{k'\uparrow} - c_{k\downarrow}^\dagger c_{k'\downarrow})) \quad (2.3)$$

with an effective exchange coupling given by

$$J_{kk'} = V_k^* V_{k'} \left\{ \frac{1}{U + \epsilon_d - \epsilon_{k'}} + \frac{1}{\epsilon_k - \epsilon_d} \right\} \quad (2.4)$$

together with a potential scattering term

$$\sum_{kk'\sigma\sigma'} K_{kk'} c_{k\sigma}^\dagger c_{k'\sigma} \quad , \quad (2.5)$$

where

$$K_{kk'} = \frac{V_k^* V_{k'}}{2} \left\{ \frac{1}{\epsilon_k - \epsilon_d} - \frac{1}{U + \epsilon_d - \epsilon_{k'}} \right\}. \quad (2.6)$$

Above correspondence is valid for conduction band energies below the threshold (level spacing  $U$ ) which can be expressed by  $|\epsilon_k| \ll |\epsilon_d - \epsilon_F|$  and  $|\epsilon_k| \ll |U + \epsilon_d - \epsilon_F|$ .

Kondo, in his seminal paper (Kondo 1969), considered a local magnetic moment with spin  $S = \frac{1}{2}$  coupled via a constant exchange interaction  $J$  with the conduction band electrons. He has shown in the third order perturbation theory in coupling  $J$  the appearance of  $\ln T$  term in the resistivity calculation

$$R(T) = aT^5 + c_{imp}R_0 - c_{imp}R_1 \ln(k_B T/D), \quad (2.7)$$

where  $c_{imp}$  is impurity concentration,  $R_0$ ,  $R_1$  - some constants,  $D$  - bandwidth. That calculation explained the observed resistance minimum, though obviously broke down at small temperatures.

A huge number of theoretical works devoted to this problem appeared in 60s and early 70s (Suhl 1965, Suhl and Wong 1967, Nagaoka 1965, Abrikosov 1965, Zitzartz and Müller-Hartmann 1974, Bloomfield and Hamann 1967, Hamann 1967)). People succeeded in identifying an energy scale

$$k_B T_K \sim D e^{-\frac{1}{2J\rho_0}} \quad (2.8)$$

called the Kondo temperature, beyond which standard perturbation approaches fail. Here  $D$  is the bandwidth,  $\rho_0$  is the density of states at the Fermi energy. Non-analytic dependence of  $T_K$  on Kondo coupling demanded non-perturbative methods to determine system properties at low temperatures  $T < T_K$ . In 60s Anderson and co-workers introduced "poor-man" scaling approach (Anderson 1967, Anderson and Yuval 1969, Anderson, Yuval and Hamann 1970, Anderson and Yuval 1970) based on continuous reduction of bandwidth  $D$  of the conduction electrons. Elimination of high energy excitations leads to a strong renormalization of the effective coupling between an impurity moment and conduction electrons, and even becomes divergent at low energies  $T \ll T_K$ . Natural conclusion follows that such a scaling picture corresponds to the ground state with the infinite coupling between an impurity and the conduction band forming a singlet state (Mattis 1967, Nagaoka 1967).

In 1974 Wilson developed numerical renormalization group approach (NRG) (Wilson 1974, Wilson 1975) which enabled him to derive an effective low-energy Hamiltonian of the problem and confirmed existence of the singlet state for  $S = 1/2$  Kondo model. Wilson got numerical results for impurity contribution to thermodynamic and transport properties which were also confirmed by Nozières (1974) using phenomenological Fermi-liquid picture of low-lying energy excitations. They both got the same result for Sommerfeld ratio of linear coefficient

$\gamma_{imp}$  in the specific heat  $C_{imp}$

$$C_{imp} = \gamma_{imp}T \quad (2.9)$$

to impurity magnetic susceptibility  $\chi_{imp}$  at zero frequency defined as

$$\chi_{imp}(\omega + i\delta) = -(g\mu_B)^2 \langle \langle d^\dagger d; d^\dagger d \rangle \rangle_{\omega+i\delta}, \quad (2.10)$$

where double brackets stand for autocorrelator. Sommerfeld ratio (for the Kondo model it is sometimes called Wilson ratio) then equals to

$$R = \frac{\chi_{imp}/\chi_c}{\gamma_{imp}/\gamma_c} = \frac{4\pi^2 k_B^2}{3(g\mu_B)^2} \frac{\chi_{imp}}{\gamma_{imp}} = 2 \quad (2.11)$$

with  $c$  meaning conduction electron values without the impurity. In non-interacting case, for  $U = 0$  and constant hybridization function  $V_k$ , this ratio is 1 or 4 depending on the magnetic susceptibility definition: if the definition is local meaning the magnetic field acts only on the impurity site then this ratio is 4; if we use the global magnetic field acting on both the conduction band as well as the impurity site then the Wilson ratio is 1.

Both the NRG and the Fermi-liquid approach give the same values for  $T^2$  coefficient in the conductivity

$$\sigma_{imp}(T) = \sigma_0 \left( 1 + \frac{\pi^4 w^2}{16} \left( \frac{T}{T_K} \right)^2 + O(T^4) \right) \quad (2.12)$$

where  $w = 0.4128$  so-called Wilson number and  $\sigma_0 = ne^2\pi\rho_0(0)/2mc_{imp}$  – conductivity at the "unitarity" limit when the  $s$ -wave phase shift of scattering electrons at the Fermi level is equal to  $\pi/2$ . Later Yamada (1975) derived the microscopic Fermi-liquid theory of the Kondo model from the Anderson Hamiltonian (2.1).

Another source of theoretical insight came from an exact analytical solution of the  $s$ - $d$  model using Bethe ansatz (Bethe 1931) applied by Andrei (1980) and Wiegmann (1980). They have succeeded in calculating thermodynamic properties of the Kondo model, providing the same results to Wilson's NRG. This approach works for the linear dispersion Kondo model with the infinite bandwidth. Exact calculation of the excitation spectrum gives all thermodynamic properties as well as analytical expressions for the Kondo temperature and Wilson number  $w$ . The method can be generalized to provide exact results for the ground state and thermodynamics of  $S > \frac{1}{2}$  magnetic impurity models, which are different from the usual spin 1/2 problem, since in the ground state an impurity spin is underscreened and equal to  $S - \frac{1}{2}$ .  $N$ -fold degenerate problem was particularly interesting for experimentalists who have already been working with rare earth elements ( $Ce$  and  $Yb$ ), which have spin degeneracy higher

than two. Since the Bethe ansatz cannot be used for calculation of dynamical response functions directly measured in experiment, a number of approximate techniques was invented, treating  $1/N$  as a small parameter. Results of these theories become asymptotically exact in the limit  $N \rightarrow \infty$  (mean field point). Many very good approximations around this limit can be obtained by different methods: perturbation theory (Ramakrishnan and Sur 1982, Rasul and Hewson 1984, Bickers 1987, Brandt, Keiter and Liu 1985), Fermi-liquid theories (Schlottmann 1983, Yoshimori 1976, Newns and Hewson 1980), non-crossing approximation (Kuromoto and Müller-Hartmann 1985, Kuromoto and Kojima 1984, Bickers, Cox and Wilkins 1987), slave-boson and mean field theory (Newns and Read 1987, Read and Newns 1983a, Read and Newns 1983b), variational  $1/N$  expansions (Gunnarsson and Schönhammer 1983a, Gunnarsson and Schönhammer 1983b), bosonization and conformal field theories (Affleck and Ludwig 1991a, Affleck and Ludwig 1991b, Affleck and Ludwig 1991c, Affleck and Ludwig 1993, Affleck and Ludwig 1994, Affleck and Ludwig 1992, Affleck and Ludwig 1991d). All these methods were successfully applied to the investigation of the bulk Kondo effect manifested in different properties of rare earth and actinide compounds.

## 2.2 Time-dependent Kondo Hamiltonian

We start from the Kondo Hamiltonian which describes the coupling between the conduction band Fermi sea and the impurity orbital in the local moment regime

$$H = \sum_{k,\alpha} \epsilon_k c_{k\alpha}^\dagger c_{k\alpha} + \sum_i J_i(t) \sum_{\alpha,\beta} c_{0\alpha}^\dagger S_i \sigma_i^{\alpha\beta} c_{0\beta}. \quad (2.13)$$

Here  $c_{0\alpha}^\dagger, c_{0\alpha}$  is the localized electron orbital at the impurity site which are defined as

$$c_{0\alpha}^\dagger \stackrel{def}{=} \sum_k \frac{c_k^\dagger}{\sqrt{L}}, \quad c_{0\alpha} \stackrel{def}{=} \sum_k \frac{c_k}{\sqrt{L}}. \quad (2.14)$$

We allow for anisotropic couplings

$$J_i = (J_\perp(t), J_\perp(t), J_\parallel(t)). \quad (2.15)$$

Such a generalization is essential for the exact analytical solution at the so-called Toulouse point. At all couplings equal to each other (isotropic coupling) we get the original Kondo Hamiltonian (2.3). Dispersion relation is linear

$$\epsilon_k = \hbar v_F k, \quad (2.16)$$

which is also necessary for the exact solution. However, it is not needed for the flow-equation approach applied in the small coupling limit. In the following we

generally set  $v_F = \hbar = 1$ . Sometimes we will restore these constants to get the right dimension of an evaluated quantity.

According to the introduction chapter we consider two types of non-equilibrium preparations:

I) The impurity spin is fixed for all negative times by a large magnetic field term  $h(t)S_z$  that is switched off at  $t = 0$ :  $h(t) \gg T_K$  for  $t < 0$  and  $h(t) = 0$  for  $t \geq 0$

$$H = \sum_{k,\alpha} \epsilon_k c_{k\alpha}^\dagger c_{k\alpha} + \sum_i J_i(t) \sum_{\alpha,\beta} c_{0\alpha}^\dagger S_i \sigma_i^{\alpha\beta} c_{0\beta} + h(t)S_z . \quad (2.17)$$

This case corresponds to the absence of spin-flip processes at negative times, although impurity is coupled to the conduction band:  $J_\perp(t) = 0$ ,  $J_\parallel(t) = J_\parallel > 0$  for  $t < 0$  and  $J_i = J_i > 0$  for  $t \geq 0$

$$H(t < 0) = \sum_{k,\alpha} \epsilon_k c_{k\alpha}^\dagger c_{k\alpha} + J_\parallel \sum_{\alpha,\beta} c_{0\alpha}^\dagger S_z \sigma_z^{\alpha\beta} c_{0\beta} \quad (2.18)$$

and

$$H(t > 0) = \sum_{k,\alpha} \epsilon_k c_{k\alpha}^\dagger c_{k\alpha} + \sum_i J_i \sum_{\alpha,\beta} c_{0\alpha}^\dagger S_i \sigma_i^{\alpha\beta} c_{0\beta} . \quad (2.19)$$

II) The impurity spin is completely decoupled from the bath degrees of freedom for all negative times:  $J_i(t) = 0$  for  $t < 0$

$$H(t < 0) = \sum_{k,\alpha} \epsilon_k c_{k\alpha}^\dagger c_{k\alpha} . \quad (2.20)$$

Similar to situation I) we assume a certain projection of spin  $\langle S_z(t \leq 0) \rangle = +1/2$ , which is realized by a infinitesimally small magnetic field. Then the coupling is switched on at  $t = 0$  and becomes finite  $J_i(t) = J_i > 0$  and time-independent for  $t \geq 0$

$$H(t > 0) = \sum_{k,\alpha} \epsilon_k c_{k\alpha}^\dagger c_{k\alpha} + \sum_i J_i \sum_{\alpha,\beta} c_{0\alpha}^\dagger S_i \sigma_i^{\alpha\beta} c_{0\beta} . \quad (2.21)$$

This situation is rather more interesting than situation I) since it can be realized in future quantum dot experiments where the quantum dot is suddenly switched into the Kondo regime by applying a time-dependent gate voltage (Nordlander et al. 1999).

## Bosonization of the Kondo Hamiltonian

For our purposes it is more convenient to treat this Hamiltonian in its bosonized form. There are two main reasons for it

- the model becomes quadratic at the Toulouse point;
- in the flow-equation approach the Toulouse point corresponds to the *fixed* point of the Hamiltonian flow.

We will follow general bosonization rules reviewed in work by von Delft and Schoeller (1998).

One introduces bosonic spin-density modes

$$\sigma = \frac{1}{\sqrt{2|p|}} \sum_q (c_{p+q\uparrow}^\dagger c_{q\uparrow} - c_{p+q\downarrow}^\dagger c_{q\downarrow}) \quad , \quad (2.22)$$

with the commutator

$$[\sigma(-q), \sigma(q')] = \delta_{qq'} \frac{L}{2\pi} = \delta_{qq'} \frac{1}{\Delta_L} \quad (2.23)$$

for  $q, q' > 0$ . Here  $L$  is the system size,  $\Delta_L$  is the momentum spacing. The bosonic field is defined in a standard way

$$\Phi(x) = -\Delta_L i \sum_{q \neq 0} \frac{\sqrt{q}}{q} e^{-iqx - a|q|/2} \sigma(q) \quad (2.24)$$

and obeys the following commutation relation

$$[\Phi(x), \partial_y \Phi(y)] = -2\pi i \delta(x - y). \quad (2.25)$$

The parameter  $a > 0$  generates the UV regularization of our model and can be interpreted as the bandwidth. The type of regularization does not play any role, while we are concerned in the universal properties of our model at energies  $|E| \ll a^{-1}$ . We will discuss the cut-off procedure later in Section 4.4 where we link UV parameter with the flat band width.

Charge density modes in the Hamiltonian (2.13) decouple completely and one only has to look at the spin-density part

$$H = H_0 + H_{\parallel} + H_{\perp}. \quad (2.26)$$

For a linear dispersion relation of the conduction band the kinetic part of the Hamiltonian  $H_0$  can be expressed via density modes as (Kronig 1935)

$$H_0 = \Delta_L \sum_{q>0} q \sigma(q) \sigma(-q) = \frac{1}{2} \int \frac{dx}{2\pi} : (\partial_x \Phi(x))^2 : \quad , \quad (2.27)$$

where  $: \dots :$  stands for normal ordering.

$H_{\parallel}$  is the longitudinal interaction between impurity spin and the conduction band

$$H_{\parallel} = -\frac{J_{\parallel}}{\sqrt{2}2\pi}\partial_x\Phi(0)S^z. \quad (2.28)$$

$H_{\perp}$  is the transverse part

$$H_{\perp} = \frac{J_{\perp}}{4\pi a}\left(e^{i\sqrt{2}\Phi(0)}S^- + e^{-i\sqrt{2}\Phi(0)}S^+\right). \quad (2.29)$$

The longitudinal spin coupling can be eliminated by a unitary transformation

$$U = \exp [i\mu S^z \Phi(0)] \quad (2.30)$$

with an appropriate choice of  $\mu$

$$\mu = \frac{J_{\parallel}}{\sqrt{2}2\pi}. \quad (2.31)$$

Applying this transformation to the conduction band part  $H_0$ , one generates exactly minus second term in (2.26), up to irrelevant constant

$$\begin{aligned} UH_0U^\dagger &= e^{i\mu S^z \Phi(0)}\left(\frac{1}{2}\int\frac{dx}{2\pi} : (\partial_x\Phi(x))^2 : \right)e^{-i\mu S^z \Phi(0)} = \\ &= H_0 + \frac{1}{2}i\mu S_z \int\frac{dx}{2\pi} [\Phi(0), (\partial_x\Phi(0))^2] = \\ &= H_0 + \mu S_z \partial_x\Phi(0). \end{aligned} \quad (2.32)$$

In both cases for  $t > 0$  we arrive at after the bosonization procedure

$$\tilde{H}_{\text{I,II}}(t > 0) \stackrel{\text{def}}{=} U^\dagger H_{\text{I,II}} U = H_0 + g_0 [V(\lambda_0, 0)S^- + V(-\lambda_0, 0)S^+] \quad (2.33)$$

with the coupling constant

$$g_0 = \frac{J_{\perp}}{4\pi a} \quad (2.34)$$

and scaling dimension

$$\lambda_0 = \sqrt{2} - \frac{J_{\parallel}}{\sqrt{2}2\pi}. \quad (2.35)$$

Here vertex operators have been introduced

$$V(\lambda, x) \equiv \exp [i\lambda\Phi(x)] \quad (2.36)$$

After applying the unitary transformation for negative times in case I) one gets

$$\tilde{H}_{\text{I}}(t < 0) = H_0 \quad (2.37)$$

In case II)

$$\boxed{\tilde{H}_{\text{II}}(t < 0) = H_0 + \frac{J_{\parallel}}{\sqrt{2}2\pi} \partial_x \Phi(0) S^z} \quad , \quad (2.38)$$

since the unitary transformation  $U$ , in spite of canceling longitudinal coupling term for positive times, generates it for negative times.

For a future reference we also give the value of the scaling dimension with restored dimension constants

$$\lambda_0 = \sqrt{2} - \frac{J_{\parallel}}{\sqrt{2}2\pi\hbar v_F}. \quad (2.39)$$

Bosonized Hamiltonian (2.33) is our starting point for a further study.



### 3. NON-EQUILIBRIUM KONDO MODEL AT THE TOULOUSE POINT

At the Toulouse point, which is defined by the unity scaling dimension  $\lambda_0$

$$\lambda_0 = \sqrt{2} - \frac{J_{\parallel}}{\sqrt{2}2\pi} = 1, \quad (3.1)$$

vertex operators (2.36) obey fermionic commutation relations (von Delft and Schoeller 1998):

$$\{V(1, x), V(-1, x')\} = 2\pi a \delta(x - x') \quad (3.2)$$

or for the normal-ordered version

$$\{ :V(1, x) :, :V(-1, x') : \} = L \delta(x - x'). \quad (3.3)$$

Both versions are connected with each other by

$$:V(1, x) := \left( \frac{L}{2\pi a} \right)^{\frac{1}{2}} V(1, x) \quad (3.4)$$

Then one may introduce standard fermionic operators according to

$$\Psi(x) \stackrel{\text{def}}{=} :V(1, x) : . \quad (3.5)$$

Thus, transformed Hamiltonian  $\tilde{H} = U^\dagger H U$  can be refermionized (see Leggett et al. (1987))

$$\tilde{H}(t > 0) = \sum_k k \Psi_k^\dagger \Psi_k + \sum_k V_k \left( \Psi_k^\dagger d + d^\dagger \Psi_k \right) . \quad (3.6)$$

where the hybridization constant  $V_k$  is connected with the exchange coupling constant  $J_{\perp}$  via

$$V_k = g_0 \left( \frac{2\pi a}{L} \right)^{\frac{1}{2}} = \frac{J_{\perp}}{4\pi a} \left( \frac{2\pi a}{L} \right)^{\frac{1}{2}} . \quad (3.7)$$

Here the spinless fermions  $\Psi(x)$  correspond to non-trivial soliton type excitations built from the bosonic spin-density waves (see the definition (2.36) of the vertex

operators). Fermionic impurity orbital  $d^\dagger, d$  is connected with the original spin degree of freedom by the identities

$$S_z = d^\dagger d - \frac{1}{2}, \quad (3.8)$$

$$S^+ = d^\dagger, \quad S^- = d. \quad (3.9)$$

Eq. (3.6) in these notations is simply the resonant level model with the hybridization function

$$\Delta(\epsilon) \stackrel{\text{def}}{=} \pi \sum_k V_k^2 \delta(\epsilon - k). \quad (3.10)$$

This is a well-known model with a lot of results already obtained (Schlottmann 1982).

Summarizing, for positive times models I) and II) are represented by the resonant level model with the hybridization function (3.10). For negative times model I) is described only by the free conduction band part (2.37), because the large magnetic field suppresses all exchange processes between the impurity orbital and the conduction band, leaving in (2.26) only the longitudinal coupling, which is, finally, removed by the unitary transformation  $U$ . In model II) the spin is decoupled from the conduction band for negative times: this leads to a time-dependent potential scattering term (again due to the polaron transformation  $U$ ), according to (2.38). All conditions can be summarized giving for both cases a Hamiltonian of the following structure:

$$H = \sum_k k \Psi_k^\dagger \Psi_k + \begin{cases} \sum_{kk'} g_{kk'} \Psi_k^\dagger \Psi_{k'} (d^\dagger d - 1/2) & , t < 0 \\ \sum_k V_k (\Psi_k^\dagger d + d^\dagger \Psi_k) & , t > 0 \end{cases} \quad (3.11)$$

with the non-zero hybridization function (3.10) for positive times

$$\Delta(\epsilon; t \geq 0) = \Delta = \frac{J_\perp^2}{16\pi a \hbar v_F} = \frac{T_K}{\pi w}. \quad (3.12)$$

Couplings  $J_i$  scales as  $L$  with the system size because of the definition (2.14), thus, one sometimes uses rescaled couplings

$$J' = \frac{J}{L} \quad (3.13)$$

which have dimension of energy. With this redefinition and using the standard expression for the flat band density of states at the Fermi energy

$$\rho_0 = \frac{L}{2\pi \hbar v_F} \quad (3.14)$$

we can re-write (3.12) as

$$\Delta = \frac{\pi(\rho_0 J')^2 \hbar v_F}{4 a} \quad (3.15)$$

and link the Kondo temperature with the transverse coupling  $J_\perp$

$$T_K = \frac{\pi^2 w (\rho_0 J')^2 \hbar v_F}{4 a} \quad (3.16)$$

The last term in the product has dimension of energy and is proportional to the highest energy difference or simply to the band width. Above definition of the Kondo temperature at the Toulouse point is necessary to obtain right dimension constants for connection our results with results of Leggett et al. (1987) and Lesage and Saleur (1998)

Potential-scattering coupling is constant and equals to

$$g_{kk'} = 0 \quad (3.17)$$

for case I) and

$$g_{kk'} = \frac{\sqrt{2} - 1}{\rho_0} \quad (3.18)$$

for case II).

## Correlation functions

Correlation functions, which we are interested in, are magnetization

$$P(t) \stackrel{\text{def}}{=} \langle S_z(t) \rangle = \langle d^\dagger(t) d(t) \rangle - 1/2 \quad (3.19)$$

and spin-spin correlator

$$C(t_w + \tau, t_w) \stackrel{\text{def}}{=} \langle S_z(t_w + \tau) S_z(t_w) \rangle \quad (3.20)$$

where  $\langle \dots \rangle$  means the average with respect to either state I) or II). Last correlation function has real and imaginary parts. Calculation of both parts is of particular interest, since they have different physical meaning. The real part describes equilibrium fluctuations of the spin

$$\begin{aligned} \text{Re } C(t_w + \tau, t_w) = \\ C_{\{S_z, S_z\}}(t_w + \tau, t_w) \stackrel{\text{def}}{=} \frac{1}{2} \langle \{S_z(t_w + \tau), S_z(t_w)\} \rangle, \end{aligned} \quad (3.21)$$

whereas, the imaginary part is proportional to a response function

$$\begin{aligned} \text{Im } C(t_w + \tau, t_w) = \\ C_{[S_z, S_z]}(t_w + \tau, t_w) \stackrel{\text{def}}{=} \frac{1}{2} \langle [S_z(t_w + \tau), S_z(t_w)] \rangle. \end{aligned} \quad (3.22)$$

In equilibrium both parts are connected by the fluctuation-dissipation theorem, which in our situation does not hold (Lobaskin and Kehrein 2005b).

All averages are taken with respect to the initial state, which is equilibrium ground state of the Hamiltonian  $\tilde{H}_{\text{I,II}}(t < 0)$ . The most intriguing in the following study is that such a state is orthogonal with respect to the ground state of the Hamiltonian of the resonant level model in the thermodynamic limit. Moreover, these states have different energies. Therefore, possibility to investigate the problem in the Schrödinger picture is questionable. Our approach suggests simply to avoid this difficulty by translating our problem into the language of the Heisenberg picture. All operators then acquire time dependence leaving wave functions time independent.

## In the Heisenberg picture

In order to evaluate the non-equilibrium spin dynamics we use the quadratic form of  $\tilde{H}_{\text{I,II}}$  (3.11) to solve the Heisenberg equations of motion for  $d(t)$  and  $d^\dagger(t)$ . Diagonalizing Hamiltonians by a unitary transformation

$$A^\dagger \tilde{H}_{\text{I,II}} A \quad (3.23)$$

for positive times we arrive to

$$A^\dagger \tilde{H}_{\text{I,II}}(t > 0) A = \sum_{\varepsilon} \varepsilon a_{\varepsilon}^\dagger a_{\varepsilon}, \quad (3.24)$$

where the constant has been dropped. Dynamics of the operators  $a_{\varepsilon}$  in diagonal basis is trivial

$$a_{\varepsilon}(t) = a_{\varepsilon}(0) e^{-i\varepsilon t} \quad (3.25)$$

and

$$a_{\varepsilon}^\dagger(t) = a_{\varepsilon}^\dagger(0) e^{i\varepsilon t}. \quad (3.26)$$

Only thing we need to do is to connect expectation values of the product of several such operators at time  $t = 0$  with expectation values of the product of original operators  $d$  and  $\Psi_k$ . New operators  $a_{\varepsilon}$  and  $a_{\varepsilon}^\dagger$  are linked with the old ones via

$$a_{\varepsilon} = \sum_{n=k,d} A_{\varepsilon n} a_n = \sum_k A_{\varepsilon k} \Psi_k + A_{\varepsilon d} d. \quad (3.27)$$

and

$$a_\varepsilon^\dagger = \sum_{n=k,d} A_{\varepsilon n}^\dagger a_n^\dagger = \sum_k A_{\varepsilon k}^\dagger \Psi_k^\dagger + A_{\varepsilon d}^\dagger d^\dagger. \quad (3.28)$$

For simplicity we have denoted

$$a_k \stackrel{\text{def}}{=} \Psi_k, \quad a_k^\dagger \stackrel{\text{def}}{=} \Psi_k^\dagger \quad \text{and} \quad a_d \stackrel{\text{def}}{=} d, \quad a_d^\dagger \stackrel{\text{def}}{=} d^\dagger. \quad (3.29)$$

Here and in the following discussion all operators with omitted time dependence assumed to be taken at time  $t = 0$ . Our task is to find matrix elements of the transformation  $A_{\varepsilon n}$  (3.23).

In case I) after this transformation we are left with expectation values which are simply an initial occupation of the impurity level and the unperturbed Fermi-sea. In case II), however, one has to transform the operators  $\Psi_k \equiv a_k$  in (3.27) to new operators  $a_p$  defined as

$$\Psi_k \equiv a_k = \sum_p A_{kp} a_p, \quad (3.30)$$

to make potential-scattering part of the Hamiltonian (3.11) diagonal:

$$\tilde{H}_{\text{II}}(t < 0) = \sum_p p a_p^\dagger a_p + \text{const} . \quad (3.31)$$

Finding coefficients  $A_{kp}$  is very similar task to finding  $A_{\varepsilon n}$ . We do both in the next section.

## 3.1 Diagonalization of the Effective Hamiltonian

### Diagonalization for positive times

Diagonalization of the Hamiltonian (3.6) conceptually follows the review by von Delft and Schoeller (1998). Equations for  $A_{\varepsilon n}$  can be found using equations of motion for fermionic operators  $a_\varepsilon$

$$[H, a_\varepsilon] = -\varepsilon a_\varepsilon. \quad (3.32)$$

and

$$[H, a_\varepsilon^\dagger] = \varepsilon a_\varepsilon^\dagger. \quad (3.33)$$

Substituting (3.27) and (3.28) into these commutators we get

$$\begin{aligned} A_{\varepsilon k} &= \frac{V_k}{\varepsilon - k} A_{\varepsilon d}, \\ \varepsilon A_{\varepsilon d} &= \sum_k V_k A_{\varepsilon k}. \end{aligned} \quad (3.34)$$

This equations together with commutation relations for operators  $a_\varepsilon$

$$\{a_\varepsilon^\dagger, a_{\varepsilon'}\} = \delta_{\varepsilon\varepsilon'} \quad (3.35)$$

or equivalently

$$\sum_n A_{\varepsilon n} A_{n\varepsilon'} = \delta_{\varepsilon\varepsilon'}, \quad (3.36)$$

produce a closed system of equations for coefficients  $A_{n\varepsilon}$ .

For these equations to be consistent condition for the spectrum must be fulfilled

$$\varepsilon = \sum_k \frac{V_k^2}{\varepsilon - k}, \quad (3.37)$$

which one can get by multiplying first equation in (3.34) by  $V_k$ , summing over  $k$ , and substituting the result for the sum  $\sum_k V_k A_{\varepsilon k}$  into the second equation. For a constant hybridization function

$$V_k \equiv V \quad (3.38)$$

and initial spectrum

$$k = \Delta_L \left( n + \frac{1}{2} \right) \quad \text{with } n \in \mathbb{Z}, \quad (3.39)$$

we get

$$\sum_k \frac{1}{\varepsilon - k} = \sum_n \frac{1}{\varepsilon - \Delta_L(n + 1/2)} = -\frac{\pi}{\Delta_L} \tan \left( \frac{\pi\varepsilon}{\Delta_L} \right). \quad (3.40)$$

Second equality follows from the meromorphic expansion of  $\tan(z)$  function.

Writing (3.36) at  $\varepsilon = \varepsilon'$  one gets

$$|A_{\varepsilon d}|^2 + \sum_k |A_{\varepsilon k}|^2 = 1. \quad (3.41)$$

Substituting equations (3.34) and (3.40) into (3.41) we obtain

$$\begin{aligned} |A_{\varepsilon d}|^2 \left( 1 + \sum_k \frac{V^2}{(\varepsilon - k)^2} \right) &= |A_{\varepsilon d}|^2 \left( 1 - V^2 \frac{\partial}{\partial \varepsilon} \sum_k \frac{1}{\varepsilon - k} \right) = \\ &= |A_{\varepsilon d}|^2 \left( 1 + \left( \frac{\pi}{\Delta_L} \right)^2 V^2 \frac{1}{\cos^2 \frac{\pi\varepsilon}{\Delta_L}} \right) = |A_{\varepsilon d}|^2 \left( 1 + \left( \frac{\pi}{\Delta_L} \right)^2 V^2 + \frac{\varepsilon^2}{V^2} \right) \end{aligned} \quad (3.42)$$

Thus, we get for  $A_{\varepsilon d}$  in the thermodynamic limit

$$\boxed{A_{\varepsilon d} = \frac{\Delta_L}{\pi} \left( \frac{\Delta}{\varepsilon^2 + \Delta^2} \right)^{\frac{1}{2}}}, \quad (3.43)$$

with allowed energies

$$\varepsilon_n = \left\{ 0, \Delta_L \left( n + \frac{1}{2} \right) + \Delta_L \frac{\delta_n}{\pi} \right\}, \quad n \in Z. \quad (3.44)$$

One finds the new spectrum after summation over  $k$  in (3.37) getting the transcendental equation

$$\varepsilon = -\Delta \tan \left( \frac{\pi \varepsilon}{\Delta_L} \right). \quad (3.45)$$

Energy shifts  $\delta_n$  follow from (3.45)

$$\tan \delta_n = \frac{\Delta}{\varepsilon_n}. \quad (3.46)$$

## Diagonalization for negative times

In the non-equilibrium situation II), when one needs to diagonalize the Hamiltonian for negative times (3.30), calculation is completely analogous to the above one. In the case of the constant potential-scattering function we can define the scattering phase shift via

$$g_{kk'} \equiv g \stackrel{\text{def}}{=} \frac{\Delta_L}{\pi} \tan \delta. \quad (3.47)$$

From the commutation relations for operators  $a_p$  and  $a_p^\dagger$  with each other

$$\{a_p^\dagger, a_{p'}\} = \delta_{pp'} \quad (3.48)$$

or equivalently

$$\sum_k A_{pk} A_{kp'} = \delta_{pp'}, \quad (3.49)$$

and with the Hamiltonian (3.31)

$$[H, a_p] = -p a_p \quad (3.50)$$

and

$$[H, a_p^\dagger] = p a_p^\dagger \quad (3.51)$$

one obtains

$$A_{pk} = \frac{g \sum_k A_{pk}}{p - k}. \quad (3.52)$$

If we sum both sides of this equation over  $k$  again we get equation for the spectrum

$$\frac{\pi}{\Delta_L} \frac{1}{\tan \delta} = \sum_k \frac{1}{p - k}. \quad (3.53)$$

Using original spectrum (3.39) and scattering phase shift definition (3.47) we get similar to Eq.(3.45)

$$\frac{1}{\tan \delta} = -\tan \left( \frac{\pi p}{\Delta_L} \right). \quad (3.54)$$

From (3.49) one obtains

$$\sum |A_{pk}|^2 = 1. \quad (3.55)$$

Thus,

$$\sum |A_{pk}|^2 = \sum \left| \frac{g \sum_{k'} A_{pk'}}{p-k} \right|^2 = \left| \sum_{k'} A_{pk'} \right|^2 \sum_k \frac{g^2}{(p-k)^2} = 1. \quad (3.56)$$

Using that

$$\begin{aligned} \sum_k \frac{1}{(p-k)^2} &= -\frac{\partial}{\partial p} \sum_k \frac{1}{p-k} = \frac{\pi}{\Delta_L} \frac{1}{\cos^2 \frac{\pi p}{\Delta_L}} = \\ &= \frac{\pi}{\Delta_L} \left( 1 + \tan^2 \frac{\pi p}{\Delta_L} \right) = \left( \frac{\pi}{\Delta_L} \right)^2 \left( 1 + \frac{1}{\tan^2 \delta} \right), \end{aligned} \quad (3.57)$$

one obtains for  $|\sum_k A_{pk}|^2$

$$\left| \sum_k A_{pk} \right|^2 = \frac{1}{g^2 \left( \frac{\pi}{\Delta_L} \right)^2 \left( 1 + \frac{1}{\tan^2 \delta} \right)} = \frac{1}{1 + \tan^2 \delta}. \quad (3.58)$$

Hence, coefficients of transformation (3.30) are given by

$$A_{pk} = \frac{\Delta_L}{\pi} \left( \frac{\tan^2 \delta}{1 + \tan^2 \delta} \right)^{\frac{1}{2}} \frac{1}{p-k}. \quad (3.59)$$

It is clear from (3.53) that new energies  $p$  are indeed shifted by a constant term

$$p_n = \Delta_L \left( n + \frac{1}{2} \right) + \Delta_L \frac{\delta}{\pi}, \quad n \in Z. \quad (3.60)$$

## 3.2 Magnetization

Now we are prepared to calculate desirable non-equilibrium correlation functions. We start with the magnetization of the impurity spin (3.19).  $P(t)$  in the diagonal basis is given by

$$P(t) = \left\langle \sum_{\varepsilon, \varepsilon'} A_{d\varepsilon}^\dagger e^{i\varepsilon t} a_\varepsilon^\dagger A_{d\varepsilon'} e^{-i\varepsilon' t} a_{\varepsilon'} \right\rangle - 1/2. \quad (3.61)$$

Then we reexpress expectation values of the operators  $a_\varepsilon^\dagger, a_\varepsilon$  at  $t = 0$  in terms of expectation values of  $a_n^\dagger, a_n$

$$P(t) = \sum_{\varepsilon, \varepsilon'} |A_{d\varepsilon}|^2 e^{i(\varepsilon - \varepsilon')t} |A_{d\varepsilon'}|^2 \langle d^\dagger d \rangle + \sum_{\varepsilon, \varepsilon', k, k'} A_{d\varepsilon}^\dagger A_{\varepsilon k}^\dagger A_{kp}^\dagger A_{d\varepsilon'} A_{\varepsilon' k'} A_{k' p'} e^{i(\varepsilon - \varepsilon')t} \langle a_p^\dagger a_{p'} \rangle - \frac{1}{2}. \quad (3.62)$$

Result, however, does not depend on the type of the initial preparation. In our case it means that *dynamics of the expectation value of the observable, which state is factorized from the bath, is independent on the initial state of the bath itself.*

One can support this idea by looking at the formula (3.62) for  $P(t)$ . If the initial state is an equilibrium one, meaning  $n_d(0) = \frac{1}{2}$  or equivalently  $\langle S_z \rangle = 0$ , then there should be no spin dynamics at all. That automatically gives relation between the first and the second lines in (3.62): one must be equal minus another for the equilibrium initial occupation number. This allows to calculate, for example, only the first term in (3.62), the simplest one. Direct calculation of the whole expression justifies this reasoning.

Therefore, result for (3.19) can be rewritten as

$$P(t) = (n_d - 1/2) \left| \sum_{\varepsilon} |A_{d\varepsilon}|^2 e^{i\varepsilon t} \right|^2. \quad (3.63)$$

After substitution of  $A_{d\varepsilon}$  from (3.43) in (3.63) one gets

$$P(t) = (n_d - 1/2) \left( \frac{1}{\pi} \int_{-\infty}^{\infty} d\varepsilon e^{i\varepsilon t} \frac{\Delta}{\varepsilon^2 + \Delta^2} \right)^2 = (n_d - 1/2) e^{-2t\Delta} \quad (3.64)$$

Substituting (3.15) one obtains the result of Leggett et al. (1987)

$$P(t) = (n_d - 1/2) e^{-2t/t_B}, \quad (3.65)$$

where

$$t_B \stackrel{\text{def}}{=} \pi w t_K = \pi w / T_K = \frac{1}{\Delta}. \quad (3.66)$$

As we see the final solution is independent on the potential scattering shift  $\delta$ .

### 3.3 Spin-spin Correlation Function

Same algebra might be applied for calculation of  $C(t_w + \tau, t_w)$ . This calculation is lengthy but straightforward. Although no such a simple reasoning as above can be used there, results are still the same for both cases I) and II). Particularly, for the symmetrized (real) part of the correlation function (3.20) one obtains

$$\boxed{C_{\{S_z, S_z\}}(t_w + \tau, t_w) = \frac{1}{4}e^{-2\tau/t_B} - (s(\tau) - s(t_w + \tau)e^{-t_w/t_B} + s(t_w)e^{-(t_w+\tau)/t_B})^2}$$
(3.67)

and for the antisymmetrized (imaginary) part

$$\boxed{C_{[S_z, S_z]}(t_w + \tau, t_w) = -ie^{-\tau/t_B} (s(\tau) - s(t_w + \tau)e^{-t_w/t_B} + s(t_w)e^{-(t_w+\tau)/t_B})}$$
(3.68)

where

$$s(\tau) \stackrel{\text{def}}{=} \frac{t_B}{\pi} \int_0^\infty d\omega \frac{\sin(\omega\tau)}{1 + \omega^2 t_B^2}$$
(3.69)

To derive these equations one rewrites spin-spin correlation function (3.20) on the basis of the effective Hamiltonian (3.11)

$$\begin{aligned} C(t, t') &= \left\langle \left( d^\dagger(t)d(t) - \frac{1}{2} \right) \left( d^\dagger(t')d(t') - \frac{1}{2} \right) \right\rangle \\ &= \langle n_d(t)n_d(t') \rangle - \frac{1}{2}(\langle n_d(t) \rangle + \langle n_d(t') \rangle) + \frac{1}{4} \end{aligned}$$
(3.70)

One has to do with an average product of several  $d, d^\dagger$  operators. Each of them can be transformed according to (3.27) and (3.30) as

$$\begin{aligned} d(t) &= \sum_\varepsilon A_{d\varepsilon} e^{-i\varepsilon t} a_\varepsilon = \\ &= \sum_\varepsilon A_{d\varepsilon} e^{-i\varepsilon t} A_{\varepsilon d} d + \sum_{\varepsilon k} A_{d\varepsilon} e^{-i\varepsilon t} A_{\varepsilon k} A_{kp} a_p \end{aligned}$$
(3.71)

Here all operators in the r.h.s. are taken at time  $t = 0$ . Substitution of (3.71)

into (3.70) gives six non-vanishing quartic

$$\begin{aligned}
\langle n_d(t)n_d(t') \rangle &= \\
&= \sum A_{d\varepsilon}^\dagger A_{d\varepsilon'} A_{d\varepsilon_1}^\dagger A_{d\varepsilon'_1} e^{i(\varepsilon-\varepsilon')t} e^{i(\varepsilon_1-\varepsilon'_1)t'} \times \\
&\left\{ A_{\varepsilon k}^\dagger A_{kp}^\dagger A_{\varepsilon'k'} A_{k'p'} A_{\varepsilon_1 k_1}^\dagger A_{k_1 p_1}^\dagger A_{\varepsilon'_1 k'_1} A_{k'_1 p'_1} \langle a_p^\dagger a_{p'}^\dagger a_{p_1}^\dagger a_{p'_1}^\dagger \rangle + \right. \\
&A_{\varepsilon k}^\dagger A_{kp}^\dagger A_{\varepsilon'k'} A_{k'p'} A_{\varepsilon_1 d}^\dagger A_{\varepsilon'_1 d} \langle a_p^\dagger a_{p'} \rangle n_d + \\
&A_{\varepsilon k}^\dagger A_{kp}^\dagger A_{\varepsilon' d} A_{\varepsilon_1 d}^\dagger A_{\varepsilon'_1 k'_1} A_{k'_1 p'_1} \langle a_p^\dagger a_{p'_1} \rangle (1 - n_d) + \\
&A_{\varepsilon d}^\dagger A_{\varepsilon'k'} A_{k'p'} A_{\varepsilon_1 k_1}^\dagger A_{k_1 p_1}^\dagger A_{\varepsilon'_1 d} \langle a_{p'}^\dagger a_{p'_1} \rangle n_d + \\
&A_{\varepsilon d}^\dagger A_{\varepsilon' d} A_{\varepsilon_1 k_1}^\dagger A_{k_1 p_1}^\dagger A_{\varepsilon'_1 k'_1} A_{k'_1 p'_1} \langle a_{p_1}^\dagger a_{p'_1} \rangle n_d + \\
&\left. A_{\varepsilon d}^\dagger A_{\varepsilon' d} A_{\varepsilon_1 d}^\dagger A_{\varepsilon'_1 d} n_d^2 \right\} \quad (3.72)
\end{aligned}$$

and four quadratic expectation values

$$\begin{aligned}
\langle n_d(t) \rangle + \langle n_d(t') \rangle &= \\
&= \sum \left( e^{i(\varepsilon-\varepsilon')t} + e^{i(\varepsilon-\varepsilon')t'} \right) \times \\
&\left\{ A_{d\varepsilon}^\dagger A_{\varepsilon d}^\dagger A_{d\varepsilon'} A_{\varepsilon' d} n_d + \right. \\
&\left. A_{d\varepsilon}^\dagger A_{\varepsilon k}^\dagger A_{kp}^\dagger A_{d\varepsilon'} A_{\varepsilon'k'} A_{k'p'} \langle a_p^\dagger a_{p'} \rangle \right\}. \quad (3.73)
\end{aligned}$$

We assume summation over all repeating indices. All expectation values now are initial impurity site occupation and unperturbed Fermi sea.

### Evaluation of Eq.(3.71)

Main difficulty is to calculate the sums inside of (3.71), which is the main building block of (3.72) and (3.73). Some of these sums are not regular and cannot be evaluated through integration. Now we consider all important steps of such a calculation in full.

First term in (3.71) is regular and easily integrated giving

$$\sum_{\varepsilon} |A_{d\varepsilon}|^2 e^{i\varepsilon t} = \frac{1}{\pi} \int_{-\infty}^{\infty} d\varepsilon e^{i\varepsilon t} \frac{\Delta}{\varepsilon^2 + \Delta^2} = e^{-t\Delta}. \quad (3.74)$$

Second one is non-regular and all summations must be done explicitly. Omitting all irrelevant constants in front of the sum one gets using (3.34), (3.43) and (3.59)

$$\sum_{\varepsilon k} A_{d\varepsilon} e^{-i\varepsilon t} A_{\varepsilon k} A_{kp} \sim \sum_{\varepsilon k} \frac{e^{-i\varepsilon t}}{(\varepsilon^2 + \Delta^2)(\varepsilon - k)(p - k)}. \quad (3.75)$$

Sum over  $k$  might be evaluated with the help of the spectrum conditions (3.37) and (3.53)

$$\begin{aligned} \sum_k \frac{1}{(\varepsilon - k)(p - k)} &= \frac{1}{\varepsilon - p} \left[ \sum_k \frac{1}{p - k} - \sum_k \frac{1}{\varepsilon - k} \right] \\ &= \frac{\pi}{\Delta_L} \frac{1}{\varepsilon - p} \left[ \frac{1}{\tan \delta} - \frac{\varepsilon}{\Delta} \right]. \end{aligned} \quad (3.76)$$

Resulting summation over  $\varepsilon$  is then given by

$$\begin{aligned} \sum_\varepsilon \frac{e^{-i\varepsilon t}(\Delta - \varepsilon \tan \delta)}{(\varepsilon^2 + \Delta^2)(\varepsilon - p)} &= \frac{\Delta - p \tan \delta}{p^2 + \Delta^2} e^{-ipt} \sum_\varepsilon \frac{e^{-i(\varepsilon - p)t}}{\varepsilon - p} - \\ &\frac{\Delta - p \tan \delta}{p^2 + \Delta^2} \sum_\varepsilon \frac{e^{-i\varepsilon t}(\varepsilon + p)}{\varepsilon^2 + \Delta^2} - \sum_\varepsilon \frac{e^{-i\varepsilon t} \tan \delta}{\varepsilon^2 + \Delta^2}. \end{aligned} \quad (3.77)$$

The second term is regular

$$\sum_\varepsilon \frac{e^{-i\varepsilon t}(\varepsilon + p)}{\varepsilon^2 + \Delta^2} = \frac{\pi}{\Delta_L} \frac{p + i\Delta}{\Delta} e^{-\Delta t} \quad (3.78)$$

and the third one is the same to (3.74).

However, the first term has a non-regular real part. Indeed, we can write the sum in it as

$$\sum_\varepsilon \frac{e^{-i(\varepsilon - p)t}}{\varepsilon - p} = \sum_\varepsilon \frac{\cos(\varepsilon - p)t}{\varepsilon - p} - i \sum_\varepsilon \frac{\sin(\varepsilon - p)t}{\varepsilon - p}. \quad (3.79)$$

Imaginary part is regular

$$\sum_\varepsilon \frac{\sin(\varepsilon - p)t}{\varepsilon - p} = \frac{1}{\Delta_L} \int_{-\infty}^{\infty} dx \frac{\sin xt}{x} = \frac{\pi}{\Delta_L}, \quad (3.80)$$

but the real part is divergent at  $\varepsilon = p$ . Thus we cannot simply interchange the sum by the integral and have to sum up all terms explicitly taking the spectrum discretization into account. The real part of (3.79) obeys several equalities in the thermodynamic limit. First equality we need is

$$\sum_\varepsilon \frac{\cos(\varepsilon - p)t}{\varepsilon - p} = \sum_\varepsilon \frac{1}{\varepsilon - p}. \quad (3.81)$$

It is always valid while we take the thermodynamic limit before the limit  $t \rightarrow \infty$ . The second relation is less trivial

$$\sum_\varepsilon \frac{1}{\varepsilon - p} = \frac{\pi}{\Delta_L} \frac{p + \Delta \tan \delta}{\Delta - p \tan \delta}. \quad (3.82)$$

To prove it one should note that

$$\frac{p + \Delta \tan \delta}{\Delta - p \tan \delta} \equiv \frac{1}{\tan(\delta_p - \delta)} \equiv \sum_n \frac{1}{\pi(n - n_p) + \delta_p - \delta}, \quad (3.83)$$

where  $p = \Delta_L(n_p + 1/2) + \delta$ ,  $\delta_p = \arctan \frac{\Delta}{p}$ . Subtracting obtained sum from the l.h.s. of (3.82) and using (3.44)-(3.46), one can show that this difference vanishes in the thermodynamic limit, which finishes the proof of (3.82). One can find a detailed discussion of all steps of this proof in Appendix. Gathering all constants we find for (3.75)

$$\sum_{\varepsilon k} A_{d\varepsilon} A_{\varepsilon k} A_{kp} e^{-i\varepsilon t} = \left( \frac{\Delta_L}{\pi} \right)^{\frac{1}{2}} \frac{\Delta^{\frac{1}{2}}}{(1 + \tan^2 \delta)^{\frac{1}{2}}} \frac{(p + \Delta \tan \delta) - i(\Delta - p \tan \delta)}{p^2 + \Delta^2} [e^{-ipt} - e^{-\Delta t}] \quad (3.84)$$

Finally, only summation over  $p$  is left, all expressions are no longer singular and can be integrated exactly.

### Checking result (3.65) for magnetization

Let us check the result for the magnetization (3.65) using obtained identity (3.84). First term in (3.62) is already calculated. For the second term one gets

$$\begin{aligned} \sum_{\varepsilon, \varepsilon', k, k'} A_{d\varepsilon}^\dagger A_{\varepsilon k}^\dagger A_{kp}^\dagger A_{d\varepsilon'} A_{\varepsilon' k'} A_{k' p'} e^{i(\varepsilon - \varepsilon')t} n(p) \delta_{pp'} &= \\ &= \frac{\Delta}{\pi} \int_0^\infty dp \frac{(e^{ipt} - e^{-\Delta t})(e^{-ipt} - e^{-\Delta t})}{p^2 + \Delta^2} = \end{aligned} \quad (3.85)$$

$$= \frac{1}{2} (1 - e^{-2\Delta t}) \quad (3.86)$$

which justified the previous result.

### Complete calculation of Eqs.(3.72) and (3.73)

First term in (3.72) can be divided into two parts after averaging of four operators  $a_p, a_p^\dagger$

$$\begin{aligned} \sum A_{d\varepsilon}^\dagger A_{\varepsilon k}^\dagger A_{kp}^\dagger e^{i\varepsilon t} \times A_{d\varepsilon'} A_{\varepsilon' k'} A_{k' p'} e^{-i\varepsilon' t} \times \\ A_{d\varepsilon_1}^\dagger A_{\varepsilon_1 k_1}^\dagger A_{k_1 p_1}^\dagger e^{i\varepsilon_1 t'} \times A_{d\varepsilon'_1} A_{\varepsilon'_1 k'_1} A_{k'_1 p'_1} e^{-i\varepsilon'_1 t'} \times \delta_{pp'} \delta_{p_1 p'_1} n(p) n(p_1) \end{aligned} \quad (3.87)$$

and

$$\begin{aligned} & \sum A_{d\varepsilon}^\dagger A_{\varepsilon k}^\dagger A_{kp}^\dagger e^{i\varepsilon t} \times A_{d\varepsilon'} A_{\varepsilon' k'} A_{k' p'} e^{-i\varepsilon' t} \times \\ & A_{d\varepsilon_1}^\dagger A_{\varepsilon_1 k_1}^\dagger A_{k_1 p_1}^\dagger e^{i\varepsilon_1 t'} \times A_{d\varepsilon'_1} A_{\varepsilon'_1 k'_1} A_{k'_1 p'_1} e^{-i\varepsilon'_1 t'} \times \delta_{pp'_1} \delta_{p_1 p'_1} n(p) n(-p_1) \end{aligned} \quad (3.88)$$

with  $n(p)$  unperturbed Fermi sea distribution. Substituting (3.84) we get for the first part

$$\begin{aligned} \sum \dots &= \\ &= \left(\frac{\Delta}{\pi}\right)^2 \int_0^\infty dp \frac{(e^{ipt} - e^{-\Delta t})(e^{-ipt} - e^{-\Delta t})}{p^2 + \Delta^2} \times \\ &\times \int_0^\infty dp_1 \frac{(e^{ip_1 t'} - e^{-\Delta t'})(e^{-ip_1 t'} - e^{-\Delta t'})}{p_1^2 + \Delta^2} = \\ &= \frac{1}{4} (1 - e^{-2\Delta t}) (1 - e^{-2\Delta t'}). \end{aligned} \quad (3.89)$$

The second part is less trivial and contains both real and imaginary contributions

$$\begin{aligned} \sum \dots &= \\ &= \left(\frac{\Delta}{\pi}\right)^2 \int_0^\infty dp \frac{(e^{-ipt} - e^{-\Delta t})(e^{ipt'} - e^{-\Delta t})}{p^2 + \Delta^2} \times \\ &\times \int_0^\infty dp_1 \frac{(e^{-ip_1 t'} - e^{-\Delta t'})(e^{ip_1 t'} - e^{-\Delta t'})}{p_1^2 + \Delta^2} = \\ &= \left(\frac{\Delta}{\pi}\right)^2 \left[ \int_0^\infty dp \frac{(e^{-ipt} - e^{-\Delta t})(e^{ipt'} - e^{-\Delta t})}{p^2 + \Delta^2} \right]^2 = \\ &= \text{Re} \sum \dots + \text{Im} \sum \dots \end{aligned} \quad (3.90)$$

Writing  $e^{ipt}$  in the trigonometric form we get integrals of two kinds

$$\int_0^\infty d\omega \frac{\cos(\omega\tau)}{\Delta^2 + \omega^2} \quad \text{and} \quad \int_0^\infty d\omega \frac{\sin(\omega\tau)}{\Delta^2 + \omega^2} \quad . \quad (3.91)$$

We denote the second one according to (3.69) and then get for the real part

$$\begin{aligned} \text{Re} \sum \dots &= \frac{1}{4} \left[ e^{-\Delta|t-t'|} - e^{\Delta(t+t')} \right]^2 - \\ &- \left[ s(t-t') - s(t)e^{-\Delta t'} + s(t')e^{-\Delta t} \right]^2, \end{aligned} \quad (3.92)$$

and for the imaginary part

$$\begin{aligned} \text{Im} \sum \dots &= \left[ e^{-\Delta|t-t'|} - e^{\Delta(t+t')} \right] \times \\ &\times \left[ s(t-t') - s(t)e^{-\Delta t'} + s(t')e^{-\Delta t} \right]^2. \end{aligned} \quad (3.93)$$

Expression for the second term in (3.72) is given by

$$\begin{aligned} & \sum A_{d\varepsilon}^\dagger A_{\varepsilon k}^\dagger A_{kp}^\dagger e^{i\varepsilon t} \times A_{d\varepsilon'} A_{\varepsilon' k'} A_{k' p'} e^{-i\varepsilon' t} \times \\ & \times A_{d\varepsilon_1}^\dagger A_{\varepsilon_1 d}^\dagger e^{i\varepsilon_1 t'} \times A_{d\varepsilon'_1} A_{\varepsilon'_1 d} e^{-i\varepsilon'_1 t'} \times \delta_{pp'} n(p) n_d, \end{aligned} \quad (3.94)$$

using (3.74) and (3.84) one obtains

$$\begin{aligned} \sum \dots &= \\ &= \frac{\Delta}{\pi} n_d e^{-2\Delta t'} \int_0^\infty dp \frac{(e^{ipt} - e^{-\Delta t}) (e^{-ipt} - e^{-\Delta t})}{p^2 + \Delta^2} = \\ &= \frac{n_d}{2} e^{-2\Delta t'} (1 - e^{-2\Delta t}). \end{aligned} \quad (3.95)$$

For the third term one gets

$$\begin{aligned} & \sum A_{d\varepsilon}^\dagger A_{\varepsilon k}^\dagger A_{kp}^\dagger e^{i\varepsilon t} \times A_{d\varepsilon'} A_{\varepsilon' d} e^{-i\varepsilon' t} \times \\ & \times A_{d\varepsilon_1}^\dagger A_{\varepsilon_1 d}^\dagger e^{i\varepsilon_1 t'} \times A_{d\varepsilon'_1} A_{\varepsilon'_1 k'_1} A_{k'_1 p'_1} e^{-i\varepsilon'_1 t'} \times \delta_{pp'_1} n(p) (1 - n_d). \end{aligned} \quad (3.96)$$

Inserting (3.74) and (3.84) we find

$$\begin{aligned} \sum \dots &= \\ &= \frac{\Delta}{\pi} (1 - n_d) e^{-\Delta(t+t')} \int_0^\infty dp \frac{(e^{-ipt} - e^{-\Delta t}) (e^{ipt'} - e^{-\Delta t'})}{p^2 + \Delta^2} = \\ &= \frac{\Delta}{\pi} (1 - n_d) e^{-\Delta(t+t')} \int_0^\infty dp \frac{e^{-ip(t-t')} - e^{-ipt} e^{-\Delta t'} - e^{ipt'} e^{-\Delta t} + e^{-\Delta(t+t')}}{p^2 + \Delta^2} = \\ &= \text{Re} \sum \dots + \text{Im} \sum \dots \quad . \end{aligned} \quad (3.97)$$

Result for the real part

$$\text{Re} \sum \dots = \frac{1 - n_d}{2} e^{-\Delta(t+t')} \left( e^{-\Delta|t-t'|} - e^{-\Delta(t+t')} \right) \quad (3.98)$$

and for the imaginary part

$$\text{Im} \sum \dots = -(1 - n_d) e^{-\Delta(t+t')} \left[ s(t - t') - s(t) e^{-\Delta t'} + s(t') e^{-\Delta t} \right]. \quad (3.99)$$

For the fourth term one gets

$$\begin{aligned} & \sum A_{d\varepsilon}^\dagger A_{\varepsilon d}^\dagger e^{i\varepsilon t} \times A_{d\varepsilon'} A_{\varepsilon' k'} A_{k' p'} e^{-i\varepsilon' t} \times \\ & \times A_{d\varepsilon_1}^\dagger A_{\varepsilon_1 k_1}^\dagger A_{k_1 p_1}^\dagger e^{i\varepsilon_1 t'} \times A_{d\varepsilon'_1} A_{\varepsilon'_1 d} e^{-i\varepsilon'_1 t'} \times \delta_{p_1 p'_1} n_d n(-p_1). \end{aligned} \quad (3.100)$$

Using (3.74) and (3.84) we find

$$\begin{aligned}
\sum \dots &= \\
&= \frac{\Delta}{\pi} n_d e^{-\Delta(t+t')} \int_0^\infty dp_1 \frac{(e^{-ip_1 t} - e^{-\Delta t})(e^{ip_1 t'} - e^{-\Delta t'})}{p_1^2 + \Delta^2} = \\
&= \frac{\Delta}{\pi} n_d e^{-\Delta(t+t')} \int_0^\infty dp_1 \frac{e^{-ip_1(t-t')} - e^{-ip_1 t} e^{-\Delta t'} - e^{ip_1 t'} e^{-\Delta t} + e^{-\Delta(t+t')}}{p_1^2 + \Delta^2} = \\
&= \text{Re} \sum \dots + \text{Im} \sum \dots \quad , \tag{3.101}
\end{aligned}$$

where

$$\text{Re} \sum \dots = \frac{n_d}{2} e^{-\Delta(t+t')} \left( e^{-\Delta|t-t'|} - e^{-\Delta(t+t')} \right) \tag{3.102}$$

and

$$\text{Im} \sum \dots = -n_d e^{-\Delta(t+t')} \left[ s(t-t') - s(t) e^{-\Delta t'} + s(t') e^{-\Delta t} \right]. \tag{3.103}$$

For the fifth term one gets

$$\begin{aligned}
&\sum A_{d\varepsilon}^\dagger A_{\varepsilon d}^\dagger e^{i\varepsilon t} \times A_{d\varepsilon'} A_{\varepsilon' d} e^{-i\varepsilon' t} \times \\
&\quad \times A_{d\varepsilon_1}^\dagger A_{\varepsilon_1 k_1}^\dagger A_{k_1 p_1}^\dagger e^{i\varepsilon_1 t'} \times A_{d\varepsilon'_1} A_{\varepsilon'_1 k'_1} A_{k'_1 p'_1} e^{-i\varepsilon'_1 t'} \times \delta_{p_1 p'_1} n_d n(p_1). \tag{3.104}
\end{aligned}$$

Using (3.74) and (3.84) one arrives at

$$\begin{aligned}
\sum \dots &= \\
&= \frac{\Delta}{\pi} n_d e^{-2\Delta t} \int_0^\infty dp \frac{(e^{ipt'} - e^{-\Delta t'})(e^{-ipt'} - e^{-\Delta t'})}{p^2 + \Delta^2} = \\
&= \frac{n_d}{2} e^{-2\Delta t} \left( 1 - e^{-2\Delta t'} \right), \tag{3.105}
\end{aligned}$$

which is purely real and symmetric to the second term if we change  $t$  and  $t'$ .

Finally, sixth term is equal to

$$\sum A_{d\varepsilon}^\dagger A_{\varepsilon d}^\dagger e^{i\varepsilon t} \times A_{d\varepsilon'} A_{\varepsilon' d} e^{-i\varepsilon' t} \times A_{d\varepsilon_1}^\dagger A_{\varepsilon_1 d}^\dagger e^{i\varepsilon_1 t'} \times A_{d\varepsilon'_1} A_{\varepsilon'_1 d} e^{-i\varepsilon'_1 t} \times n_d^2. \tag{3.106}$$

Only Eq.(3.74) is needed and one obtains

$$\sum \dots = n_d^2 e^{-2\Delta(t+t')}. \tag{3.107}$$

For  $\langle n_d(t) \rangle$  in (3.73) we can use result for the magnetization (3.65)

$$\langle n_d(t) \rangle = \frac{1}{2} + \left( n_d - \frac{1}{2} \right) e^{-2\frac{t}{t_B}}. \tag{3.108}$$

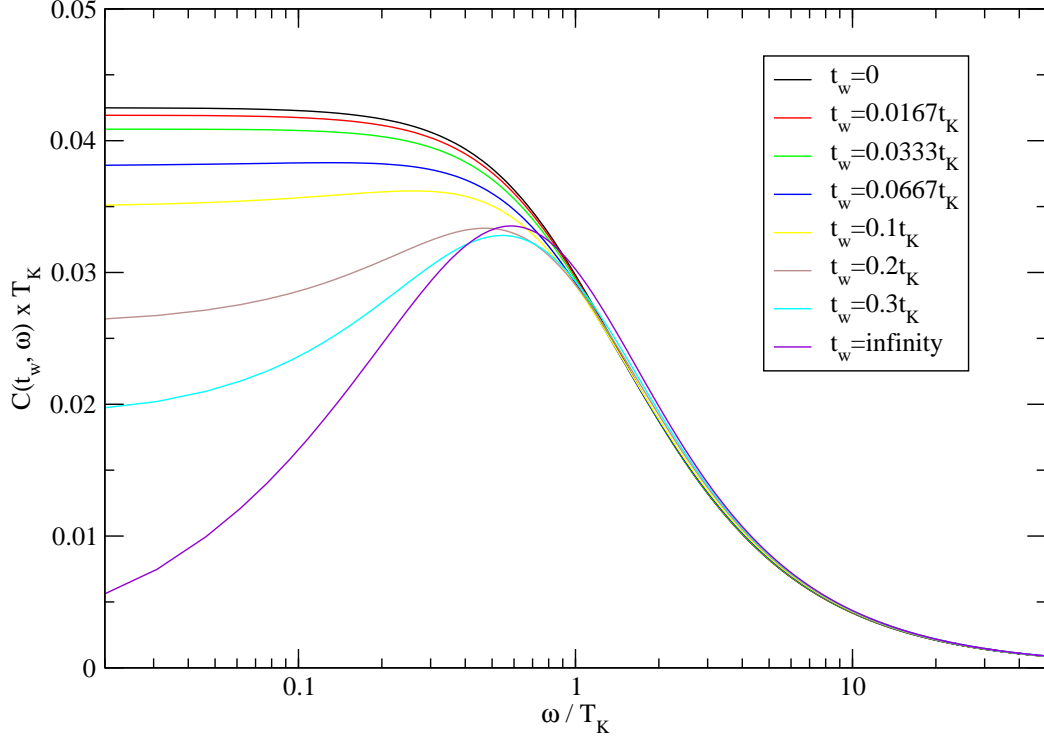


**Figure 3.1:** Universal curves for the symmetrized correlation function  $C(t_w, \omega)$  at the Toulouse point for various waiting times.

Collecting all real contributions we get

$$\text{Re } C(t, t') = C_{\{S_z, S_z\}}(t, t') = \frac{1}{4} e^{-2\Delta|t-t'|} - \left( s(t-t') - s(t)e^{-\Delta t'} + s(t')e^{-\Delta t} \right)^2. \quad (3.109)$$

For the imaginary part we obtain

$$\text{Im } C(t, t') = C_{[S_z, S_z]}(t, t') = -i e^{-\Delta|t-t'|} \left( s(t-t') - s(t)e^{-\Delta t'} + s(t')e^{-\Delta t} \right). \quad (3.110)$$

Using new notations

$$t_w = t' \quad , \quad \tau = t - t_w \quad \text{and} \quad t_B = \frac{1}{\Delta} \quad (3.111)$$

we come to (3.67) and (3.68).

The normalized curves (e.g. multiplied by  $T_K$ ) for the symmetrized correlator are presented in Fig.3.1.

We introduce here a one-sided Fourier transform of the spin-spin correlation function with respect to the time difference  $\tau$ . Algebraic  $\propto 1/\tau^2$  long-time behavior of  $C_{\text{eq}}(\tau)$  gives  $\propto |\omega|$  behavior at small frequencies. Here it is indicated by the non zero first derivative at the origin immediately after the switching on the Kondo coupling.

### 3.4 Conclusion

We have calculated the magnetization of the impurity spin defined as the average of the spin operator with respect to the non-equilibrium initial states I) or II). Result of Leggett et al. (1987) was obtained. Although the result is already known the method we used is useful for calculation of other correlation functions at the Toulouse point as well as away from it in the Kondo limit.

Developed approach have been used for evaluation of the spin-spin correlation function defined as an average of spin measurements at two different times with respect to either I) or II) initial states. In equilibrium, it is known that this quantity should decay algebraically at large times. However, if one of the measurements happens at zero time then this function is identical to the magnetization and should vanish exponentially. To resolve this puzzle we have used the bosonization and the refermionization approach to derive spin-spin correlation function at the exactly solvable Toulouse point. Final expressions are given for the symmetrized (real) part of the spin-spin correlator by Eq.(3.67) and for the antisymmetrized (imaginary) part by Eq.(3.68) One may see exponential approach to the equilibrium algebraic long time decay with waiting time  $t_w$  going to infinity. This is purely Fermi liquid property which cannot be obtained, for example, by the non-crossing approximation (Nordlander et al. 1999), which does not work at the zero temperature limit. It is the *first analytic result* regarding this exponential to algebraic non-equilibrium crossover.

The question is whether this result preserves in the physical Kondo limit as well. The answer is "yes" with a proof given in the next chapter.

## 4. NON-EQUILIBRIUM KONDO MODEL IN THE KONDO LIMIT

Study of the non-equilibrium Kondo effect has a long history. First experimental and theoretical works were made in 1960s when the tunneling between two metals through insulating barriers was investigated as a function of applied bias voltage (Appelbaum and Shen 1972, Wallis and Wyatt 1974, Wolf and Losee 1970, Shen and Rowell 1968, Nielsen 1970, Bermon, Paraskevopoulos and Tedrow 1978). Further progress came during study of the Kondo effect in quantum nanodevices since in experiment one can continuously control various parameters of the system such as applied bias and gate voltages, strength of the coupling of a charged region with leads, applied (generally, time-dependent) external fields. It has been observed that applied bias voltage  $V$  quenches the Kondo effect when it becomes larger than the Kondo temperature  $V \gg T_K$ , and that the applied magnetic field splits the zero-bias conductance into two distinct peaks with a distance of Zeeman splitting of the dot spin between them (Goldhaber-Gordon, Shtrikman, Mahalu, Abusch-Magder, Meirav and Kastner 1998, Cronenwett, Oosterkamp and Kouwenhoven 1998, Schmid, Weis, Eberl and von Klitzing 1998, Nygard, Cobden and Lindelhof 2000, van der Wiel, Franceschi, Fujisawa, Elzerman, Tarucha and Kouwenhoven 2000, Goldhaber-Gordon, Göres, Kastner, Shtrikman, Mahalu and Meirav 1998). Such a splitting by a dc bias voltage was observed in experiment by Francheshi et al (van der Wiel et al. 2000). Another type of non-equilibrium can be studied measuring response to time-dependent external fields induced, for example, microwave radiation with a frequency  $\omega$  (Goldin and Avishai 1998, Lopez, Aguado, Platero and Tejedor 1998, Ng 1996, Hettler and Schoeller 1995, Kaminski, Nazarov and Glazman 2000, Kaminski, Nazarov and Glazman 1999, Goldin and Avishai 2000). This experiment was recently done by Kogan et al. (2004), where they have observed satellites of the Kondo effect separated by the frequency  $\omega$ .

### Known theoretical approaches

A number of theoretical methods were generalized to be applied to study the non-equilibrium Kondo effect: perturbation theory (Appelbaum 1966, Appelbaum 1967, Solyom and Zawadowski 1968a, Appelbaum, Phillips and

Tzouras 1967, Kaminski et al. 1999, Kaminski et al. 2000, Solyom and Zawadowski 1968b, Sivan and Wingreen 1996, Herschfield, Davies and Wilkins 1991, Fujii and Ueda 2003, Oguri 2002, Rosch, Paaske, Kroha and Wölfle 2003, Paaske, Rosch and Wölfle 2004, Paaske, Rosch, Kroha and Wölfle 2004, Parcolett and Hooley 2002), equations of motions and self-consistent diagrammatic methods (non-crossing approximation) (Ng 1996, Wingreen and Meir 1994, Hettler, Kroha and Herschfield 1994, Hettler, Kroha and Herschfield 1998, König, Schmidt, Schoeller and Schön 1996, Schiller and Herschfield 2000, Rosch, Kroha and Wölfle 2001, Krawiec and Wysokinski 2002, Meir, Wingreen and Lee 1993, Nordlander et al. 1999, Nordlander et al. 2000, Plihal et al. 2000), slave-boson mean-field theories (Aguado and Langreth 2000, Han 2003, Coleman, Hooley, Avishai, Goldin and Ho 2002), approximations of the scattering states starting from Bethe ansatz solution (Konik, Saleur and Ludwig 2002, Konik, Saleur and Ludwig 2001), form-factor approach (Lesage and Saleur 1998), perturbative renormalization group (Kaminski et al. 1999, Kaminski et al. 2000, Rosch, Paaske, Kroha and Wölfle 2003, Rosch, Costi, Paaske and Wölfle 2003), numerical renormalization group (Costi 1997), exact solutions for specific values of coupling constants (Schiller and Herschfield 1995, Schiller and Herschfield 1998, Lee and Lee 2002, Majumdar et al. 1998). Main difficulty encountered is that even in the simplest case of non-equilibrium steady-state, such a state of the system is a highly excited many-body state. Consequently, all methods used for calculations of the equilibrium properties cannot be directly applied. In addition to that, the equilibrium Kondo effect is a highly non-trivial strong-coupling problem and most of the methods mentioned are already approximate at this point, therefore, their generalization out of equilibrium might demand further approximations.

## 4.1 Flow Equation Approach

In 1994 Wegner suggested a new non-perturbative version of the renormalization group which he called flow-equation approach (Wegner 1994). Main idea was to deal with strong-coupling Hamiltonians converting them by the infinitesimal unitary transformations to the diagonal form. Special choice of the generator of the transformation allows to eliminate high energy *differences* preserving all energy scales of the Hamiltonian, in contrast with the ordinary renormalization group approach which gradually cut the spectrum during the flow. That distinguishable feature allows to use it in many strong-coupling problems where the traditional renormalization group study fails. Flow-equation method was successfully applied to obtain correlation functions of the spin-boson model (Kehrein and Mielke 1997), sine-gordon model (Kehrein 2001), Anderson impurity model (Kehrein and Mielke 1996) etc. Successful implementation of the flow-equation method to the equilibrium Kondo problem (Hofstetter and Kehrein 2001) sug-

gested to use the same approach for out of equilibrium Kondo problem as well.

There are two main advantages of the flow–equation scheme in comparison with the other approaches: the possibility to investigate the full range of coupling values including the strong–coupling regime; straightforward extension to time–dependent models, since the transformed Hamiltonian is diagonal and gives trivial equations of motions for observables in Heisenberg picture.

The Toulouse point exhibits many universal features of the strong–coupling phase of the Kondo model like local Fermi liquid properties, however, other universal properties like the Wilson ratio depend explicitly on the coupling  $J_{\parallel}$ . This raises the question which of the above non–equilibrium to equilibrium crossover properties are generic in the strong–coupling phase. We investigate this question by using the flow equation method that allows us to extend our analysis away from the Toulouse point in a controlled expansion. In this part of the work we focus on the experimentally most relevant limit of small Kondo couplings. The flow equation approach is not restricted to this limit and can be used for general  $J_{\parallel}$  (Lobaskin and Kehrein 2005c), hence, connecting the Kondo regime continuously with the results at the exactly solvable Toulouse point.

Let us discuss most important details of this method. The main goal is to construct a one–parameter family of unitarily equivalent Hamiltonians  $H(B)$

$$H(B) = U(B)HU^{\dagger}(B) \quad (4.1)$$

where  $H(0)$  is the initial Hamiltonian and  $H(B = \infty)$  is the final diagonal Hamiltonian.  $U(B)$  is a unitary operator. Above unitary transformation can be equivalently formulated by setting up the flow in differential form

$$\frac{dH(B)}{dB} = [\nu(B), H(B)] \quad (4.2)$$

with the anti-Hermitian generator  $\nu(B) = -\nu^{\dagger}(B)$ . This generator  $\nu(B)$  is connected with the unitary operator  $U(B)$  by the identities

$$\nu(B) = \frac{dU(B)}{dB}U^{-1}(B) \quad (4.3)$$

or equivalently

$$\begin{aligned} U(B) &= T_B \exp \int_0^{\infty} dB' \nu(B') = \\ &= 1 + \sum_{n=1}^{\infty} \frac{1}{n!} \int_0^B dB_1 \dots dB_n T_B \{\nu(B_1) \dots \nu(B_n)\}. \end{aligned} \quad (4.4)$$

Here  $T_B$  denotes  $B$ –ordering, that is the generator  $\nu(B_i)$  with largest  $B_i$  is commuted to the left, similar to the usual time–ordering.

From the differential formulation (4.2) is clear that when  $B$  has the meaning of  $|\Delta E|^{-2}$ , where  $\Delta E$  denotes the energy difference, then  $\nu(B)$  is constructed in the way to eliminate interaction matrix elements with an energy difference  $\Delta E \propto B^{-1/2}$ . Transformed Hamiltonian  $H(B)$  at this stage contains only matrix elements which couple energy differences less than  $B^{-1/2}$ . Thus, our Hamiltonian become more and more diagonal during the flow.

Of course, the main task is to find appropriate flow generator  $\nu(B)$  which possesses above properties. Wegner chooses the generator as the commutator of the diagonal part of the Hamiltonian  $H_0$  with the interaction part  $H_{\text{int}}$  (Wegner 1994)

$$\nu(B) = [H_0(B), H_{\text{int}}(B)] \quad (4.5)$$

where

$$H(B) = H_0(B) + H_{\text{int}}(B) . \quad (4.6)$$

With this choice the flow parameter  $B$  has the dimension of  $[Energy]^{-2}$  and one can even get the following relation

$$\frac{d}{dB} \text{Tr} H_{\text{int}}^2(B) \leq 0 . \quad (4.7)$$

According to this inequality the off-diagonal part of the Hamiltonian  $H(B)$  becomes smaller during the flow. However, the energy spectrum for a typical many-body Hamiltonian is unbounded and this statement cannot be made rigorous. But the reasonable choice of the generator  $\nu(B)$  makes this inequality to be true.

The evaluation of any correlation functions in this approach is performed very differently from the other many-body technics as well. The final Hamiltonian is diagonal and the equations of motions for any observable are very simple, but, unfortunately, initial observables also change during the flow

$$\frac{dO(B)}{dB} = [\nu(B), O(B)] \quad (4.8)$$

with  $O(B=0) = O$ . Thus, although the Hamiltonian becomes simpler during the flow, observables typically take on a more complicated structure due to the above transformation.

A ground state correlation function of any two operators  $O_1$  and  $O_2$  can be calculated in the final diagonal basis according to

$$\begin{aligned} C(t, t') &\stackrel{\text{def}}{=} \langle GS | O_1(t) O_2(t') | GS \rangle = \\ &= \langle GS | e^{iHt} O_1 e^{-iHt} e^{iHt'} O_2 e^{-iHt'} | GS \rangle = \\ &= \langle \widetilde{GS} | e^{iH(B=\infty)t} O_1(B=\infty) e^{-iH(B=\infty)t} \times \\ &\quad \times e^{iH(B=\infty)t'} O_2(B=\infty) e^{-iH(B=\infty)t'} | \widetilde{GS} \rangle \end{aligned} \quad (4.9)$$

Here  $|GS\rangle$  stands for the ground state of the initial basis and  $|\widetilde{GS}\rangle = U(B=\infty)|GS\rangle$  the ground state in the diagonal basis.

## 4.2 Effective Hamiltonian

In the following we implement the flow equation approach described above to the non-equilibrium Kondo model out of the Toulouse point. Physically the most relevant limit is the isotropic and small exchange couplings  $J_\perp$  and  $J_\parallel$ .

Since under the flow the Hamiltonian is transformed into its diagonal basis, we can follow the same steps as in the Toulouse point analysis:

- Write the Heisenberg equations of motion for the unitarily transformed observables and solve them with respect to the diagonal Hamiltonian.
- Re-expresses the time-evolved operators through the operators in the initial (non-diagonal) basis for time  $t = 0$ .
- Evaluate the correlation functions (3.20) for general  $t_w$ .

The general procedure for this calculation is developed by Hofstetter and Kehrein (2001). The Kondo Hamiltonian (2.33) is rewritten in more general form

$$H(B) = H_0 + \sum_p g_p(B) (V_p^\dagger(\lambda(B))S^- + V_p(\lambda(B))S^+) + \sum_p \omega_p(B) [V_p^\dagger(\lambda(B_p)), V_p(\lambda(B_p))] . \quad (4.10)$$

Here we introduce spatial dependence in vertex operators  $V(\lambda(B), x)$  (2.36) and in coupling constants  $g(B, x)$  and  $\omega(B, x)$  and take their Fourier transform. Last term with coupling  $\omega_p(B)$  is the potential scattering term. It is generated during the flow and initially equals to zero. Constants  $g(B, x)$  and  $\omega(B, x)$  are flow dependent with initial values  $g(B = 0, x) = g_0$  and  $\omega(B = 0, x) = 0$ . We also use notation  $B_p \stackrel{\text{def}}{=} p^{-2}$ .

One uses generator (4.5) to derive the following flow equations for the parameters in (4.10)

$$\frac{dg_p}{dB} = -p^2 g_p + \frac{2\pi}{\Gamma(\lambda^2)} \sum_{q \neq p} \frac{p+q}{p-q} g_p g_q^2 |qa|^{\lambda^2-1} + \frac{1}{4} g_p \ln(B/a^2) \frac{d\lambda^2}{dB} , \quad (4.11)$$

$$\frac{d\omega_q}{dB} = \frac{2\pi}{\Gamma(\lambda^2)} q g_q^2 |qa|^{\lambda^2-1} \quad (4.12)$$

and a differential equation for the flow of the scaling dimension

$$\frac{d\lambda^2}{dB} = \frac{8\pi\lambda^2(1-\lambda^2)}{\Gamma(\lambda^2)} \sum_q g_q g_{-q} |qa|^{\lambda^2-1} . \quad (4.13)$$

The above procedure can be used quite generally to apply the flow equation method to time-dependent Hamiltonians of the above kind. However, for the Kondo model, one can simplify the calculation by using the results obtained by Slezak, Kehrein, Pruschke and Jarrell (2003). In this work it was shown that the resonant level model (3.6)

$$H_{\text{RLM}} = \sum_k \epsilon_k c_k^\dagger c_k + \epsilon_d d^\dagger d + \sum_k V_k (c_k^\dagger d + d^\dagger c_k) \quad (4.14)$$

with a universal non-trivial hybridization function  $\Delta_{\text{eff}}(\epsilon) \neq \text{const}$

$$\Delta_{\text{eff}}(\epsilon) = \Delta_{\text{eff}}^0 \tilde{\Delta}_{\text{eff}}(\epsilon/\Delta_{\text{eff}}^0) \quad (4.15)$$

can be used as an effective model for the spin dynamics on all time scales; the only free parameter is the low-energy scale  $\Delta_{\text{eff}}^0 \propto T_K$  which determines the magnitude of the hybridization at small energies.

Indeed, the flow equations for the resonant level model are

$$\frac{dV_k}{dB} = -V_k(\epsilon_d - \epsilon_k)^2 + \sum_{q \neq k} V_k V_q^2 \frac{\epsilon_k + \epsilon_q - 2\epsilon_d}{\epsilon_k - \epsilon_q}, \quad (4.16)$$

$$\frac{d\epsilon_d}{dB} = -2 \sum_k V_k^2 (\epsilon_k - \epsilon_d), \quad (4.17)$$

$$\frac{d\epsilon_k}{dB} = 2V_k^2 (\epsilon_k - \epsilon_d). \quad (4.18)$$

If we introduce the substitution

$$\boxed{V_k^2 = \frac{2\pi}{\Gamma(\lambda^2(B))} g_k^2 |ka|^{\lambda^2-1}} \quad (4.19)$$

we may notice that two sets of the flow equations for the Kondo model and the resonant level model are equivalent for  $\epsilon_d = 0$ , with the exception of the logarithmic term in (4.11). Another approximation usually done is to substitute the flow parameter  $B$  by  $B_p = 1/p^2$  as in Hofstetter and Kehrein (2001).

The effective hybridization parameters  $V_k$  are derived by Slezak et al. (2003) from the comparison of  $\langle S^+ S^- \rangle$  correlation function in the Kondo model using the full flow equation solution to  $\langle d^\dagger d \rangle$  in the noninteracting resonant level model. Above reasoning means that we can use the effective Hamiltonian (3.11) with  $\Delta(\epsilon; t > 0) = \Delta_{\text{eff}}(\epsilon)$  from Slezak et al. (2003) to evaluate the  $S_z$ -spin dynamics for both non-equilibrium situations I) and II) in the time-dependent case. Result for the effective hybridization function  $\tilde{\Delta}_{\text{eff}}(\epsilon)$  is shown in Fig.4.1

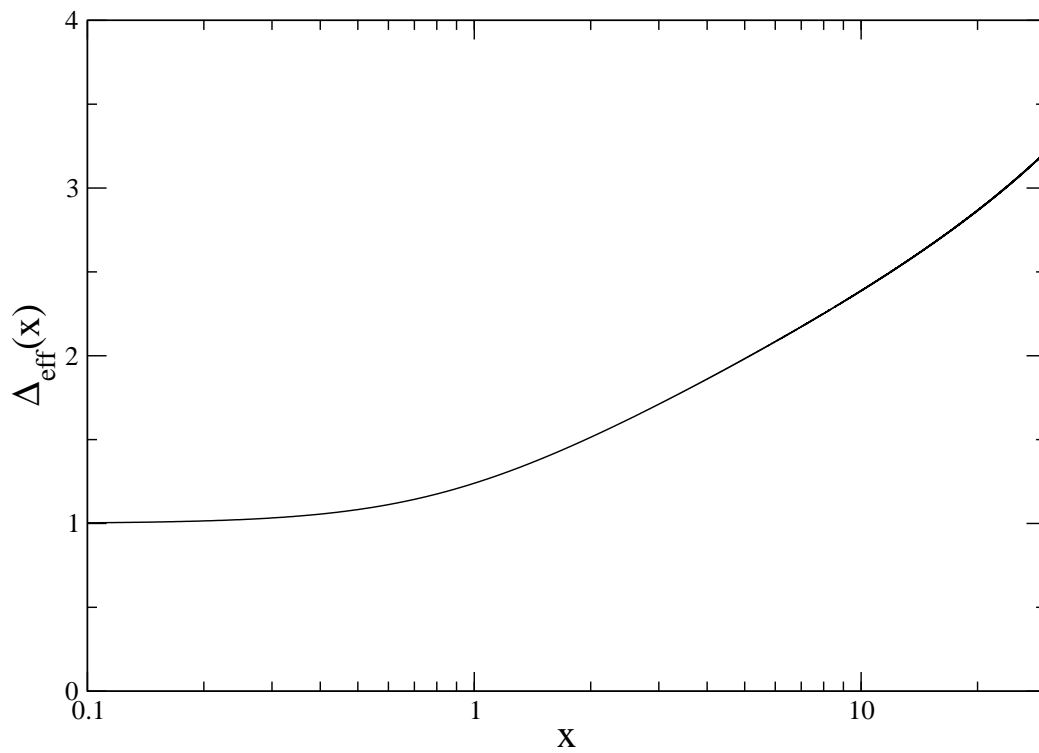


**Figure 4.1:** The dimensionless effective hybridization function  $\Delta_{\text{eff}}(x)$ . The function slowly grows for energies less than the Kondo temperature (first logarithmic term in (4.20)) and becomes linear with logarithmic corrections for energies much larger than  $T_K$ .

$a_0$	$a_1$	$a_2$
0.829	0.536	0.00324

**Tab. 4.1:** Result of the fit (4.20) to the effective hybridization  $\tilde{\Delta}_{\text{eff}}(x)$

Analytical fit for this hybridization function is given by formula

$$\tilde{\Delta}(x) = 1 + \frac{1}{2}a_1 \ln \left( 1 + \left( \frac{x}{a_0} \right)^2 \right) + a_2 \left( \arctan \left| \frac{x}{a_0} \right| - \left| \frac{x}{a_0} \right| \right) \left( 1 - \ln \left| \frac{x}{a_0} \right| \right), \quad (4.20)$$

where all constants  $a_0, a_1$  and  $a_2$  are given in Table 4.1.

A careful analysis (Lobaskin and Kehrein 2005c) shows that the only effect not captured by the resonant level model is a polaron-like transformation that is contained in the complete flow equation approach. Each time when we gradually eliminate high energy differences applying the flow transformation (4.2) we generate the term of the structure (Hofstetter and Kehrein 2001)

$$H_{\text{new}} = \int dx f(x) S^z \partial_x \Phi(x) \quad (4.21)$$

with some function  $f(x)$ . The term obviously coincides with the longitudinal coupling which have already eliminated before starting the procedure by the unitary transformation  $U$  (2.30). Therefore on each step of the flow we should apply the polaron transformation again

$$U = \exp \left\{ i \int dx r(x) \Phi(x) S^z \right\} \quad (4.22)$$

where function  $r(x)$  is connected with  $f(x)$  (Hofstetter and Kehrein 2001). On some step  $B_p$  of the flow only the matrix elements with energy differences less than  $p$  are modified. Thus diagonal elements are mostly changed. Accumulation of these polaron transformations leads to an initial potential scattering term with coupling  $g_{kk'}$  like in (3.11) with

$$g_{kk'}(t < 0) = (\lambda(B_{\text{eff}}) - \sqrt{2})/\rho_0, \quad (4.23)$$

where

$$B_{\text{eff}} = \frac{1}{\epsilon_k^2 + \epsilon_{k'}^2} \quad (4.24)$$

and  $\lambda(B)$  is the flowing scaling dimension according to Hofstetter and Kehrein (2001) ( $\lambda(B=0) = \sqrt{2}$  and  $\lambda(B \rightarrow \infty) = 1$ ). Notice that this initial potential scattering term has a negligible effect (relative error  $< 5\%$ ) which is probably just a numerical error since we expect the solution to be independent on the initial state of the bath.

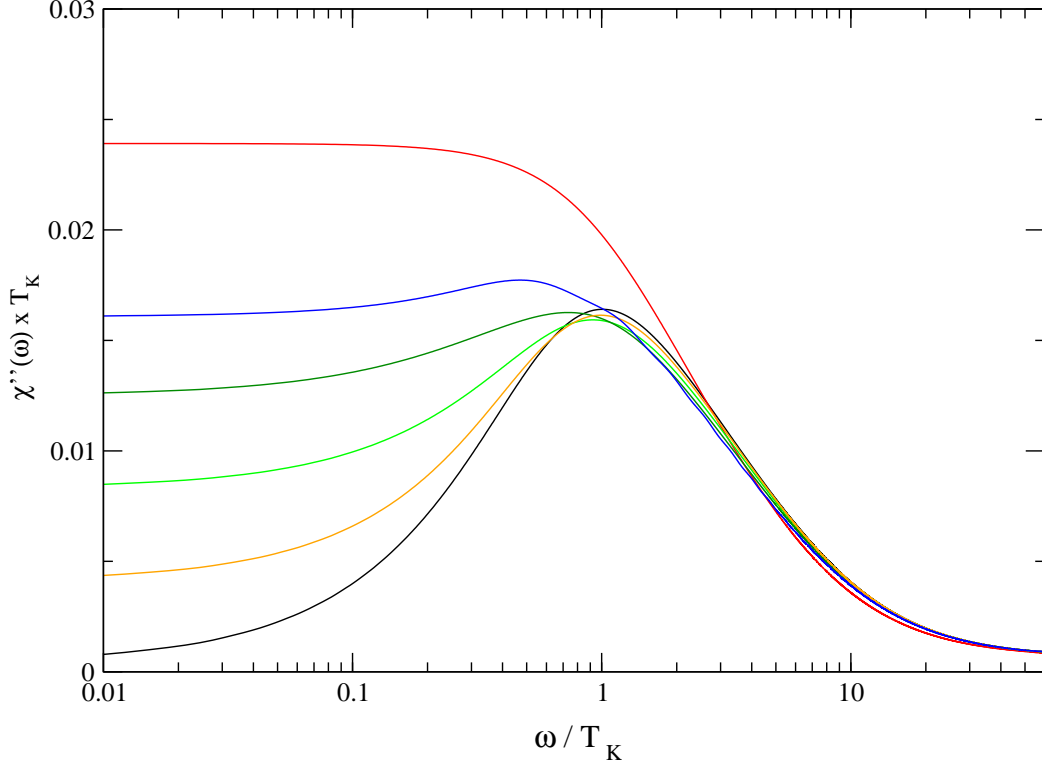


**Figure 4.2:** Universal curves for the dynamic spin susceptibility  $\chi''(t_w, \omega)$  in the limit of small Kondo couplings (Kondo limit) for various waiting times ( $t_w = 0, t_K/4, t_K/2, t_K, 2t_K, \infty$  from top to bottom like in Fig. 3.1).

### 4.3 Numerical Results

From the effective quadratic Hamiltonian (3.11) with these coupling constants one can evaluate the non-equilibrium correlation functions. Results are depicted in Fig. 4.2. The key observations from the Toulouse point analysis hold in the Kondo limit as well, only the crossover behavior is more complicated:

- The system approaches equilibrium behavior exponentially fast as a function of  $t_w/t_K$ . One can notice that the initial approach for small  $t_w$  in Fig. 4.2 is faster than at the Toulouse point (Fig. 3.1).
- An algebraic long-time decay  $\propto t^{-2}$  dominates for all nonzero waiting times  $t_w > 0$ .

For zero waiting time  $t_w = 0$  we have calculated spin expectation value  $P(t)$  in the Kondo limit which is shown in Fig. 4.3 and which has not been previously calculated explicitly on all time scales. For large  $t/t_K$  the behavior crosses over into an exponential decay which agrees very well with the exact asymptotic result

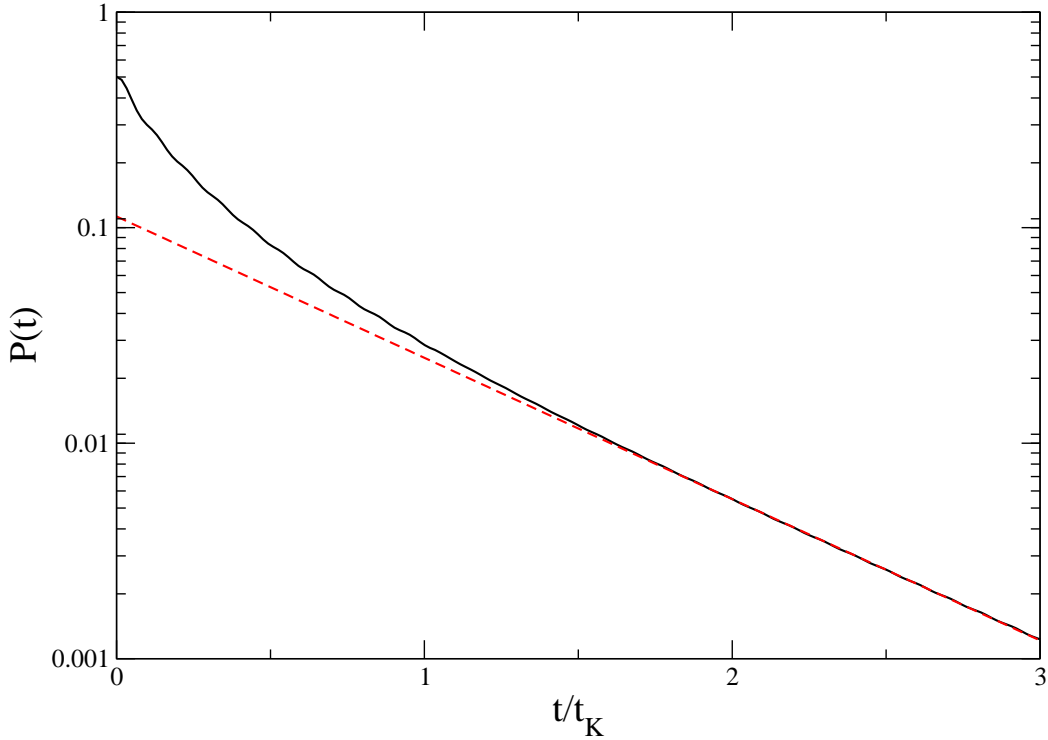


**Figure 4.3:** Spin expectation value  $P(t)$ : the dashed line is an asymptotic fit  $P_{\text{asym}}(t) = 0.11 \exp(-1.51 t/t_K)$ .

from Lesage and Saleur (1998):  $P_{\text{exact}}(t) \propto \exp(-2t/\pi w t_K) \propto \exp(-1.54t/t_K)$ . On shorter time scales the decay is faster, which is due to unrenormalized coupling constants at large energies that dominate the short-time behavior.

#### 4.4 Analytical Estimations of the Asymptotics

Our prime interest is in calculation of the asymptotics of  $P(t)$  at large and small times.

Analytical results in the limit of small couplings  $J$  might be calculated using the equivalence of the Kondo model to the resonant level model with a non-constant hybridization function (Slezak et al. 2003). This nontrivial hybridization encodes the quasiparticle interaction in the Kondo limit with the hybridization function (3.10) shown in Fig.4.1 and with the analytical fit (4.20). These effective couplings grow linearly at high energies with some logarithmical corrections. If we try to perform here the procedure similar to the Toulouse point calculations we have all summations divergent. At the Toulouse point the effective model of non-interacting fermions has a constant hybridization function. This allows to neglect any band-edge behavior and go to the infinite band limit easily. However

in the Kondo limit we have to introduce a cut-off explicitly and it can affect small time results. However, for a large time behavior the way how we introduce a cut-off is unimportant.

## Large time asymptotics

To find the asymptotics of  $P(t)$  at  $t \gg t_K$  we use expression (3.63). In the case of the non-constant hybridization function, result for  $A_{d\varepsilon}$  is no longer given by (3.43), but still regular as a function of  $\varepsilon$ . It allows us to go in (3.63) from summation to integration. Since the coefficients  $A_{d\varepsilon}$  are simply connected with an impurity equilibrium density of states  $\rho_d(\varepsilon)$  via

$$|A_{d\varepsilon}|^2 \equiv \Delta_L \rho_d(\varepsilon), \quad (4.25)$$

one may write (3.63) in the form

$$P(t) = (n_d - 1/2) \left[ \int d\varepsilon \rho_d(\varepsilon) e^{i\varepsilon t} \right]^2. \quad (4.26)$$

The impurity density of states for non-constant hybridization function is given by (see Hewson (1993), for example)

$$\rho_d(\varepsilon) = \frac{1}{\pi} \frac{\Delta(\varepsilon)}{(\varepsilon - \Lambda(\varepsilon))^2 + \Delta(\varepsilon)^2} \quad (4.27)$$

where

$$\Lambda(\varepsilon) = \frac{1}{\pi} \text{P} \int_{-D/2}^{D/2} dx \frac{\Delta(x)}{\varepsilon - x}. \quad (4.28)$$

Behavior of  $\Lambda(x)$  is shown in Fig.4.4. The negative first derivative at the origin is very important for fulfillment of the Wilson ratio (Slezak et al. 2003). This derivative is zero for a non-interacting Toulouse point case. At large times  $t \gg t_K$  the integral in (4.26) is determined by a region of small  $\varepsilon \ll T_K$ . Therefore, leading contribution to  $P(t)$  in this limit is given by

$$\begin{aligned} \lim_{t \rightarrow \infty} P(t) &\sim \left[ \int d\varepsilon \rho(\varepsilon) e^{i\varepsilon t} \right]^2 \sim \\ &\sim \left[ \int d\varepsilon \frac{\Delta(0) e^{i\varepsilon t}}{(1 - \Lambda'(0))^2 \varepsilon^2 + \Delta(0)^2} \right]^2 = e^{-\frac{2\Delta(0)}{1 - \Lambda'(0)} t}. \end{aligned} \quad (4.29)$$

Finally, using  $T_K$  definition via the Sommerfeld coefficient

$$\gamma_{\text{imp}} = \frac{\pi^2 w k_B}{3 T_K} \quad (4.30)$$

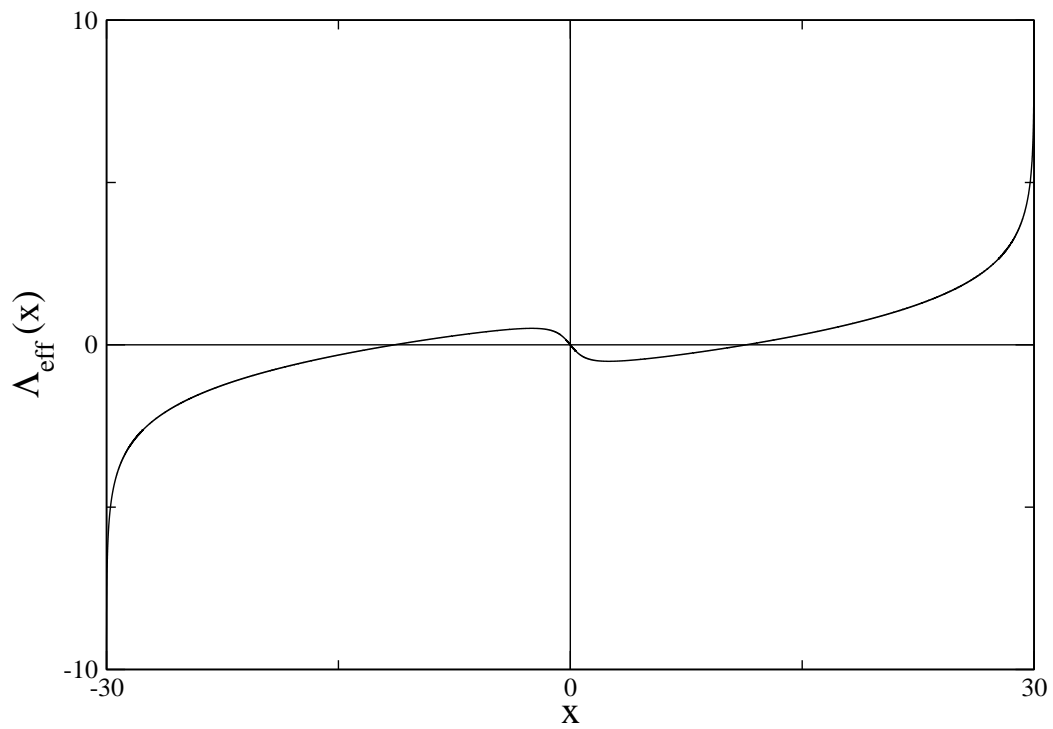


**Figure 4.4:** The dimensionless function  $\Lambda(x)$ . The first derivative is negative at the origin. Its non-zero value provide the fulfillment of the Wilson's ratio in the strong coupling case.

and its value for the noninteracting resonant level model (Slezak et al. 2003)

$$\gamma_{\text{imp}} = \frac{\pi^2 k_{\text{B}}^2}{3} \rho_d(0) (1 - \Lambda'(0)) = \frac{\pi k_{\text{B}}^2}{3\Delta(0)} (1 - \Lambda'(0)), \quad (4.31)$$

one gets the exact asymptotic result of Lesage and Saleur (Lesage and Saleur 1998)

$$\boxed{P(t) \sim e^{-2t/t_{\text{B}}} = e^{-2\pi\omega t/t_{\text{K}}}} \quad . \quad (4.32)$$

## Short time behavior

While the calculation of large  $t$  asymptotics using (3.63) is straightforward, it is rather problematic in the small time limit, since the full knowledge of  $\Delta(\varepsilon)$  behavior, until the band edges, is required. Therefore, to find small  $t$  asymptotics of  $P(t)$  we use a different approach, namely, non-equilibrium perturbation expansion in powers of bare coupling  $J$ .

In interaction picture expectation value of the impurity spin is given by

$$P(t) = \langle U^\dagger S_z(t) U \rangle \quad (4.33)$$

with the  $T$ -ordered time-evolution operator

$$U \equiv \text{T exp} \left( -i \int_0^t H_{\text{int}}(t') dt' \right) , \quad (4.34)$$

and  $H_{\text{int}}$  in the interaction picture

$$H_{\text{int}}(t) = \frac{J}{L} \sum_{kk'} (S^+ c_{k\downarrow}^\dagger c_{k'\uparrow} + S^- c_{k\uparrow}^\dagger c_{k'\downarrow} + S_z (c_{k\uparrow}^\dagger c_{k'\uparrow} - c_{k\downarrow}^\dagger c_{k'\downarrow})) e^{i(\epsilon_k - \epsilon_{k'})t} . \quad (4.35)$$

Expanding time-ordered exponent up to a second order in bare coupling one finds

$$\begin{aligned} P(t) \simeq & \frac{1}{2} + \left\langle \int_0^t dt_1 H_{\text{int}}(t_1) S_z \int_0^t dt_2 H_{\text{int}}(t_2) \right\rangle - \\ & - \left\langle \int_0^t dt_1 \int_0^{t_1} dt_2 H_{\text{int}}(t_1) H_{\text{int}}(t_2) S_z \right\rangle - \left\langle S_z \int_0^t dt_1 \int_0^{t_1} dt_2 H_{\text{int}}(t_2) H_{\text{int}}(t_1) \right\rangle \end{aligned} \quad (4.36)$$

Initial factorized state  $|IS\rangle$  is the product of the spin-up and the Fermi sea states

$$|IS\rangle = |\uparrow\rangle \otimes |FS\rangle \quad (4.37)$$

The only nonzero expectation values in (4.37) are

$$\begin{aligned} \langle IS | H_{\text{int}}(t_1) S_z H_{\text{int}}(t_2) | IS \rangle & = \\ & = \frac{J^2}{L^2} \langle \uparrow | S^+ S_z S^- | \uparrow \rangle \langle FS | c_{k\downarrow}^\dagger c_{k'\uparrow} c_{k_1\uparrow}^\dagger c_{k_1\downarrow} | FS \rangle e^{i(\epsilon_k - \epsilon_{k'})t_1} e^{-i(\epsilon_k - \epsilon_{k'})t_2} = \\ & = -\frac{J^2}{L^2} \frac{1}{2} n(k) (1 - n(k')) \delta_{kk_1} \delta_{k'k_1} e^{i(\epsilon_k - \epsilon_{k'})t_1} e^{-i(\epsilon_k - \epsilon_{k'})t_2}, \end{aligned} \quad (4.38)$$

$$\begin{aligned}
\langle IS|H_{int}(t_1)H_{int}(t_2)S_z|IS\rangle &= \\
&= \frac{J^2}{L^2} \langle \uparrow |S^+S^-S_z| \uparrow \rangle \langle FS|c_{k_1\downarrow}^\dagger c_{k'\uparrow} c_{k_1\uparrow}^\dagger c_{k'\downarrow}|FS\rangle e^{i(\epsilon_k - \epsilon_{k'})t_1} e^{-i(\epsilon_k - \epsilon_{k'})t_2} = \\
&= \frac{J^2}{L^2} \frac{1}{2} n(k)(1 - n(k')) \delta_{kk'} \delta_{k'k_1} e^{i(\epsilon_k - \epsilon_{k'})t_1} e^{-i(\epsilon_k - \epsilon_{k'})t_2} \quad (4.39)
\end{aligned}$$

and

$$\begin{aligned}
\langle IS|S_z H_{int}(t_1)H_{int}(t_2)|IS\rangle &= \\
&= \frac{J^2}{L^2} \langle \uparrow |S_z S^+ S^-| \uparrow \rangle \langle FS|c_{k_1\downarrow}^\dagger c_{k'\uparrow} c_{k_1\uparrow}^\dagger c_{k'\downarrow}|FS\rangle = e^{i(\epsilon_k - \epsilon_{k'})t_1} e^{-i(\epsilon_k - \epsilon_{k'})t_2} \\
&= \frac{J^2}{L^2} \frac{1}{2} n(k)(1 - n(k')) \delta_{kk'} \delta_{k'k_1} e^{i(\epsilon_k - \epsilon_{k'})t_1} e^{-i(\epsilon_k - \epsilon_{k'})t_2}. \quad (4.40)
\end{aligned}$$

We substitute these three terms into (4.37) and perform  $t$  integration first. Integration in the first term of (4.37) gives purely real contribution, imaginary parts of second and third terms cancel each other since they are conjugated.

Simple calculation gives

$$\begin{aligned}
P(t) &= \frac{1}{2} - \frac{J^2}{L^2} \sum_{kk'} \frac{2(1 - \cos(\epsilon_k - \epsilon_{k'})t)}{(\epsilon_k - \epsilon_{k'})^2} n(k)(1 - n(k')) = \\
&= \frac{1}{2} - \frac{J^2}{L^2} \sum_{k,k'>0} \frac{2(1 - \cos(\epsilon_k + \epsilon_{k'})t)}{(\epsilon_k + \epsilon_{k'})^2}. \quad (4.41)
\end{aligned}$$

We make substitution  $\epsilon_k + \epsilon_{k'} = \epsilon_{k''}$  and use the flat band with allowed energies  $-D/2 < \epsilon_k < D/2$  and density of states  $\rho_0$ . After simple integration we arrive at

$$P(t) = \frac{1}{2} - \frac{\pi(\rho_0 J)^2 D}{4L^2} t. \quad (4.42)$$

Using scaled coupling  $J' = J/L$  as in (3.15) we get

$$\boxed{P(t) = \frac{1}{2} - \frac{\pi(\rho_0 J')^2 D}{4} t}. \quad (4.43)$$

This result is in a full agreement with the exact formula (3.65) at the Toulouse point if one puts UV cut-off  $a$  to be equal to

$$\frac{\hbar v_F}{a} = D. \quad (4.44)$$

This is, actually, one of the possible ways to define a cut-off  $a$ , since after bosonization and refermionization of the initial Hamiltonian we lose the knowledge about

the high energy spectrum. One way to restore it is to use the standard perturbation expansion at the exactly solvable point to identify a cut-off explicitly depending on the band type.

Our result is non-universal. Although at the Toulouse point

$$T_K \sim (\rho_0 J')^2 D, \quad (4.45)$$

it is no longer true in the Kondo limit, where

$$T_K \sim D e^{-1/(\rho_0 J')}. \quad (4.46)$$

Therefore, obtained small time behavior of  $P(t)$  is nonuniversal on the scale of order  $t \sim 1/(\rho_0 J' D)$  and depends on two parameters  $\rho_0 J'$  and  $D$ , in contrast with the long time asymptotics, where  $P(t)$  is scaled only by  $T_K$ . This fact makes it impossible to connect asymptotics in two regions of small and large times by this approach, since one cannot get a non-perturbative exponent in any finite order of the perturbation theory.

Search for another theoretical tool to derive exactly universal analytic results in this limit is one of the possible topics of our further study of the non-equilibrium Kondo problem.

## 4.5 Conclusion

Summing up, we have investigated the crossover to equilibrium behavior for a Kondo model that is prepared in an initial non-equilibrium state in the physically relevant limit. We calculated the non-equilibrium spin-spin correlation function on all time scales and could show that it evolves exponentially fast towards its equilibrium form for large waiting time of the first spin measurement  $t_w \gg t_K$ . Our results also established that the flow equation method is a very suitable approach for studying such non-equilibrium problems: it agrees with very good accuracy with exact results for both  $t_w = 0$  and  $t_w = \infty$ , and can describe the crossover regime as well.

Finally, it is worthwhile to recall the fundamental quantum mechanical observation that the overlap between the initial non-equilibrium state and the true ground state of the Kondo model is always *time-independent*. Therefore it is not strictly accurate to conclude from our results that an initial non-equilibrium state "decays" into the ground state: rather, quantum observables which exhibit equilibration behavior are probes for which the time-evolved initial non-equilibrium state eventually "looks like" the ground state.



---

## 5. VIOLATION OF THE FLUCTUATION-DISSIPATION THEOREM IN THE NON-EQUILIBRIUM KONDO MODEL

### 5.1 Fluctuation-Dissipation Theorem

The fluctuation-dissipation theorem (FDT)(Callen and Welton 1951) is of fundamental importance for the theoretical understanding of many-body problems. It establishes a relation between the equilibrium properties of a system and its response to an external perturbation. In nonequilibrium situations this powerful tool is in general not available: typical nonequilibrium situations are e.g. systems prepared in an excited state, or systems driven into an excited state by pumping energy into them. Since such nonequilibrium systems occur everywhere in nature, the investigation of nonequilibrium many-body physics has become one of the key challenges of modern theoretical physics. The violation of the FDT in a nonequilibrium system plays an important role in such studies as it characterizes "how far" the system is driven out of equilibrium.

Most widely investigated in this context are glassy systems, that is systems with a very long relaxation time compared to the typical time scale of measurements. Due to the long relaxation times it is experimentally possible to measure the deviation from the FDT, i.e. to study the *ageing effects*: one observes a relaxation of the nonequilibrium initial state towards equilibrium. For a review of this field see reviews by Fisher and Hertz (1991), Calabrese and Gambassi (2005).

However, these are classical systems at finite temperature and therefore the classical limit of the FDT is studied. Nonequilibrium zero temperature quantum systems provide a very different limit which has been studied very little in the literature. Notable exceptions are the nonequilibrium dynamics of Heisenberg spin chains in a dissipative environment (Cugliandolo and Lozano 1999, Biroli and Parcollet 2002, Cugliandolo, Grepel, Lozano, Lozza and da Silva Santos 2002, Cugliandolo, Grepel, Lozano and Lozza 2004), quantum brownian motion (Pottier and Mauger 2000), and one-dimensional quantum phase transitions (Iglói and Rieger 2000, Calabrese and Cardy 2005). This provides one of the main motivations for our work which looks at the FDT violation in the time-dependent Kondo model at zero temperature. Time-dependence is

here introduced by freezing the impurity spin at negative times, and then allowing it to relax at positive times.

Besides being of fundamental theoretical importance as the paradigm for strong-coupling impurity physics in condensed matter theory, Kondo physics is also experimentally realizable in quantum dots. The Kondo effect has been observed in quantum dot experiments (Goldhaber-Gordon, Shtrikman, Mahalu, Abusch-Magder, Meirav and Kastner 1998, Cronenwett et al. 1998), and time-dependent switching of the gate potential amounts to a realization of the time-dependent Kondo model (Nordlander et al. 1999) which should be possible in future experiments.

Our calculations in this chapter are based on analytical results for the Toulouse point and results in a controlled approximation in the experimentally relevant Kondo limit (Lobaskin and Kehrein 2005a) described before. We will see that the FDT is maximally violated at intermediate time scales of order the inverse Kondo temperature: the effective temperature becomes of order the Kondo temperature due to heating of the conduction band electrons by the formation of the Kondo singlet. The system then relaxes towards equilibrium and the FDT becomes fulfilled exponentially fast at larger times.

## Basic definitions

Consider an observable  $A$  which is coupled linearly to a time-dependent external field  $h(t)$ . The Hamiltonian of the system is then given by

$$H = H_0 - h(t) A , \quad (5.1)$$

where  $H_0$  is the unperturbed part of the Hamiltonian. The generalized susceptibility (or *response*)  $R(t, t')$  of the observable  $A$  at time  $t$  to the external small perturbation  $h(t')$  at time  $t'$  is defined as

$$R(t, t') = \left. \frac{\delta \langle \overline{A(t)} \rangle}{\delta h(t')} \right|_{h=0} . \quad (5.2)$$

Here  $\langle \overline{A(t)} \rangle \equiv \langle A(t) \rangle_h - \langle A(t) \rangle_0$  is the deviation of the expectation value from its equilibrium value. If the system is in equilibrium before its perturbation by the field  $h$ , then  $R(t, t')$  depends only on the time difference  $\tau = t - t'$ . One introduces the Fourier transform of  $R(\tau)$

$$R(\omega) = \int_0^\infty R(\tau) e^{i\omega\tau} d\tau , \quad (5.3)$$

where the integration runs only over positive times as a consequence of causality. A simple calculation shows that the imaginary part of  $R(\omega)$  is proportional

to the energy dissipated by the system for a small periodic perturbation with frequency  $\omega$  (see, for example, Landau and Lifshitz (1980)). Thus the response function determines the dissipation properties of the equilibrium system.

For calculating the response function one defines the two-time correlation function

$$C_{A,A}(t, t') \equiv \langle A(t)A(t') \rangle = \frac{1}{Z} \text{Tr} [A(t)A(t')\rho] , \quad (5.4)$$

with the operators in the Heisenberg picture

$$A(t) \equiv \exp(iHt) A(0) \exp(-iHt) . \quad (5.5)$$

The trace runs over all the states in the Hilbert space,  $\rho$  is the density matrix and  $Z$  the partition function. Symmetrized and antisymmetrized correlation functions  $C_{\{A,A\}}(t, t')$ ,  $C_{[A,A]}(t, t')$  are defined in the same way

$$C_{\{A,A\}}(t, t') \equiv \frac{1}{2} \langle \{A(t), A(t')\} \rangle \quad (5.6)$$

$$C_{[A,A]}(t, t') \equiv \frac{1}{2} \langle [A(t), A(t')] \rangle . \quad (5.7)$$

The cumulant of the symmetrized correlation function is

$$C_{\{A,A\}}^{(\text{cum})}(t, t') \equiv C_{\{A,A\}}(t, t') - \langle A(t) \rangle \langle A(t') \rangle . \quad (5.8)$$

In the framework of linear response theory (that is for small perturbations) one then proves the famous Kubo formula(Kubo 1956)

$$\boxed{R(t, t') = 2i\theta(t - t')C_{[A,A]}(t, t')} . \quad (5.9)$$

Here the time dependence of all operators is given by the unperturbed part of the Hamiltonian  $H_0$ . Since in equilibrium all correlation functions depend only on the time difference  $\tau = t - t'$ , one defines their Fourier transform with respect to  $\tau$

$$C_{\{A,A\}}^{(\text{cum})}(\omega) = \int_{-\infty}^{\infty} C_{\{A,A\}}^{(\text{cum})}(\tau) e^{i\omega\tau} d\tau . \quad (5.10)$$

If the initial state is the equilibrium state for a given temperature,  $R(\omega)$  and  $C_{\{A,A\}}^{(\text{cum})}(\omega)$  are related by the famous Callen-Welton relation(Callen and Welton 1951), which is also known as *the* Fluctuation-Dissipation theorem

$$\boxed{\text{Im} R(\omega) = \tanh\left(\frac{\beta\omega}{2}\right) C_{\{A,A\}}^{(\text{cum})}(\omega)} . \quad (5.11)$$

Here  $\beta$  is the inverse temperature. For  $T = 0$  Eq. (5.11) reads

$$\boxed{\text{Im} R(\omega) = \text{sgn}(\omega) C_{\{A,A\}}^{(\text{cum})}(\omega)} . \quad (5.12)$$

Eqs. (5.11) and (5.12) relate dissipation with equilibrium fluctuations, which is the fundamental content of the FDT. These equations are often formulated with the connected correlation function instead of its cumulant appearing on the rhs. One can easily verify that this makes no difference in equilibrium. However, using the cumulant is the suitable generalization for nonequilibrium situations (see e.g. Sollich, Fielding and Mayer (2002)).

## 5.2 FDT Violation in Nonequilibrium

Let us recapitulate why the FDT (5.11) in general will not hold in quantum nonequilibrium systems. We will only consider the zero temperature case since it brings out the quantum effects most clearly; the generalization to nonzero temperatures is straightforward.

We first consider how a typical experiment is actually performed: the system is prepared in some initial state at time  $t = 0$  (not necessarily its ground state) and then evolves according to its Hamiltonian. A response measurement is then done by applying the external field after a *waiting time*  $t_w > 0$ , and the response to this is measured a time difference  $\tau$  later. The Fourier transform with respect to (positive) time difference will then in general depend on the waiting time  $t_w$

$$R(\omega, t_w) = \int_0^\infty R(t_w + \tau, t_w) e^{i\omega\tau} d\tau . \quad (5.13)$$

Likewise in an experimental measurement of the correlation function the first measurement of the observable will be performed after the waiting time  $t_w$ , and then at time  $t_w + \tau$  the second measurement follows. From the experimental point of view this leads again to a one-sided Fourier transform

$$C_{\{A,A\}}^{(\text{cum})}(\omega, t_w) = 2 \int_0^\infty C_{\{A,A\}}^{(\text{cum})}(t_w + \tau, t_w) \cos(\omega\tau) d\tau . \quad (5.14)$$

If the system is prepared in its ground state, or if the system equilibrates into its ground state for sufficiently long waiting time  $t_w \rightarrow \infty$ , then we can replace this one-sided Fourier transform by the symmetric version and arrive at the conventional equilibrium definition (5.10).

However, for a nonequilibrium preparation at  $t = 0$  Eqs. (5.13) and (5.14) are the suitable starting point for the discussion of the FDT (5.12). Let us therefore look at the FDT in the framework of (5.13) and (5.14). We follow the standard derivation (Landau and Lifshitz 1980) and introduce a complete set of eigenstates  $|n\rangle$  of the Hamiltonian  $H$ ,  $H|n\rangle = E_n|n\rangle$ . The matrix elements of the operator  $A$  are denoted by  $A_{nm} = \langle n|A|m\rangle$  in this basis. Then a matrix element of the

susceptibility is given by

$$R(t, t_w)_{nn'} = i\theta(t - t_w) \sum_m A_{nm} A_{mn'} \quad (5.15)$$

$$\times \left( e^{i(E_n - E_m)t} e^{i(E_m - E_{n'})t_w} - e^{i(E_n - E_m)t_w} e^{i(E_m - E_{n'})t} \right)$$

The imaginary part of (5.13) is

$$\text{Im } R(\omega, t_w)_{nn'} = \text{Re} \sum_m A_{nm} A_{mn'} \quad (5.16)$$

$$\times \int_0^\infty (e^{i\omega_{nm}\tau} - e^{i\omega_{mn'}\tau}) e^{i\omega_{nn'}t_w} e^{i\omega\tau} d\tau$$

with  $\omega_{nm} \equiv E_n - E_m$ . For diagonal matrix elements  $n = n'$  this implies

$$\text{Im } R(\omega, t_w)_{nn} = \quad (5.17)$$

$$\frac{1}{2} \sum_m A_{nm} A_{mn} (\delta(\omega + \omega_{nm}) - \delta(\omega + \omega_{mn})) .$$

Likewise for the correlation function

$$C_{\{A,A\}}(\omega, t_w)_{nn'} = \sum_m A_{nm} A_{mn'} \quad (5.18)$$

$$\times \int_0^\infty (e^{i\omega_{nm}\tau} + e^{i\omega_{mn'}\tau}) e^{i\omega_{nn'}t_w} \cos(\omega\tau) d\tau$$

and the diagonal matrix elements are

$$C_{\{A,A\}}^{(\text{cum})}(\omega, t_w)_{nn} = \quad (5.19)$$

$$\frac{1}{2} \sum_{m \neq n} A_{nm} A_{mn} (\delta(\omega + \omega_{nm}) + \delta(\omega + \omega_{mn})) .$$

If we take  $|n\rangle = |\text{GS}\rangle$  as the ground state of our Hamiltonian, i.e. the system is in equilibrium, then we know  $\omega_{nm} = E_{\text{GS}} - E_m \leq 0$  and  $\omega_{mn} = E_m - E_{\text{GS}} \geq 0$  for all  $m$ . For positive  $\omega$  therefore only the first terms in (5.17) and (5.19) contribute, and for negative  $\omega$  the second terms contribute: this just proves the zero temperature FDT (5.12) with its  $\text{sgn}(\omega)$ -coefficient.

Now let us assume the nonequilibrium situation described above where the system is prepared in some arbitrary initial state  $|\text{NE}\rangle$  at  $t = 0$ . One can expand  $|\text{NE}\rangle$  in terms of the eigenstates  $|n\rangle$  of the Hamiltonian

$$|\text{NE}\rangle = \sum_n c_n |n\rangle \quad (5.20)$$

with suitable coefficients  $c_n$ . Then the relations (5.16) and (5.18) are modified like

$$\begin{aligned}\text{Im } R(\omega, t_w)_{NE} &= \sum_{m,n,n'} c_n^* c_{n'} A_{nm} A_{mn'} \times \dots \\ C_{\{A,A\}}(\omega, t_w)_{NE} &= \sum_{m,n,n'} c_n^* c_{n'} A_{nm} A_{mn'} \times \dots ,\end{aligned}$$

where "... " stands for the same expressions as in (5.16) and (5.18). In general this will lead to a nonzero difference

$$\text{sgn}(\omega) C_{\{A,A\}}^{(\text{cum})}(\omega, t_w)_{NE} - \text{Im } R(\omega, t_w)_{NE} \neq 0 \quad (5.21)$$

and therefore the FDT is violated. We will next study the violation of the FDT explicitly in the time-dependent Kondo model, and in particular also show that the difference (5.21) vanishes exponentially fast for large waiting times  $t_w$ .

### 5.3 Toulouse Point

At the Toulouse point (Toulouse 1969) with  $J_{\parallel}/2\pi v_F = 1 - 1/\sqrt{2}$  the mapping to the effective resonant level model (3.11) is exact and the effective parameters  $g_{kk'}$  and  $V_k$  are independent of  $k, k'$ . This allowed us to express the spin-spin correlation functions in closed analytical form (Lobaskin and Kehrein 2005a)

$$\begin{aligned}C_{\{S_z, S_z\}}^{(\text{cum})}(\tau, t_w) &\stackrel{\text{def}}{=} \\ &= \frac{1}{2} \langle \{S_z(t_w), S_z(t_w + \tau)\} \rangle - \langle S_z(t_w) \rangle \langle S_z(t_w + \tau) \rangle \\ &= \frac{1}{4} e^{-2\tau/t_B} (1 - e^{-4t_w/t_B}) \\ &\quad - (s(\tau) - s(t_w + \tau)) e^{-t_w/t_B} + s(t_w) e^{-(t_w + \tau)/t_B})^2\end{aligned} \quad (5.22)$$

for the symmetrized part and

$$\begin{aligned}C_{[S_z, S_z]}(\tau, t_w) &\stackrel{\text{def}}{=} \frac{1}{2} \langle [S_z(t_w), S_z(t_w + \tau)] \rangle \\ &= -i e^{-\tau/t_B} \left( s(\tau) - s(t_w + \tau) e^{-t_w/t_B} \right. \\ &\quad \left. + s(t_w) e^{-(t_w + \tau)/t_B} \right)\end{aligned} \quad (5.23)$$

for the antisymmetrized part. Here again as in (3.69)  $s(t) \stackrel{\text{def}}{=} (t_B/\pi) \int_0^\infty d\omega \sin(\omega\tau)/(1 + \omega^2 t_B^2)$  with the shorthand notation  $t_B = \pi w t_K$ ,  $w = 0.4128$  is the Wilson number and  $t_K = 1/T_K$  is the Kondo time scale, i.e. the

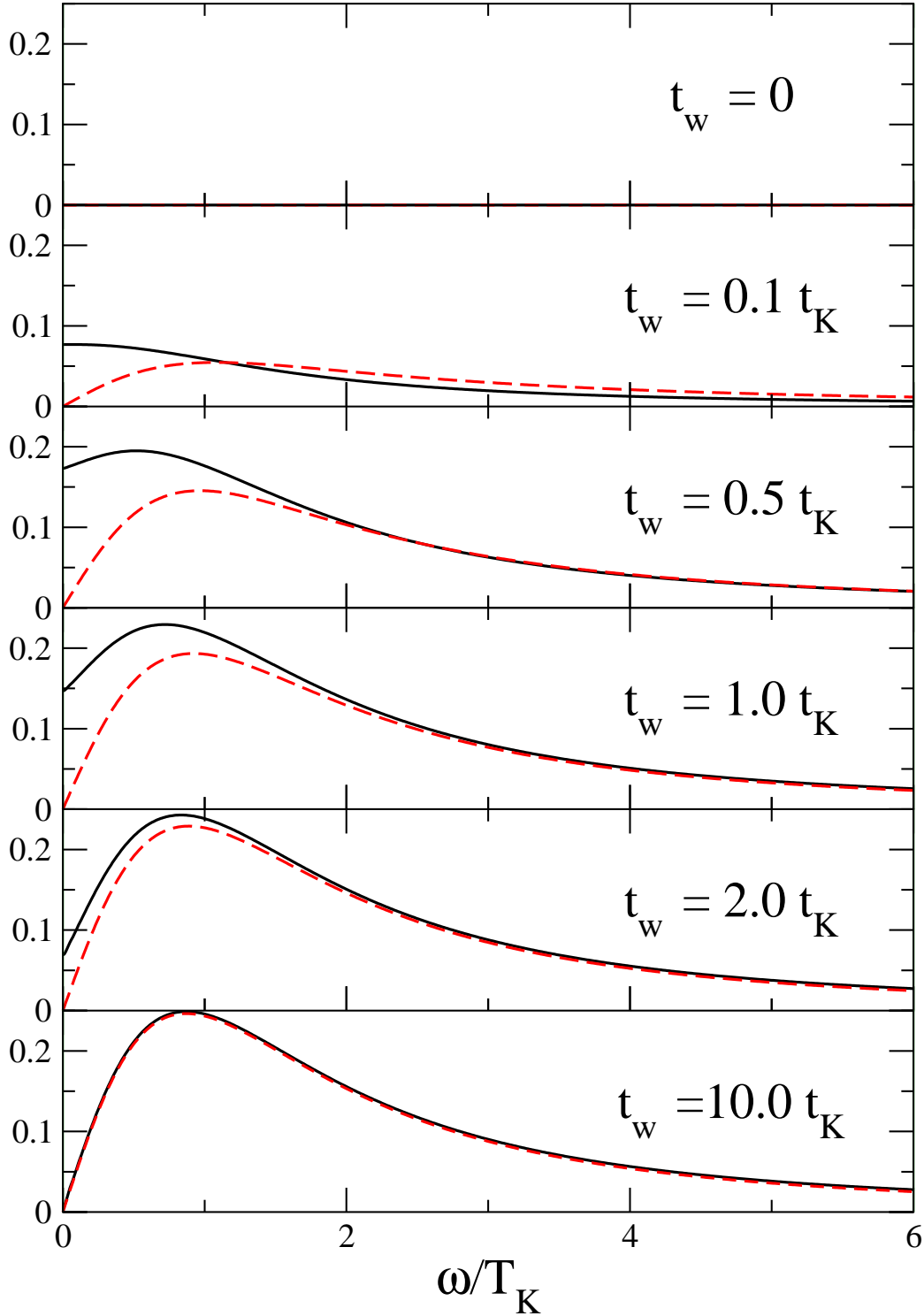


**Figure 5.1:** Universal curves for the spin-spin correlation function  $T_K \times C_{\{S_z, S_z\}}^{(\text{cum})}(\omega, t_w)$  (solid line) and response function  $T_K \times \text{Im} R(\omega, t_w)$  (dashed line) at the Toulouse point. Notice the normalization of the equilibrium curve ( $t_w \rightarrow \infty$ ) which follows from (5.6) with the operator identity  $S_z^2 = 1/4$ : this gives  $\int_0^\infty C_{\{S_z, S_z\}}^{(\text{cum})}(\omega, t_w = \infty) d\omega = \pi/4$ .

inverse Kondo temperature. As before we use the definition of the Kondo temperature  $T_K$  via the zero temperature impurity contribution to the Sommerfeld coefficient,  $\gamma_{\text{imp}} = w\pi^2/3T_K$ .

From (3.67) and (3.68) one can obtain the Fourier transforms (5.13) and (5.14). Results for  $C_{\{S_z, S_z\}}^{\text{cum}}(\omega, t_w)$  and  $\text{Im}R(\omega, t_w)$  for various waiting times  $t_w$  are shown in Fig. 5.1. For zero waiting time  $t_w = 0$  the FDT is trivially fulfilled since the system is prepared in an eigenstate of  $S_z$  and therefore both functions vanish identically,  $C_{\{S_z, S_z\}}^{\text{cum}}(\omega, t_w = 0) = \text{Im}R(\omega, t_w = 0) = 0$ . For increasing waiting time the curves start to differ, which indicates the violation of the FDT in nonequilibrium. For large waiting time as compared to the Kondo time scale one can then see nicely that the curves coincide again, which shows that the system reaches equilibrium behavior for  $t_w \rightarrow \infty$  where the FDT is known to hold.

From the curves in Fig. 5.1 one also notices that the maximum violation of the FDT occurs at zero frequency, while it becomes fulfilled more rapidly at higher frequencies. We interpret this as showing that high-energy excitations find “equilibrium-like” behavior faster than low-energy excitations probed by the small  $\omega$  response. The high-energy components of the initial nonequilibrium state can “decay” more quickly for a given waiting time.

At zero frequency  $C_{\{S_z, S_z\}}^{\text{cum}}(\omega = 0, t_w)$  is non-zero for  $0 < t_w < \infty$  as if one were studying the spin dynamics of the equilibrium system at finite temperature. This leads to the definition of the *effective temperature*  $T_{\text{eff}}$  via the zero frequency limit of (5.11)

$$\lim_{\omega \rightarrow 0} \frac{\text{Im} R(\omega)}{\omega} = \frac{1}{2T_{\text{eff}}} C_{\{A, A\}}^{\text{cum}}(\omega = 0). \quad (5.24)$$

This concept of an “effective temperature” is frequently used and well-established in the investigation of classical nonequilibrium systems. (Cugliandolo, Kurchan and Peliti 1997) We suggest that it is also useful in a quantum nonequilibrium system by giving a measure for the “effective temperature” of our bath (i.e. the conduction band electrons) in the vicinity of the impurity.

We can see this explicitly by using (5.24) to evaluate the effective temperature as a function of the waiting time; the results are shown in Fig. 5.2. One sees that the effective temperature goes up very quickly as a function of the waiting time until it reaches a maximum of  $T_{\text{eff}} \approx 0.4T_K$  at  $t_w \approx 0.1t_K$ . After that the system cools down again. We can understand this by noticing that the conduction band is initially in its ground state with respect to the Hamiltonian for  $t < 0$ , therefore its effective temperature vanishes. As the spin dynamics is turned on at  $t = 0$  the Kondo singlet starts building up. Its nonzero binding energy therefore initially “heats up” the conduction band electrons. After a sufficiently long time the Kondo singlet has been formed and then the process of energy diffusion takes over: the binding energy that has initially been stored in the vicinity of the Kondo impurity

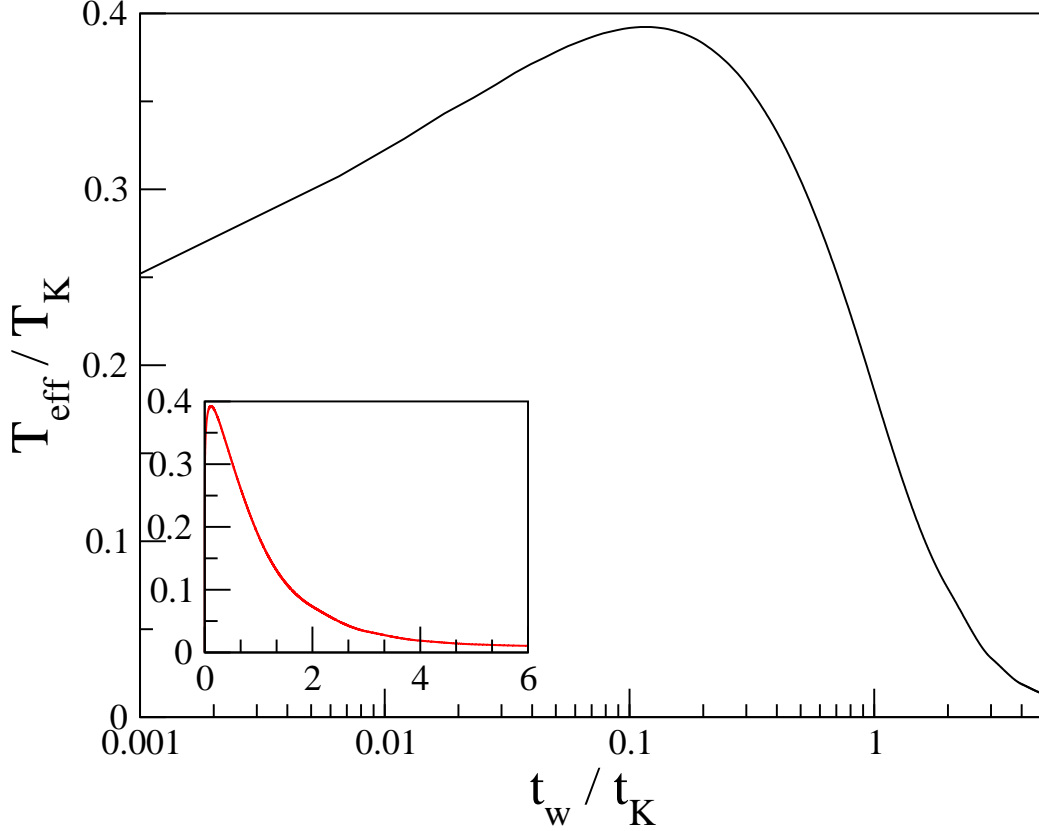


**Figure 5.2:** Effective temperature  $T_{\text{eff}}$  as a function of the waiting time  $t_w$  at the Toulouse point. The inset shows the same curve on a linear scale to illustrate how fast the initial heating occurs.

diffuses away, the system equilibrates and the effective temperature goes back to zero. The behavior of the effective temperature therefore traces this competition of release of binding energy and energy diffusion away from the impurity.

### Asymptotics of $T_{\text{eff}}$

Now we will derive several analytical results. First, we consider the case of a very small waiting time  $t_w \ll t_K$ . The one-sided Fourier transform of the symmetrized autocorrelator at zero frequency obeys

$$C_{\{S_z, S_z\}}^{\text{cum}}(\omega = 0, t_w) = 2 \int_0^\infty d\tau C_{\{S_z, S_z\}}^{\text{cum}}(\tau, t_w). \quad (5.25)$$

Now we have to choose most slowly vanishing terms when  $t_w$  goes to zero. Symmetrized autocorrelation function (5.23) has the first term equal to

$$\frac{1}{4} e^{-2\tau}, \quad (5.26)$$

the second long bracket

$$- (s(\tau) + s(t_w)e^{-\tau+t_w} - s(\tau + t_w)e^{-t_w})^2 \quad (5.27)$$

and minus the product of two averages of  $S_z(\tau + t_w)$  and  $S_z(t_w)$

$$-\frac{1}{4}e^{-2\tau-4t_w}. \quad (5.28)$$

Here for simplicity we omit the denominator  $t_B$  in all exponents.

The first term minus the third one gives

$$\frac{1}{4}e^{-2\tau} (1 - e^{-4t_w}) \simeq t_w e^{-2\tau} \quad (5.29)$$

and for the Fourier transform at zero frequency we get

$$2 \int_0^\infty d\tau t_w e^{-2\tau} = t_w. \quad (5.30)$$

Let us check that the second term gives the contribution of the next order in  $t_w$ . One finds that the function  $s(t_w)$  behaves at small  $t_w$  as

$$s(t_w) \sim t_w \ln t_w \quad (5.31)$$

Indeed,

$$\begin{aligned} s(t_w) &= \frac{1}{\pi} \int_0^\infty dx \frac{\sin xt_w}{1+x^2} = \\ &= \frac{1}{\pi} \left( \int_0^{1/t_w} \frac{\sin xt_w}{1+x^2} + \int_{1/t_w}^\infty \frac{\sin xt_w}{1+x^2} \right) \simeq \\ &\simeq \frac{1}{\pi} \left( \int_0^{1/t_w} \frac{xt_w}{1+x^2} + \int_{1/t_w}^\infty \frac{\sin xt_w}{1+x^2} \right). \end{aligned} \quad (5.32)$$

Last integral for small  $t_w$  is proportional to  $t_w$

$$\int_{1/t_w}^\infty \frac{\sin xt_w}{1+x^2} = t_w \int_1^\infty \frac{\sin y}{t_w^2 + y^2} dy \simeq t_w \int_1^\infty \frac{\sin y}{y^2} dy \sim t_w, \quad (5.33)$$

where we have changed variables from  $x$  to  $y = t_w x$ . First integral, however, vanishes slower than  $t_w$  and one obtains

$$\int_0^{1/t_w} \frac{\sin xt_w}{1+x^2} \simeq \int_0^{1/t_w} \frac{xt_w}{1+x^2} \simeq t_w \ln |t_w|. \quad (5.34)$$

Therefore, for  $s(t_w)$  the following asymptotic expression at small  $t_w$  is valid

$$\boxed{s(t_w) \simeq \frac{t_w t_B}{\pi} \ln \left| \frac{t_w}{t_B} \right|}. \quad (5.35)$$

Consequently, the long bracket (5.27) in  $C(\tau, t_w)$  contributes as

$$\begin{aligned} & (s(\tau) + s(t_w)e^{-\tau}e^{-t_w} - s(\tau + t_w)e^{-t_w}) = \\ & \simeq (s(\tau) + s(t_w)e^{-\tau} - s(\tau) + O(t_w \ln t_w)) \end{aligned} \quad (5.36)$$

and can be omitted since everything is of order  $t_w^2 \ln^2 t_w$ . Last estimation of  $s(\tau + t_w)$  follows from

$$\begin{aligned} s(\tau + t_w) &= \int_0^\infty dx \frac{\sin(\tau + t_w)x}{1 + x^2} = \\ &= \int_0^\infty dx \frac{\sin \tau x \cos t_w x + \cos \tau x \sin t_w x}{1 + x^2} \simeq \end{aligned} \quad (5.37)$$

$$\simeq \int_0^\infty dx \frac{\sin \tau x + \cos \tau x \sin t_w x}{1 + x^2} + O(t_w^2) \simeq \quad (5.38)$$

$$\simeq s(\tau) + \int_0^\infty dx \frac{\cos \tau x \sin t_w x}{1 + x^2} + O(t_w^2) \simeq \quad (5.39)$$

$$\simeq s(\tau) + O(t_w \ln t_w). \quad (5.40)$$

Thus, for the Fourier transform of the symmetrized autocorrelator in the small  $t_w$  limit we get

$$C_{\{S_z, S_z\}}^{cum}(\omega = 0, t_w) \simeq t_w. \quad (5.41)$$

To find the left part of the (5.24) definition we do the following. Since

$$\lim_{\omega \rightarrow 0} \frac{\text{Im } R(\omega)}{\omega} = \text{Im } R'(0, t_w) \quad (5.42)$$

we first find the Fourier transform of the antisymmetrized correlator. Then we differentiate it over the frequency and put the frequency equal to zero. In (5.23) there are three terms

$$-i e^{-\tau/t_B} s(\tau), \quad (5.43)$$

$$i e^{-\tau/t_B} s(t_w + \tau) e^{-t_w/t_B} \quad (5.44)$$

and

$$-i e^{-\tau/t_B} s(t_w) e^{-(t_w + \tau)/t_B}. \quad (5.45)$$

Taking the Fourier transform of the first term we get (omitting  $t_B$  again)

$$\begin{aligned}
& -i \frac{1}{\pi} \int_0^\infty dx \int_0^\infty d\tau \frac{\sin x\tau}{1+x^2} e^{-\tau} e^{i\omega\tau} d\tau = \\
& = -i \frac{1}{\pi} \int_0^\infty \frac{1}{1+x^2} dx \int_0^\infty e^{-\tau} e^{i\omega\tau} \frac{e^{ix\tau} - e^{-ix\tau}}{2i} d\tau = \\
& = -\frac{1}{2\pi} \int_0^\infty \frac{1}{1+x^2} dx \left\{ \frac{1}{i\omega - ix - 1} - \frac{1}{i\omega + ix - 1} \right\}. \quad (5.46)
\end{aligned}$$

Now we differentiate the expression over  $\omega$  getting

$$-\frac{1}{2\pi} \int_0^\infty dx \frac{1}{1+x^2} \left\{ \frac{-i}{(i\omega - ix - 1)^2} + \frac{i}{(i\omega + ix - 1)^2} \right\} \quad (5.47)$$

and put  $\omega = 0$

$$\begin{aligned}
& -\frac{1}{2\pi} \int_0^\infty dx \frac{1}{1+x^2} \left\{ \frac{-i}{(ix + 1)^2} + \frac{i}{(ix - 1)^2} \right\} = \\
& = \frac{2}{\pi} \int_0^\infty dx \frac{x}{(1+x^2)^3}. \quad (5.48)
\end{aligned}$$

Restoring the dimension we obtain for the first term

$$\frac{2t_B^2}{\pi} \int_0^\infty dx \frac{x}{(1+x^2)^3}. \quad (5.49)$$

Taking the Fourier transform of the second term we arrive at

$$\begin{aligned}
& \frac{i}{\pi} \int_0^\infty dx \int_0^\infty d\tau \frac{\sin x(\tau + t_w)}{1+x^2} e^{-\tau - t_w} e^{i\omega\tau} d\tau = \\
& = i \frac{1}{\pi} \int_0^\infty \frac{1}{1+x^2} dx \int_0^\infty e^{-\tau - t_w} e^{i\omega\tau} \frac{e^{ix(\tau + t_w)} - e^{-ix(\tau + t_w)}}{2i} d\tau = \\
& = \frac{1}{2\pi} e^{-t_w} \int_0^\infty \frac{1}{1+x^2} dx \left\{ \frac{e^{-it_w x}}{i\omega - ix - 1} - \frac{e^{it_w x}}{i\omega + ix - 1} \right\}. \quad (5.50)
\end{aligned}$$

Then we differentiate the expression over  $\omega$  getting

$$\frac{1}{2\pi} \int_0^\infty dx \frac{1}{1+x^2} \left\{ \frac{-ie^{-it_w x}}{(i\omega - ix - 1)^2} + \frac{ie^{it_w x}}{(i\omega + ix - 1)^2} \right\} \quad (5.51)$$

and put  $\omega = 0$

$$\begin{aligned}
& \frac{1}{2\pi} e^{-t_w} \int_0^\infty dx \frac{1}{1+x^2} \left\{ \frac{-ie^{-it_w x}}{(ix + 1)^2} + \frac{ie^{it_w x}}{(ix - 1)^2} \right\} = \\
& = -\frac{1}{2\pi} e^{-t_w} \int_0^\infty dx \frac{1}{(1+x^2)^3} \left\{ 4x \cos xt_w + 2 \sin xt_w (1 - x^2) \right\}. \quad (5.52)
\end{aligned}$$

Restoring the dimension we obtain for the second term

$$-e^{-t_w/t_B} \frac{t_B^5}{2\pi} \int_0^\infty dx \frac{1}{(1+x^2 t_B)^3} \left\{ 4 \frac{x}{t_B} \cos xt_w + 2 \sin xt_w \left( \frac{1-x^2 t_B}{t_B} \right) \right\}. \quad (5.53)$$

Finally, taking the Fourier transform of the third term we get

$$-is(t_w)e^{-t_w} \int_0^\infty d\tau e^{-2\tau} e^{i\omega\tau} = is(t_w)e^{-t_w} \frac{1}{i\omega - 2}. \quad (5.54)$$

We differentiate the expression over  $\omega$  obtaining

$$is(t_w)e^{-t_w} \frac{-i}{(i\omega - 2)^2} \quad (5.55)$$

and put  $\omega = 0$

$$s(t_w)e^{-t_w} \frac{1}{4}. \quad (5.56)$$

Restoring the dimension we obtain for the third term

$$s(t_w)e^{-t_w/t_B} \frac{t_B^2}{4}. \quad (5.57)$$

Collecting all three terms we arrive at

$$\begin{aligned} R'(0, t_w) &= 2 \left\{ \frac{2t_B^2}{\pi} \int_0^\infty dx \frac{x}{(1+x^2)^3} \right. \\ &\quad \left. - e^{-t_w/t_B} \frac{t_B^5}{2\pi} \int_0^\infty dx \frac{1}{(1+x^2 t_B)^3} \left\{ 4 \frac{x}{t_B} \cos xt_w + 2 \sin xt_w \left( \frac{1-x^2 t_B}{t_B} \right) \right\} \right. \\ &\quad \left. + s(t_w)e^{-t_w/t_B} \frac{t_B^2}{4} \right\}. \end{aligned} \quad (5.58)$$

Let us evaluate all integrals inside the bracket up to the first order in  $t_w$

$$\begin{aligned} R'(0, t_w) &= 2 \left[ \frac{2t_B^2}{\pi} \int_0^\infty dx \frac{x}{(1+x^2)^3} \right. \\ &\quad \left. - (1 - t_w/t_B) \frac{t_B^5}{2\pi} \int_0^\infty dx \frac{1}{(1+x^2 t_B)^3} \left\{ 4x + 2x \frac{t_w}{t_B} (1-x^2) \right\} \right. \\ &\quad \left. + s(t_w) \frac{t_B^2}{4} \right] + O(t_w^2 \ln t_w) = \\ &= 2 \left[ \frac{t_w t_B}{\pi} \int_0^\infty dx \frac{x}{(1+x^2)^2} + s(t_w) \frac{t_B^2}{4} \right] + O(t_w^2 \ln t_w) = \\ &= \frac{t_w t_B}{\pi} + \frac{t_w t_B}{2\pi} \ln \left| \frac{t_w}{t_B} \right| = \frac{t_w t_B}{\pi} \left( 1 + \frac{1}{2} \ln \left| \frac{t_w}{t_B} \right| \right) + O(t_w^2 \ln t_w). \end{aligned} \quad (5.59)$$

Thus using (5.24),(5.41) and (5.59) we get for  $T_{\text{eff}}$

$$T_{\text{eff}} = \frac{t_w}{2 \left( \frac{t_w t_B}{\pi} \left( 1 + \frac{1}{2} \ln \left| \frac{t_w}{t_B} \right| \right) \right)} = \frac{\pi}{t_B \left( 2 + \ln \left| \frac{t_w}{t_B} \right| \right)}. \quad (5.60)$$

Using the definition of  $t_B$  via the Kondo temperature and neglecting the constant comparing with the logarithm one arrives to

$$\boxed{\frac{T_{\text{eff}}}{T_K} \simeq \frac{1}{w} \frac{1}{\ln(\pi w t_K/t_w)}}. \quad (5.61)$$

For large time  $t_w \gg t_K$  the behavior of the effective temperature is an exponential decay to zero temperature

$$\boxed{\frac{T_{\text{eff}}}{T_K} \propto e^{-t_w/t_K}}. \quad (5.62)$$

That observation follows from the fact that in the  $t_w \rightarrow \infty$  limit the first derivative of the Fourier transform of  $R(\omega, t_w)$  at zero frequency is constant (see the first term in (5.58)), whereas for the symmetrized correlation function the Fourier transform of the equilibrium part is identically zero and the contribution of the non-equilibrium part goes to zero as  $e^{-t_w/t_B}$  which follows from (3.67).

Finally, we want to emphasize that while the effective temperature seems a useful phenomenological concept for interpreting the  $\omega = 0$  behavior in nonequilibrium, its definition (5.24) does not capture the small  $\omega$ -behavior. Since  $C_{\{S_z, S_z\}}^{(\text{cum})}(\omega, t_w) - C_{\{S_z, S_z\}}^{(\text{cum})}(\omega = 0, t_w) \propto |\omega|$  is nonanalytic for small  $\omega$  and finite waiting time (see Fig. 5.1), the long time decay of the spin-spin correlation function is always algebraic for all  $t_w > 0$  (therefore characteristic of equilibrium zero temperature behavior),  $C_{\{S_z, S_z\}}^{(\text{cum})}(\tau, t_w) \propto \tau^{-2}$ .

## 5.4 Kondo Limit

The Kondo limit with small coupling constants  $J_{\perp}, J_{\parallel} \rightarrow 0$  is the relevant regime for experiments on quantum dots. In this regime our results for the spin-spin correlation function are not exact, but were shown to be very accurate by comparison with asymptotically exact results for  $t_w = 0$  and  $\tau/t_K \gg 1$  by Lesage and Saleur (1998). For our purposes here the main difference from the Toulouse point analysis is the nontrivial structure of the effective parameters  $g_{kk'}$  and  $V_k$  from Lobaskin and Kehrein (2005a) in (3.11). This makes it impossible to give closed analytic expressions like (3.67) or (3.68), but the numerical solution of the quadratic Hamiltonian (3.11) is still straightforward. The results presented in

this section were obtained by numerical diagonalization of (3.11) with 4000 band states. The numerical errors from the discretization are very small (less than 2% relative error in all curves). Notice that a large number of band states is important for analyzing the behavior for small waiting time: one must ensure that  $t_w \gg 1/\Lambda$  where  $\Lambda$  is the ultraviolet cutoff in order to obtain universal curves that only depend on the low energy scale  $T_K$ .

Fig. 5.3 shows the behavior of the spin-spin correlation function and the response function obtained in this manner. Similar to the Toulouse point results we observe a violation of the FDT for finite nonzero waiting time,  $0 < t_w < \infty$ . For  $t_w \rightarrow \infty$  one recovers the FDT exponentially fast (5.62) as expected since the system equilibrates. The results for the effective temperature in the Kondo limit are depicted in Fig. 5.4. While the behavior of  $T_{\text{eff}}(t_w)$  is somehow more complicated than at the Toulouse point, the interpretation regarding heating and cooling effects carries over without change. The main difference is that the maximum effective temperature is already reached for  $t_w \approx 0.03t_K$  in the Kondo limit. We interpret this as being due to the (dimensionful) bare coupling constants at higher energies that are larger than the renormalized low energy scale  $T_K$  and therefore lead to faster heating.

## 5.5 Conclusion

Our investigation of the zero temperature quantum limit of the fluctuation-dissipation theorem in the time-dependent Kondo model provides some important lessons regarding its relevance in quantum nonequilibrium systems. For the Kondo system prepared in an initial state with a frozen impurity spin, i.e. in a *product state* of system and environment, the FDT is violated for all nonzero waiting times  $t_w$  of the first measurement after switching on the spin dynamics at  $t = 0$ . For large waiting times as compared to the Kondo time scale the FDT becomes fulfilled exponentially fast, which indicates the quantum equilibration of the Kondo system. A quantitative measure for the violation of the FDT is provided by the *effective temperature*  $T_{\text{eff}}$  (Cugliandolo et al. 1997) here defined via the spin dynamics (5.24) and depicted in Figs. 5.2 and 5.4. It traces the buildup of fluctuations in the conduction band: Initially, the conduction band electrons are in equilibrium with respect to the Hamiltonian for  $t < 0$ . Then in the vicinity of the impurity they get locally “heated up” to  $T_{\text{eff}}$  about  $0.4T_K$  (Toulouse point)/  $0.45T_K$  (Kondo limit) due to the release of the binding energy when the Kondo singlet is being formed. Eventually, this excess energy diffuses away to infinity and  $T_{\text{eff}}$  reaches zero again. In this sense the largest deviation from zero temperature equilibrium behavior occurs for  $t_w \approx 0.1t_K$  at the Toulouse point, and for  $t_w \approx 0.03t_K$  in the experimentally relevant Kondo limit, with very rapid initial heating (see the inset in Fig. 5.2). These observations could be relevant for

designing time-dependent (functional) nanostructures with time-dependent gate potentials (Nordlander et al. 1999) since they give a quantitative insight into how long one needs to wait after switching for the system to return to *effectively* zero temperature.

From a theoretical point of view it would be interesting to study the FDT for other observables (like the current) and in other nonequilibrium quantum impurity systems in order to see which of the above observations are generic. Notice that the “effective temperature” will generally depend on the observable chosen for its definition in (5.24) (Calabrese and Gambassi 2004), though we suggest that the qualitative behavior (rapid initial increase and exponential decrease) will be similar for all local observables. Work along such lines is in progress in order to substantiate the concept and notion of an “effective temperature” qualitatively characterizing the evolving nonequilibrium quantum state, and to explore its usefulness in quantum nonequilibrium models in general.

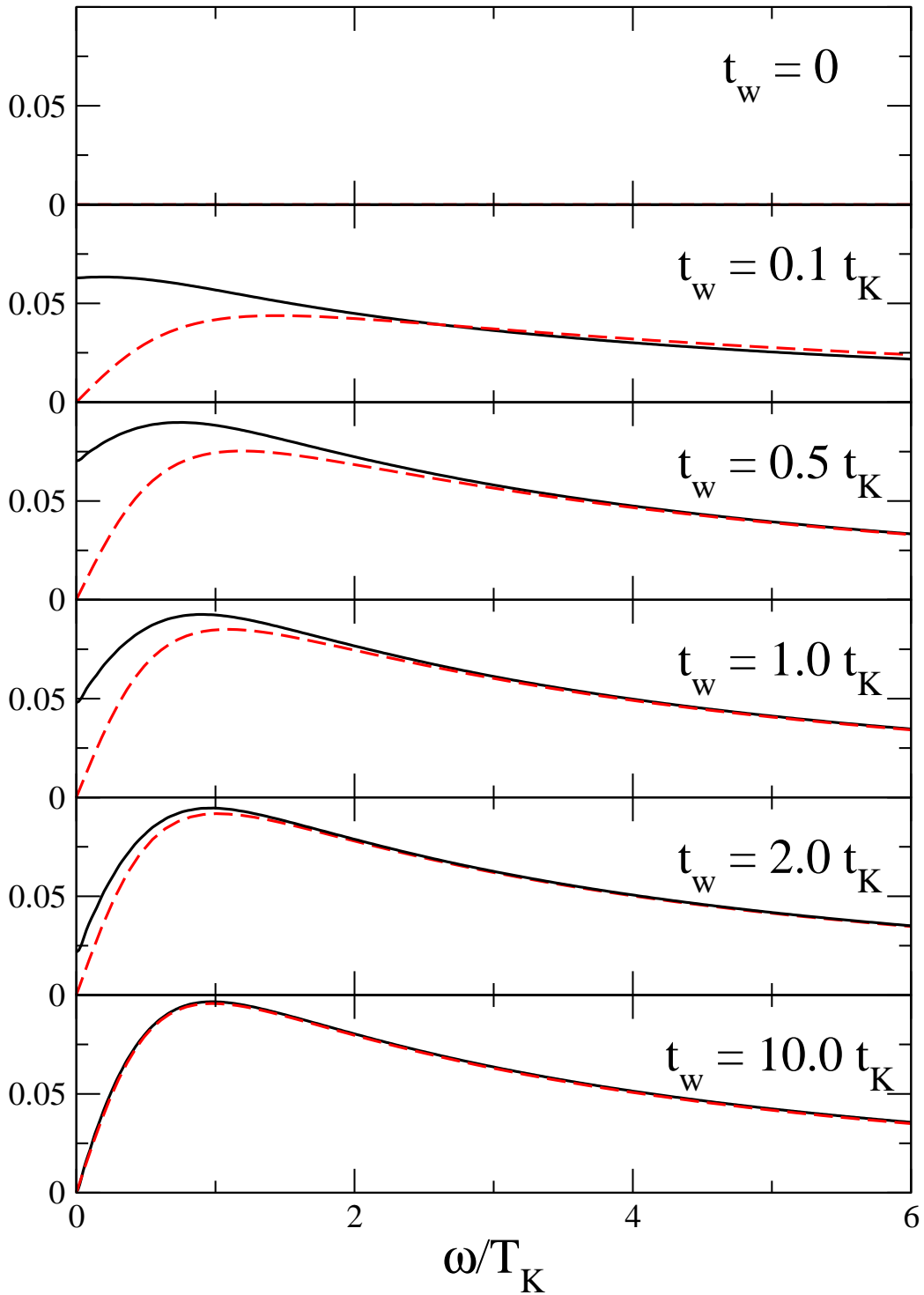


**Figure 5.3:** Universal curves for the spin-spin correlation function  $T_K \times C_{\{S_z, S_z\}}^{(\text{cum})}(\omega, t_w)$  (solid line) and response function  $T_K \times \text{Im } R(\omega, t_w)$  (dashed line) in the Kondo limit (compare with Fig. 5.1).

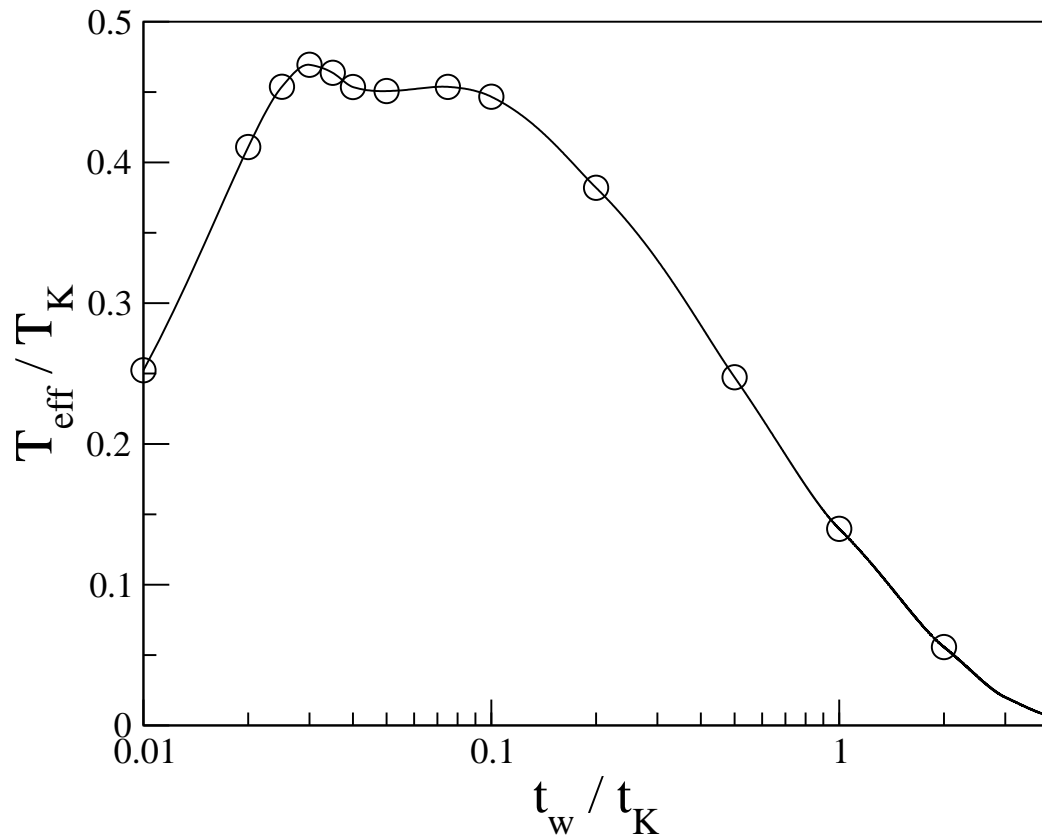


**Figure 5.4:** Effective temperature  $T_{\text{eff}}$  as a function of the waiting time  $t_w$  in the Kondo limit. The line is a guide to the eye. The size of the datapoints (circles) indicates the numerical error. The datapoint for  $t_w/t_K = 5.5$  is numerically indistinguishable from zero.

## 6. QUASIPARTICLE SPECTRAL FUNCTION

### 6.1 Nonequilibrium Spectral Density

In experiment one typically measures the conductance of a given sample. A quantum dot suddenly shifted into the Kondo regime exhibits an increase in the conductance due to a forming of the Kondo resonance at the Fermi energy. Thus, calculating the time-dependent spectral function of the dot we can determine development of the time-dependent current at a finite bias voltage (Wingreen and Meir 1992). Standard definition of the spectral function can be extended to the non-equilibrium as

$$\rho_{\text{imp}}(\epsilon, t) \stackrel{\text{def}}{=} \text{Re} \int_0^\infty \frac{d\tau}{\pi} e^{i\epsilon\tau} \left\langle \{c_{0\alpha}(t), c_{0\alpha}^\dagger(t - \tau)\} \right\rangle, \quad (6.1)$$

where  $c_{0\alpha}, c_{0\alpha}^\dagger$  is the localized electron orbital at the impurity site. All operators belong to the original Anderson Hamiltonian (2.1) and describe real conduction band electrons. Actual integration runs only from zero to  $t$ , since for all negative times impurity orbital is decoupled. In equilibrium all dependence on  $t$  should vanish. In non-equilibrium it should asymptotically reach the equilibrium value at large times.

Exact evaluation of the non-equilibrium spectral function of the original Hamiltonian (2.1) is only possible for a zero on-site interaction  $U = 0$ . Then the model is simply the non-interacting resonant level model which we have already intensively used.

### Non-equilibrium spectral function of the non-interacting resonant level model

Now we derive an expression for the time-dependent spectral density in the case of the non-interacting resonant level model. We assume the hybridization term is switched off for all negative times. The reason for this calculation is not purely pedagogical since we use this result in our further study.

For the non–equilibrium resonant level model the time dependent spectral density is naturally defined as the spectral function of dot electrons

$$\rho_{\text{imp}}^{\text{RLM}}(\epsilon, t) \stackrel{\text{def}}{=} \text{Re} \int_0^\infty \frac{d\tau}{\pi} e^{i\epsilon\tau} \langle \{d(t), d^\dagger(t-\tau)\} \rangle . \quad (6.2)$$

Time dependence of operators  $d$  and  $d^\dagger$  might be expressed in the same way as we have already done for calculation of the magnetization and spin–spin correlation function

$$d(t) = \sum_\epsilon A_{d\epsilon} a_\epsilon(t) \quad (6.3)$$

and

$$d^\dagger(t) = \sum_\epsilon A_{d\epsilon}^\dagger a_\epsilon^\dagger(t). \quad (6.4)$$

Equations of motion in diagonal basis are simple

$$a_\epsilon(t) = a_\epsilon e^{-i\epsilon t} \quad (6.5)$$

and

$$a_\epsilon^\dagger(t) = a_\epsilon^\dagger e^{i\epsilon t}. \quad (6.6)$$

Substituting them into the definition of the spectral function (6.2) we get

$$\begin{aligned} \rho_{\text{imp}}^{\text{RLM}}(\epsilon, t) &= \\ &= \text{Re} \int_0^t \frac{d\tau}{\pi} e^{i\epsilon\tau} \left\langle \left\{ \sum_{\epsilon'} A_{d\epsilon'} a_{\epsilon'}(t), \sum_{\epsilon''} A_{d\epsilon''}^\dagger a_{\epsilon''}^\dagger(t-\tau) \right\} \right\rangle = \\ &= \text{Re} \int_0^t \frac{d\tau}{\pi} e^{i\epsilon\tau} \sum_{\epsilon'\epsilon''} A_{d\epsilon'} A_{d\epsilon''}^\dagger e^{-i\epsilon't} e^{i\epsilon''(t-\tau)} \langle \{a_{\epsilon'}(0), a_{\epsilon''}^\dagger(0)\} \rangle = \\ &= \text{Re} \int_0^t \frac{d\tau}{\pi} e^{i\epsilon\tau} \sum_{\epsilon'\epsilon''} A_{d\epsilon'} A_{d\epsilon''}^\dagger e^{-i\epsilon't} e^{i\epsilon''(t-\tau)} \delta_{\epsilon'\epsilon''} = \\ &= \text{Re} \int_0^t \frac{d\tau}{\pi} \sum_{\epsilon'} |A_{d\epsilon'}|^2 e^{i(\epsilon-\epsilon')\tau} . \end{aligned} \quad (6.7)$$

If we perform the  $\tau$ –integration in above formula we obtain

$$\boxed{\rho_{\text{imp}}^{\text{RLM}}(\epsilon, t) = \frac{1}{\pi} \int d\epsilon' \frac{\sin(\epsilon - \epsilon')t}{\epsilon - \epsilon'} |A_{d\epsilon'}|^2} . \quad (6.8)$$

In  $t \rightarrow \infty$  limit we get the equilibrium spectral function, as it should be, since

$$|A_{d\epsilon'}|^2 \equiv \rho_d(\epsilon'), \quad (6.9)$$

where  $\rho_d(\epsilon)$  is the equilibrium density of states at the impurity site and

$$\lim_{t \rightarrow \infty} \frac{1}{\pi} \frac{\sin(\epsilon - \epsilon')t}{\epsilon - \epsilon'} = \delta(\epsilon - \epsilon') \quad (6.10)$$

is one of the representations of the Dirac  $\delta$ –function.

## 6.2 Results of the Fermi Liquid Theory

If we try to use the formula (6.1) in the non-equilibrium Kondo model we encounter severe complications due to non-trivial dependence of operators  $c_0$  and  $c_0^\dagger$  on the operators of the corresponding effective model. It is very hard to find the time-evolution of those operators even at the exactly solvable Toulouse point. Therefore, to calculate spectral density, we use another approach, namely, the Fermi liquid theory.

The Fermi liquid theory of Landau based on the assumption that the low-lying energy excitations of a system of interacting fermions are equivalent to excitations of the non-interacting system. As we have established in previous chapters the time-dependent Kondo model is equivalent to the resonant-level model with the constant hybridization function at the Toulouse point and strongly  $k$ -dependent in the Kondo limit of small couplings  $J$ . These effective models describe the spin sector. However since after the bosonization procedure the charge excitations are non-interacting and decoupled completely we can study only the contribution of spin excitations into the total spectral density. According to the Landau Fermi liquid picture this contribution should give the same low-energy behavior as the strongly interacting initial model. All low-energy quantities can be identified with the help of the effective model after some rescaling. While a bias voltage is much smaller than the Kondo temperature, which determine the width of the Kondo resonance, the behavior of the conductance can be formulated in the language of the effective model. If we find the time-dependent quasiparticle spectral function of the effective model we immediately get the spectral function of the original model at low energies.

According to that reasoning, if we succeed in evaluating  $\rho_{\text{eff}}(\epsilon, t)$  which is the time-dependent spectral function measured at time  $t$  after the switching on the Kondo coupling, we may claim that up to some constant factor  $z$  it is proportional to the total density of states near the Fermi energy

$$\boxed{\rho(\epsilon, t) = z\rho_{\text{eff}}(\epsilon, t)}. \quad (6.11)$$

This constant  $z$  is usually called wave-function renormalization factor in the Fermi liquid studies.

In our derivation we used the effective non-interacting resonant level model. "Conduction band" in this model is not equivalent to the real conduction band of the system made of spin 1/2 electrons. The effective resonant level model defined at the spin sector describes spinless quasiparticles which are very complicated spin excitations of real electrons. Although in the Toulouse point case they obey fermionic commutation relations, in the physical limit they are introduced by the vertex operators (2.36) which do not have simple statistics. Our usage

of the effective resonant level model with  $k$ -dependent hybridization is only an approximate solution of the flow equations, which provides the right low-energy spectrum, but does not explain the real physical nature of quasiparticles. As we have already seen in the exactly solvable case they are very complicated structures made of original electron spin-density excitations and, of course, situation does not become simpler in the Kondo limit.

Our approximation is the following: we assume that  $z$  factor remains time-independent in the non-equilibrium situation or, at least, it remains constant on the scale of order of  $t_K = 1/T_K$ . Then one is to calculate only the spectral function for the effective resonant level model, which ingredients are already given in previous section.

### 6.3 Buildup of the Kondo Resonance

At the exactly solvable Toulouse point hybridization function is constant. Using (6.8) and (3.43) we obtain the following analytic result

$$\begin{aligned}
\rho_{\text{eff}}(\epsilon, t) &= \rho_{\text{imp}}^{\text{RLM}}(\epsilon, t) = \\
&= \text{Re} \int_0^t \frac{d\tau}{\pi} \sum_{\epsilon'} \frac{\Delta}{\epsilon'^2 + \Delta^2} e^{i(\epsilon - \epsilon')\tau} = \\
&= \text{Re} \int_0^t \frac{d\tau}{\pi} e^{i\epsilon\tau} e^{-\Delta\tau} = \\
&= \text{Re} \frac{1}{\pi} \frac{e^{i\epsilon t - \Delta t} - 1}{i\epsilon - \Delta} = \\
&= \frac{1}{\pi} \frac{\Delta (1 - \cos(\epsilon t) e^{-\Delta t}) + \epsilon \sin(\epsilon t) e^{-\Delta t}}{\Delta^2 + \epsilon^2} = \\
&= \frac{t_B}{\pi} \frac{1 - \cos(\epsilon t) e^{-t/t_B} + \epsilon t_B \sin(\epsilon t) e^{-t/t_B}}{1 + \epsilon^2 t_B^2}. \tag{6.12}
\end{aligned}$$

The buildup of the quasiparticle resonance at the Toulouse point is shown in Fig. 6.1. Comparing these curves with similar curves in Nordlander et al. (Nordlander et al. 1999), one sees the same characteristic oscillations of the spectral function with the frequency equal to the time of the measurement  $t$ . Notice the presence of a local minimum at the Fermi energy, its depth tends to zero exponentially fast

$$\boxed{\rho_{\text{eff}}(0, t) = \frac{1}{\pi\Delta} (1 - \exp(-t/t_B))}. \tag{6.13}$$

Numerical results for the buildup of the quasiparticle resonance in the Kondo limit are depicted in Fig. 6.2. One observes much less spectral weight in tail

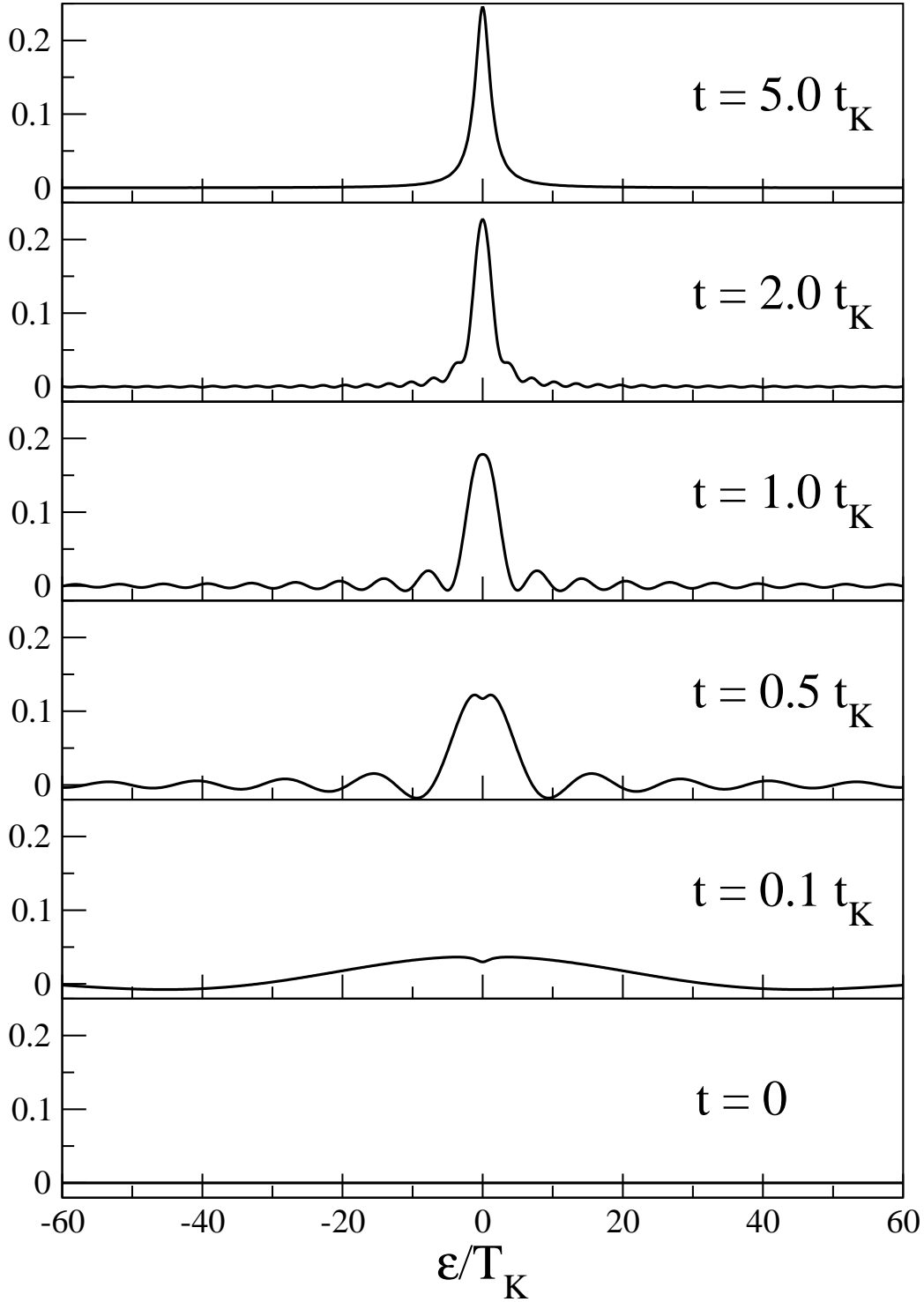


**Figure 6.1:** Universal curves for a quasiparticle density of states  $T_K \times \rho_{\text{eff}}(\epsilon, t)$  at the Toulouse point. Notice a presence of a local minimum at the Fermi energy, its depth tends to zero exponentially fast:  $\rho_{\text{eff}}(0, t) = \frac{1}{\pi\Delta} (1 - \exp(-t/t_B))$ . Equilibrium curve ( $t \rightarrow \infty$ ) is normalized to unity:  $\int \rho_{\text{eff}}(\epsilon, \infty) d\epsilon = 1$ .

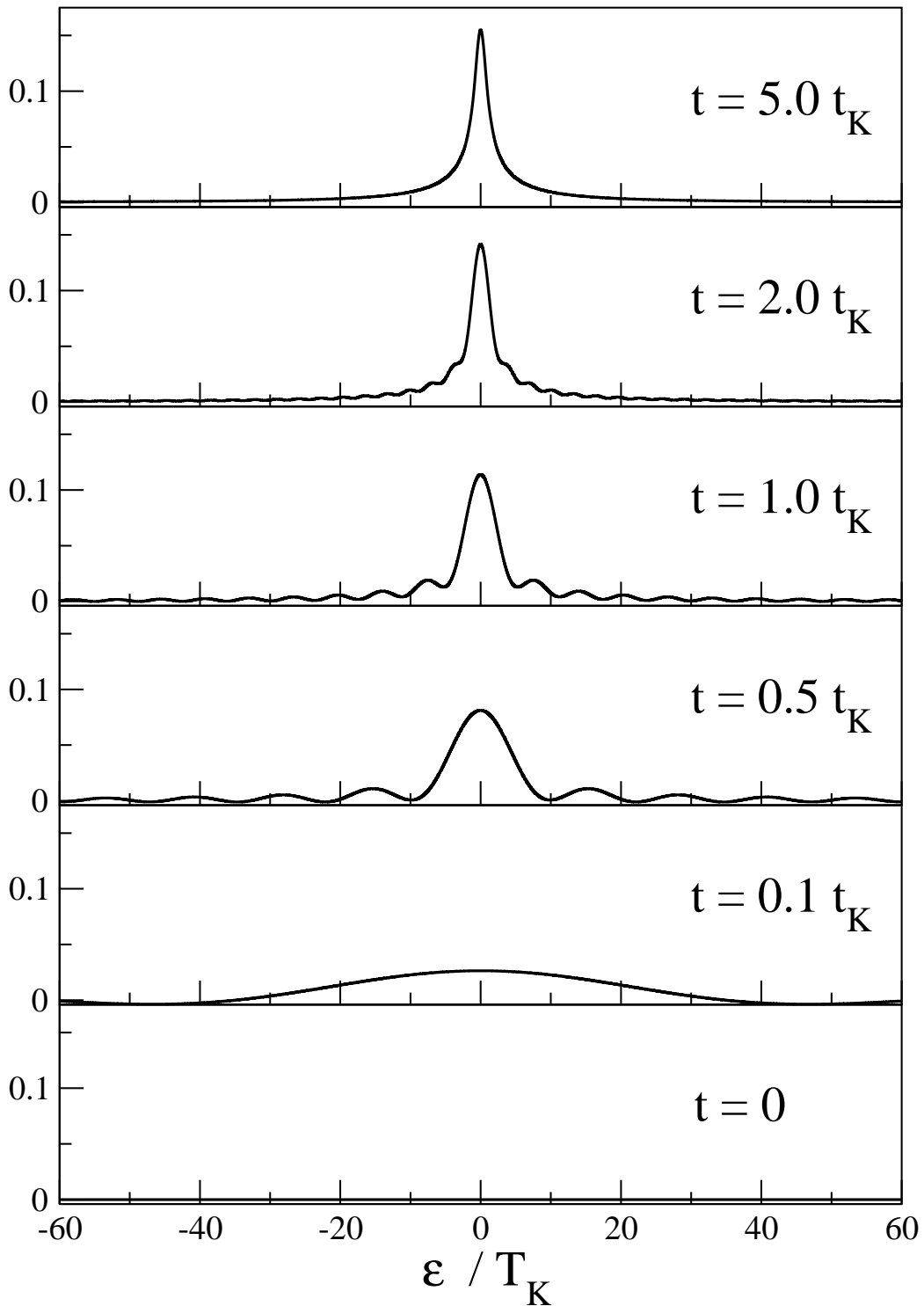


**Figure 6.2:** Universal curves for a quasiparticle density of states  $T_K \times \rho_{\text{eff}}(\epsilon, t)$  in the Kondo limit. Notice the absence of the local minimum in contrast to the Toulouse point result and much less spectral weight in the tail oscillations.

oscillations. The local minimum at the Fermi energy is absent in contrast to the Toulouse point curves.

An interesting observation which immediately follows from these pictures is negativity of the spectral functions at some values of the energy for rather small times of the measurement comparing with  $t_K$ . Of course, in equilibrium the spectral function is just the single-particle density of states and is strictly non-negative as we see in the limit  $t \rightarrow \infty$  of our non-equilibrium results. However, at intermediate times the non-equilibrium spectral function is clearly negative at some points away from the Fermi energy. Consequently, at intermediate times in some energy intervals the differential conductance might be also negative since it is the quantity proportional to the spectral density (Wingreen and Meir 1992). For instance, if we apply asymmetric bias voltage, then, in principle, we could observe this effect. Change of sign of the differential conductance will lead to non-equilibrium current oscillations around its steady state value, which, in its turn, might be observed in experiment.

## 6.4 Conclusion

We have calculated the buildup of the quasiparticle spectral function of the non-equilibrium Kondo model for two types of the initial preparations I) and II). We used the Fermi-liquid theory to connect it with the original one-particle spectral function in the vicinity of the Fermi energy. Results are not unexpected in view of our previous calculations. As all previously calculated quantities which are connected with the impurity degree of freedom, the quasiparticle spectral function decays exponentially fast towards its equilibrium value. Sharp initial condition leads to Fridel-type oscillations in energy with the frequency identified by a distance to the time of switching on the coupling. The magnitude of such oscillations decays with time but initially it is large enough to make the spectral function negative at some energies away from the Fermi level. We believe it should be very interesting to check our result in experiment to verify whether the Fermi-liquid picture stays unchanged in non-equilibrium.



## 7. SUMMARY

In conclusions we would like to present a summary of the main results of this work and give an outlook.

We have investigated the non-equilibrium Kondo problem for two types of initial non-equilibrium conditions:

- I) the impurity spin is initially decoupled from the Fermi sea and then at some time the coupling is switched on;
- II) the impurity spin is frozen for some time (e.g. by a strong magnetic field) and at a certain time constraint is released

### Exact results at the Toulouse point

We have calculated the spin-spin correlation function of the impurity spin defined as the average of the spin operators with respect to the non-equilibrium initial states I) and II). In equilibrium, it is known that this quantity should decay algebraically at large times. However, if one of the measurements happens at zero time then this function is identical to the magnetization and should vanish exponentially. To resolve this puzzle we have used the bosonization and the refermionization approach to derive spin-spin correlation function at the exactly solvable Toulouse point. The main results are given for the symmetrized (real) part of the spin-spin correlator by Eq.(3.67)

$$C_{\{S_z, S_z\}}(t_w + \tau, t_w) = \frac{1}{4} e^{-2\tau/t_B} - (s(\tau) - s(t_w + \tau)e^{-t_w/t_B} + s(t_w)e^{-(t_w+\tau)/t_B})^2, \quad (7.1)$$

and for the antisymmetrized (imaginary) part by Eq.(3.68)

$$C_{[S_z, S_z]}(t_w + \tau, t_w) = -i e^{-\tau/t_B} \left( s(\tau) - s(t_w + \tau)e^{-t_w/t_B} + s(t_w)e^{-(t_w+\tau)/t_B} \right), \quad (7.2)$$

where

$$s(\tau) \stackrel{\text{def}}{=} \frac{t_B}{\pi} \int_0^\infty d\omega \frac{\sin(\omega\tau)}{1 + \omega^2 t_B^2} \quad (7.3)$$

One may see exponential approach to the equilibrium algebraic long time decay with waiting time  $t_w$  going to infinity. This is purely Fermi liquid property which cannot be obtained, for example, by the non-crossing approximation (Nordlander et al. 1999). It is the first analytic result regarding this exponential to algebraic non-equilibrium crossover.

## Correlation functions in the Kondo limit

In the Kondo limit of small isotropic couplings we have used the results of the flow-equation approach which establish an equivalence between the Kondo model and the non-interacting resonant level model with the non-trivial hybridization function (Slezak et al. 2003). This correspondence is valid in the low energy sector and provides reliable (up to 5% error) results for any spin correlation function. The solution is qualitatively the same with the Toulouse point solution. The main result is that the relaxation of the impurity spin happens exponentially fast at large times as

$$P(t) = \langle S_z \rangle \sim e^{-\frac{2t}{t_B}} \quad (7.4)$$

with the parameter  $t_B$  proportional to the inverse Kondo temperature

$$t_B = \frac{\pi w}{T_K}. \quad (7.5)$$

At smaller times comparable with the  $t_B$  the relaxation is even faster due to unrenormalized couplings at high energies. This result obtained asymptotically by Lesage and Saleur (1998) now is available at all time scales with the help of the flow-equation method. To our knowledge it is the first result providing the full crossover at all intermediate times. It can serve further as the reference for all numerical methods used for investigation of the non-equilibrium Kondo model (e.g. numerical renormalization group, density-matrix renormalization group, Monte-Carlo etc.).

Spin-spin correlator crosses into the algebraic long time decay exponentially fast at large times of the first measurement. At shorter times the relaxation is faster than exponential as well as in the magnetization result. Qualitative equivalence with the exactly solvable Toulouse point tells us that solution for the spin-spin correlation function at this point is generic and can provide valuable insight into the physical relevant Kondo limit as well. Though, one should be very careful with such a generalization since some very important quantities like the Wilson's ratio are different from the strong coupling regime.

One of the main conclusions of our investigation is the exponential crossover to equilibrium of the time-dependent Kondo model with the prepared initial state. A very important point is that relaxation for impurity observables doesn't

depend at all on the incipient state of conduction band electrons. Although equilibration is governed by exchange processes between the impurity degree of freedom and the bath, only a coupling strength (the Kondo temperature) and an initial impurity state (the spin polarization) are essential to determine the behavior of correlation functions in such a factorized non-equilibrium situation. This important qualitative feature should hold for any observable which can be directly related with the impurity degree of freedom, which we have shown, as an important example, for a quasiparticle density of states.

## Quasiparticle spectral function

Since in experiment it is sometimes easier to measure electronic transport than magnetic properties of a sample, our results for the non-equilibrium quasiparticle spectral function is a good starting point for experimental validation of the exponential relaxation of observables in the non-equilibrium Kondo model. The spectral function is proportional to the differential conductance of a sample which means that according to our results the non-equilibrium current should reach its equilibrium linear response value exponentially fast as well. An interesting feature, which we have also observed, is the negative spectral function at some energy intervals at intermediate times. This might lead to current oscillations during its equilibration in certain experiments.

## FDT violation and effective temperature

Another important point is impossibility to interpret our zero-temperature results using the concept of the time-dependent effective temperature in a simple way. For arbitrary small time of the measurement one will immediately "see" algebraic long-time decay of the spin-spin correlation function, which is particular feature of the zero-temperature case. An attempt to introduce the effective temperature using the buildup of the non-equilibrium spectral function (Nordlander et al. 1999) is not consistent in our opinion, since in that case it is defined not by a magnitude of fluctuations in the system but by means of an average current through a quantum dot. In this manner, physically appropriate definition of the effective temperature should be given by a current-current correlator, for example.

In a field of glassy system, which is most widely investigated in this context, the concept of the effective temperature is introduced via the violation of the fluctuation-dissipation relation. We have followed this line and have investigated the zero temperature quantum limit of the fluctuation-dissipation theorem in the time-dependent Kondo model. For the Kondo system prepared in a product initial state of impurity spin and environment, the FDT is violated for all nonzero

waiting times  $t_w$  of the first measurement after switching on the spin dynamics at  $t = 0$ . For large waiting times as compared to the Kondo time scale the FDT becomes fulfilled exponentially fast, since both spin–spin correlation function and generalized response function approach their equilibrium values exponentially as well. A quantitative measure for the violation of the FDT is provided by the *effective temperature*  $T_{\text{eff}}$  which we have defined via the spin dynamics (5.24). It traces the buildup of fluctuations in the conduction band. Initially, the conduction band electrons are in equilibrium with respect to the Hamiltonian for  $t < 0$ . Then in the vicinity of the impurity they get locally “heated up” to  $T_{\text{eff}}$  about  $0.4T_K$  at the Toulouse point, and about  $0.45T_K$  in the Kondo limit of small and isotropic coupling constants due to the release of the binding energy when the Kondo singlet is being formed. Eventually, this excess energy diffuses away to infinity and  $T_{\text{eff}}$  reaches zero again. In this sense the largest deviation from zero temperature equilibrium behavior occurs for  $t_w \approx 0.1t_K$  at the Toulouse point, and for  $t_w \approx 0.03t_K$  in the experimentally relevant Kondo limit, with very rapid initial heating. These conclusions could be relevant for designing time-dependent functional nanostructures with time-dependent gate potentials since they give a quantitative insight into how long one needs to wait after switching for the system to return to effectively zero temperature.

## Some open questions

From a theoretical point of view it would be interesting to study the FDT for other observables (like the current) and in other nonequilibrium quantum impurity systems in order to see which of the above observations are generic. In principle, a direct behavior of the “effective temperature” will generally depend on the observable chosen for its definition. However, we suggest that the qualitative behavior in the non–equilibrium Kondo model with a factorized initial state, namely, rapid initial increase and exponential decrease, will be similar for all local observables. Eventually, study of different definitions of the effective temperature might be very useful in further investigations of quantum non–equilibrium models in general.

One of the possible non–equilibrium Kondo model extensions is the periodic switching on/off of the Kondo coupling, which can be, most probably, much easier realized in experiment. In this case, one is interested in calculation of the spin–spin correlation function and its equilibration as well. The natural question of the fulfillment of the fluctuation dissipation theorem arises again. We pump additional energy into the system during the time of switching on/off. Due to that the fluctuation–dissipation theorem will be inevitably violated. What is the effective temperature during such a pumping? how is it connected with the frequency of an external field? - these are the natural questions to answer.

Of course, this list of topics to be studied is quite far from being exhaustive. Non-equilibrium many-body physics in general and the non-equilibrium Kondo model in particular are extremely rich and exciting in physical content. We hope that some obtained results and developed ideas will aid in further investigations of other non-equilibrium strongly correlated models as well.



# APPENDIX



## A. DETAILS OF NON-REGULAR SUM CALCULATIONS

In this Appendix we give an extended proof of Eq.(3.82). Using trigonometric formulas the difference between left and right parts of (3.82) can be written as

$$\begin{aligned} \sum_{\varepsilon} \frac{1}{\varepsilon - p} - \frac{\pi}{\Delta_L} \frac{p + \Delta \tan \delta}{\Delta - p \tan \delta} &= \\ &= \sum_n \frac{1}{\varepsilon_n - p} - \frac{\pi}{\Delta_L} \frac{1}{\tan(\delta_p - \delta)} \end{aligned} \quad (\text{A.1})$$

where

$$\delta_p \stackrel{\text{def}}{=} \arctan \frac{\Delta}{p} \quad \text{and} \quad p = \Delta_L \left( k + \frac{1}{2} \right) + \Delta_L \frac{\delta}{\pi}. \quad (\text{A.2})$$

Substituting spectrums (3.44) and (3.60) we get for (A.1)

$$\begin{aligned} \frac{\pi}{\Delta_L} \sum_n \left[ \frac{1}{\pi \left( n + \frac{1}{2} \right) + \delta_n - \pi \left( k + \frac{1}{2} \right) - \delta} - \frac{1}{\pi n + \delta_p - \pi k - \delta} \right] &= \\ &= \frac{\pi}{\Delta_L} \sum_n \left[ \frac{1}{\pi (n - k) + \delta_n - \delta} - \frac{1}{\pi (n - k) + \delta_p - \delta} \right] = \\ &= \frac{\pi}{\Delta_L} \sum_{n'} \frac{\delta_p - \delta_{n'+k}}{(\pi n' + \delta_{n'+k} - \delta)(\pi n' + \delta_p - \delta)}. \end{aligned} \quad (\text{A.3})$$

Now we need to prove that this sum vanishes in the thermodynamic limit. One can do that showing that it is proportional to  $\Delta_L$ .

For  $p > \Delta$  the sum (A.3) has two regions of summation

$$|n'| \gtrsim \frac{\Delta}{\Delta_l} \quad \text{and} \quad |n'| \lesssim \frac{\Delta}{\Delta_l}. \quad (\text{A.4})$$

In the first region it can be estimated as

$$\sum_{n'} \dots \sim \sum_{n'} \frac{\delta_p - \delta_{n'+k}}{(\pi n')^2} \sim \frac{1}{n'} \sim \frac{\Delta_L}{\Delta}. \quad (\text{A.5})$$

since the nominator is of order of unity in this region.

In the second region we can estimate the nominator according to

$$\begin{aligned} \delta_p - \delta_{n'+k} &= \arctan \frac{\Delta}{p} - \arctan \frac{\Delta}{\varepsilon_{n'+k}} = \\ &= \arctan \frac{\Delta_L n' \Delta}{p^2 + \Delta^2 + p \Delta_L n'} \leq \arctan \frac{\Delta_L n'}{\Delta} < \frac{\Delta_L n'}{\Delta} . \end{aligned} \quad (\text{A.6})$$

Substituting the estimate for the nominator into the sum we get

$$\sum_{n'} \dots \sim \sum_{|n'| \lesssim \Delta / \Delta_L} \frac{\Delta_L n'}{\Delta (\pi n' + \delta_{n'+k} - \delta) (\pi n' + \delta_p - \delta)} \sim \Delta_L . \quad (\text{A.7})$$

Thus the sum (A.3) vanishes in the thermodynamic limit.

For the case  $\Delta > p$  we can follow the same steps just changing  $\Delta$  by  $p$  in the regions of integration and in the nominator estimate which finishes the proof.

## BIBLIOGRAPHY

- Abrikosov, A. A.: 1965, *Physics* **2**, 5.
- Affleck, I. and Ludwig, A. W. W.: 1991a, *Nucl. Phys. B* **352**, 849.
- Affleck, I. and Ludwig, A. W. W.: 1991b, *Nucl. Phys. B* **360**, 641.
- Affleck, I. and Ludwig, A. W. W.: 1991c, *Phys. Rev. Lett.* **67**, 161.
- Affleck, I. and Ludwig, A. W. W.: 1991d, *Phys. Rev. Lett.* **67**, 3160.
- Affleck, I. and Ludwig, A. W. W.: 1992, *Phys. Rev. Lett.* **68**, 1046.
- Affleck, I. and Ludwig, A. W. W.: 1993, *Phys. Rev. B* **48**, 7297.
- Affleck, I. and Ludwig, A. W. W.: 1994, *Nucl. Phys. B* **428**, 545.
- Aguado, R. and Langreth, D. C.: 2000, *Phys. Rev. Lett.* **85**, 1946.
- Alhassid, Y.: 2000, *Rev. Mod. Phys.* **72**, 4.
- Anderson, P. W.: 1961, *Phys. Rev.* **124**, 41.
- Anderson, P. W.: 1967, *Phys. Rev.* **164**, 352.
- Anderson, P. W. and Yuval, G.: 1969, *Phys. Rev. Lett.* **23**, 89.
- Anderson, P. W. and Yuval, G.: 1970, *Phys. Rev. B* **1**, 1522.
- Anderson, P. W., Yuval, G. and Hamann, D. R.: 1970, *Phys. Rev. B* **1**, 4464.
- Andrei, N.: 1980, *Phys. Rev. Lett.* **45**, 379.
- Appelbaum, J.: 1966, *Phys. Rev. Lett.* **17**, 91.
- Appelbaum, J.: 1967, *Phys. Rev.* **154**, 633.
- Appelbaum, J., Phillips, J. C. and Tzouras, G.: 1967, *Phys. Rev.* **160**, 554.
- Appelbaum, J. and Shen, L. Y.: 1972, *Phys. Rev. B* **5**, 544.
- Averin, D. V. and Likharev, K. K.: 1986, *J. Low. Temp. Phys.* **62**, 345.

- Ben-Jacob, E. and Gefen, Y.: 1985, *Phys. Lett. A* **108**, 289.
- Bermon, S., Paraskevopoulos, D. E. and Tedrow, P. M.: 1978, *Phys. Rev. B* **17**, 210.
- Bethe, H.: 1931, *Z. Phys.* **71**, 205.
- Bickers, N. E.: 1987, *Rev. Mod. Phys.* **59**, 845.
- Bickers, N. E., Cox, D. L. and Wilkins, J. H.: 1987, *Phys. Rev. B* **36**, 2036.
- Biroli, G. and Parcollet, O.: 2002, *Phys. Rev. B* **65**, 094414.
- Blandin, A. and Friedel, J.: 1959, *J. Phys. Radium* **20**, 160.
- Bloomfield, P. E. and Hamann, D. R.: 1967, *Phys. Rev.* **164**, 856.
- Brandt, U., Keiter, H. and Liu, F. S.: 1985, *Z. Phys B* **58**, 267.
- Calabrese, P. and Cardy, J.: 2005, *JSTAT* **0504**, P010.
- Calabrese, P. and Gambassi, A.: 2004, *J. Stat. Mech.* p. P07013.
- Calabrese, P. and Gambassi, A.: 2005, *J. Phys. A: Math. Gen.* **38**(18), R133–R193.
- Callen, H. B. and Welton, T. A.: 1951, *Phys. Rev.* **83**, 34.
- Coleman, P., Hooley, C., Avishai, Y., Goldin, Y. and Ho, A. F.: 2002, *J. Phys.: Condens. Matter* **14**, L205–L211.
- Costi, T. A.: 1997, *Phys. Rev. B* **55**, 3003.
- Cronenwett, S. M., Oosterkamp, T. H. and Kouwenhoven, L. P.: 1998, *Science* **281**, 540.
- Cugliandolo, L. F., Grepel, D. R., Lozano, G. and Lozza, H.: 2004, *Phys. Rev. B* **70**, 024422.
- Cugliandolo, L. F., Grepel, D. R., Lozano, G., Lozza, H. and da Silva Santos, C. A.: 2002, *Phys. Rev. B* **66**, 014444.
- Cugliandolo, L. F., Kurchan, J. and Peliti, L.: 1997, *Phys. Rev. E* **55**, 3898.
- Cugliandolo, L. F. and Lozano, G.: 1999, *Phys. Rev. B* **59**, 915.
- de Haas, W. J., de Boer, J. H. and van den Berg, G. J.: 1934, *Physica* **1**, 1115.
- Egger, R.: 2004, *Phys. Rev. Lett.* **93**, 047002.

- Fisher, K. H. and Hertz, J. A.: 1991, *Spin Glasses*, Cambridge University Press, Cambridge.
- Folk, J. A., Patel, S. R., Godijn, S. F., Huibers, A. G., Cronenwett, S. M., Markus, C. M., Campman, K. and Gossard, A. C.: 1996, *Phys. Rev. Lett.* **76**, 1699.
- Franceschi, S. D., Hanson, R., van der Wiel, W. G., Elzerman, J. M., Wijkema, J. J., Fujisawa, T., Tarucha, S. and Kouwenhoven, L. P.: 2002, *Phys. Rev. Lett.* **89**, 156801.
- Friedel, J.: 1952, *Phil. Mag.* **43**, 153.
- Friedel, J.: 1956, *Can. J. Phys.* **34**, 1190.
- Friedel, J.: 1958, *Nuovo Cimento (Suppl)* **7**, 287.
- Fujii, T. and Ueda, K.: 2003, *Phys. Rev. B* **68**, 531.
- Fulton, T. A. and Dolan, G. J.: 1987, *Phys. Rev. Lett.* **59**, 109.
- Giaever, I. and Zeller, H. R.: 1968, *Phys. Rev. Lett.* **20**, 1504.
- Glazman, L. I. and Pustilnik, M.: 2003, *in* R. Fazio, V. Gantmakher and Y. Imry (eds), *New Directions in Mesoscopic Physics (Towards Nanoscience)*, Kluwer, Dordrecht.
- Goldhaber-Gordon, D., Göres, J., Kastner, M. A., Shtrikman, H., Mahalu, D. and Meirav, U.: 1998, *Phys. Rev. Lett.* **81**, 5225.
- Goldhaber-Gordon, D., Shtrikman, H., Mahalu, D., Abusch-Magder, D., Meirav, U. and Kastner, M. A.: 1998, *Nature* **391**, 156.
- Goldin, Y. and Avishai, Y.: 1998, *Phys. Rev. Lett.* **81**, 5394.
- Goldin, Y. and Avishai, Y.: 2000, *Phys. Rev. B* **61**, 16750.
- Gunnarsson, O. and Schönhammer, K.: 1983a, *Phys. Rev. Lett.* **50**, 604.
- Gunnarsson, O. and Schönhammer, K.: 1983b, *Phys. Rev. B* **28**, 4315.
- Hamann, D. R.: 1967, *Phys. Rev.* **158**, 570.
- Han, J. H.: 2003, *preprint cond-mat/0312023*.
- Herschfield, S., Davies, J. D. and Wilkins, J. W.: 1991, *Phys. Rev. Lett.* **67**, 3720.
- Hettler, M. H., Kroha, J. and Herschfield, S.: 1994, *Phys. Rev. Lett.* **73**, 1967.

- Hettler, M. H., Kroha, J. and Herschfield, S.: 1998, *Phys. Rev. B* **58**, 5649.
- Hettler, M. H. and Schoeller, H.: 1995, *Phys. Rev. Lett.* **74**, 4907.
- Hewson, A. C.: 1993, *The Kondo Problem to Heavy Fermions*, Cambridge University Press, Cambridge.
- Hofstetter, W. and Kehrein, S.: 2001, *Phys. Rev. B* **63**, R140402.
- Iglói, F. and Rieger, H.: 2000, *Phys. Rev. Lett.* **85**, 3233.
- Kaminski, A., Nazarov, Y. V. and Glazman, L. I.: 1999, *Phys. Rev. Lett.* **83**, 384.
- Kaminski, A., Nazarov, Y. V. and Glazman, L. I.: 2000, *Phys. Rev. B* **62**, 8154.
- Kastner, M. A.: 1992, *Rev. Mod. Phys.* **64**, 849.
- Kehrein, S.: 2001, *Nucl. Phys. B* **592**, 512–562.
- Kehrein, S. and Mielke, A.: 1996, *Ann. Physics (NY)* **252**, 1–32.
- Kehrein, S. and Mielke, A.: 1997, *Ann. Physik (Leipzig)* **6**, 90.
- Kogan, A., Amasha, S. and Kastner, M. A.: 2004, *Science* **304**, 1293.
- Kondo, J.: 1969, in F. Seitz, D. Turnbull and H. Ehrenreich (eds), *Solid State Physics*, Vol. 8, Academic Press, New York.
- König, J., Schmidt, J., Schoeller, H. and Schön, G.: 1996, *Phys. Rev. B* **54**, 16820.
- Konik, R. M., Saleur, H. and Ludwig, A.: 2001, *Phys. Rev. Lett.* **87**, 236801.
- Konik, R. M., Saleur, H. and Ludwig, A.: 2002, *Phys. Rev. B* **66**, 125304.
- Krawiec, M. and Wysokinski, K. I.: 2002, *Phys. Rev. B* **66**, 165408.
- Kronig, R.: 1935, *Physica* **2**, 968.
- Kubo, R.: 1956, *Can. J. Phys.* **34**, 1274.
- Kulik, I. O. and Shekhter, R. I.: 1975, *Sov. Phys. JETP* **41**, 308.
- Kuromoto, Y. and Kojima, H.: 1984, *Z. Phys. B* **57**, 95.
- Kuromoto, Y. and Müller-Hartmann, E.: 1985, *J. Mag. Mag. Mat.* **57**, 122.
- Landau, L. D. and Lifshitz, E. M.: 1980, *Statistical Physics Part I*, Pergamon Press, New York.
- Lee, Y.-W. and Lee, Y.-L.: 2002, *Phys. Rev. B* **65**, 155324.

- Leggett, A. J., Chakravarty, S., Dorsey, A. T., Fisher, M. P. A., Garg, A. and Zwerger, W.: 1987, *Rev. Mod. Phys.* **59**, 1.
- Lesage, F. and Saleur, H.: 1998, *Phys. Rev. Lett.* **80**, 4370.
- Likharev, K. K. and Zorin, A. B.: 1985, *J. Low Temp. Phys.* **59**, 347.
- Lobaskin, D. and Kehrein, S.: 2005a, *Phys. Rev. B* **71**, 193303.
- Lobaskin, D. and Kehrein, S.: 2005b, *to be published in J. of Stat. Phys.* .
- Lobaskin, D. and Kehrein, S.: 2005c, *to be published* .
- Lopez, R., Aguado, R., Platero, G. and Tejedor, C.: 1998, *Phys. Rev. Lett.* **81**, 4688.
- Majumdar, K., Schiller, A. and Herschfield, S.: 1998, *Phys. Rev. B* **57**, 2991.
- Mattis, D. C.: 1967, *Phys. Rev. Lett.* **19**, 1478.
- Meir, Y., Wingreen, N. S. and Lee, P. A.: 1993, *Phys. Rev. Lett.* **70**, 2601.
- Nagaoka, Y.: 1965, *Phys. Rev. A* **138**, 1112.
- Nagaoka, Y.: 1967, *Prog. Theor. Phys.* **37**, 13.
- Newns, D. M. and Hewson, A. C.: 1980, *J. phys. F* **10**, 2429.
- Newns, D. M. and Read, N.: 1987, *Adv. in Phys.* **36**, 799.
- Ng, T.-K.: 1996, *Phys. Rev. Lett.* **76**, 487.
- Nielsen, P.: 1970, *Phys. Rev. B* **2**, 3819.
- Nordlander, P., Pustilnik, M., Meir, Y., Wingreen, N. S., and Langreth, D. C.: 1999, *Phys. Rev. Lett.* **83**, 808.
- Nordlander, P., Wingreen, N. S., Meir, Y. and Langreth, D. C.: 2000, *Phys. Rev. B* **61**, 2146.
- Nozières, P.: 1974, *J. Low Temp. Phys.* **17**, 31.
- Nygaard, J., Cobden, D. H. and Lindelhof, P. E.: 2000, *Nature* **408**, 342.
- Oguri, A.: 2002, *J. Phys. Soc. J.* **71**, 2969.
- Paaske, J., Rosch, A., Kroha, J. and Wölfle, P.: 2004, *Phys. Rev. B* **70**, 155301.
- Paaske, J., Rosch, A. and Wölfle, P.: 2004, *Phys. Rev. B* **69**, 155330.

- Parcolett, O. and Hooley, C.: 2002, *Phys. Rev. B* **66**, 085315.
- Plihal, M., Langreth, D. C. and Nordlander, P.: 2000, *Phys. Rev. B* **61**, R13341.
- Pottier, N. and Mauger, A.: 2000, *Physica A* **282**, 77–107.
- Ramakrishnan, T. V. and Sur, K.: 1982, *Phys. Rev. B* **26**, 1798.
- Rasul, J. W. and Hewson, A. C.: 1984, *J. Phys. C* **17**, 2555 and 3332.
- Read, N. and Newns, D. M.: 1983a, *J. Phys. C* **16**, L1055.
- Read, N. and Newns, D. M.: 1983b, *J. Phys. C* **16**, 3273.
- Rosch, A., Costi, T. A., Paaske, J. and Wölfle, P.: 2003, *Phys. Rev. B* **68**, 014430.
- Rosch, A., Kroha, J. and Wölfle, P.: 2001, *Phys. Rev. Lett.* **87**, 156802.
- Rosch, A., Paaske, J., Kroha, J. and Wölfle, P.: 2003, *Phys. Rev. Lett.* **90**, 076804.
- Sarachik, M., Corenzvit, E. and Longinotti, L. D.: 1964, *Phys. Rev. A* **135**, 1041.
- Schiller, A. and Herschfield, S.: 1995, *Phys. Rev. B* **51**, 12896.
- Schiller, A. and Herschfield, S.: 1998, *Phys. Rev. B* **58**, 14978.
- Schiller, A. and Herschfield, S.: 2000, *Phys. Rev. B* **62**, R16271.
- Schlottmann, P.: 1982, *Phys. Rev. B* **25**, 4915.
- Schlottmann, P.: 1983, *Z. Phys. B* **51**, 49.
- Schmid, J., Weis, J., Eberl, K. and von Klitzing, K.: 1998, *Physica B* **258**, 182.
- Schollwoeck, U.: 2005, *Rev. Mod. Phys.* **77**, 259.
- Schrieffer, J. R. and Wolff, P. A.: 1966, *Phys. Rev.* **149**, 491.
- Scott-Thomas, J. H. F., Field, S. B., Kastner, M. A., Smith, H. I. and Antonadis, D. A.: 1989, *Phys. Rev. Lett.* **62**, 583.
- Shen, L. Y. L. and Rowell, J. M.: 1968, *Phys. Rev.* **165**, 566.
- Sivan, N. and Wingreen, N. S.: 1996, *Phys. Rev. B* **54**, 11622.
- Slezak, C., Kehrein, S., Pruschke, T. and Jarrell, M.: 2003, *Phys. Rev. B* **67**, 184408.
- Sollich, P., Fielding, S. and Mayer, P.: 2002, *J. Phys. C: Cond. Matter* **14**, 1683.
- Solyom, J. and Zawadowski, A.: 1968a, *Phys. Kondens. Materie* **7**, 342.

- Solyom, J. and Zawadowski, A.: 1968b, *Phys. Kondens. Materie* **7**, 325.
- Suhl, H.: 1965, *Phys. Rev.* **138**, A515.
- Suhl, H. and Wong, D.: 1967, *Physics* **3**, 17.
- Toulouse, G.: 1969, *C. R. Acad. Sci. Paris* **268**, 1200.
- van der Wiel, W. G., Franceschi, S. D., Fujisawa, T., Elzerman, J. M., Tarucha, S. and Kouwenhoven, L. P.: 2000, *Science* **289**, 2105.
- von Delft, J. and Schoeller, H.: 1998, *Ann. Physik (Leipzig)* **4**, 225.
- Wallis, R. H. and Wyatt, A. F. G.: 1974, *J. Phys. C* **7**, 1293.
- Wegner, F.: 1994, *Ann. Physik (Leipzig)* **3**, 77.
- Wiegmann, P. B.: 1980, *Sov. Phys. JETP Lett.* **31**, 392.
- Wilson, K. G.: 1974, *Nobel Symposia* **24**, 68.
- Wilson, K. G.: 1975, *Rev. Mod. Phys.* **47**, 773.
- Wingreen, N. S. and Meir, Y.: 1992, *Phys. Rev. Lett.* **68**, 11040.
- Wingreen, N. S. and Meir, Y.: 1994, *Phys. Rev. B* **49**, 2512.
- Wolf, E. L. and Losee, D. L.: 1970, *Phys. Rev. B* **2**, 3660.
- Yamada, K.: 1975, *Prog. Theor. Phys.* **53**, 970.
- Yoshimori, A.: 1976, *J. Phys. C* **15**, 5241.
- Zittartz, J. and Müller-Hartmann, E.: 1974, *Z. Physik* **212**, 280.



## PUBLICATIONS

Parts of this thesis were published in the following articles:

1. **Crossover from Non-Equilibrium to Equilibrium Behavior in the Time-Dependent Kondo Model**  
D. Lobaskin and S. Kehrein  
*Phys. Rev. B* **71**, 193303-4 (2005)
2. **Violation of the Fluctuation-Dissipation Theorem and Heating Effects in the Time-Dependent Kondo Model**  
D. Lobaskin and S. Kehrein  
cond-mat/0504373, accepted in the Journal of Statistical Physics
3. **Non-Equilibrium Kondo Model with a Factorized Initial State**  
D. Lobaskin and S. Kehrein  
in preparation



## CURRICULUM VITAE

Name	Lobaskin Dmitry
Date of birth	13 December 1978
Place of birth	Kopeysk, Chelyabinsk region, USSR
Nationality	Russian

### Education

09/85 - 06/93	Secondary school in Kopeysk, Chelyabinsk region, Russia
09/93 - 06/95	Physics and Mathematics Lyceum 31, Chelyabinsk, Russia
09/95 - 06/97	Chelyabinsk Technical State University, Chelyabinsk, Russia
09/97 - 06/02	Moscow Institute for Physics and Technology, Moscow, Russia Landau Institute for Theoretical Physics, Moscow, Russia
06/02	Master of Science in Applied Mathematics and Physics <b>Advisor:</b> Dr. Igor Suslov <b>Thesis:</b> Higher order corrections to the Lipatov asymptotics in $\varphi^4$ theory <b>GPA:</b> 5.0/5.0
10/02 - 12/05	Augsburg University, Augsburg, Germany
12/05(expected)	PhD in Theoretical Physics <b>Advisors:</b> Prof. Dr. Dieter Vollhardt, PD Dr. Stefan Kehrein <b>Thesis:</b> Time-dependent Kondo model with a factorized initial state

**Awards and Scholarships**

- |           |  |
|-----------|--|
| 1995      | 3rd Prize in Russian Physics Olympiad  |
| 1995      | Gold Medal. Outstanding Graduation Record.<br>Physics and Mathematics Lyceum 31, Chelyabinsk, Russia                           |
| 1996-1998 | Soros Foundation Student Fellowship  |
| 1997      | Two Winner Prizes in Russian Student Olympiad<br>in Theoretical Mechanics  |
| 1999-2002 | Landau Institute Fellowship  |
| 2002      | Diploma with Distinction. Outstanding Graduation Record,<br>Moscow Institute for Physics and Technology, Moscow, Russia        |
| 2004      | Verband der Bayrischen Metal- und Elektro-Industrie fellowship<br>to attend the Nobel Prize Laureates Meeting, Lindau, Germany |

**Research Experience**

- |             |  |
|-------------|--|
| 1999 - 2002 | Research assistant at Landau Institute, Russia     |
| 2002 - 2005 | Research assistant at Augsburg University, Germany |

## ACKNOWLEDGEMENTS

I am grateful to Prof. Dr. Dieter Vollhardt for the possibility to work in his group and to attend a lot of interesting conferences and workshops during my stay here. In addition to a big variety of exciting topics, which he suggests to work on to group members, he always manages to maintain very friendly atmosphere and good relationships in our collective.

I sincerely thank PD Dr. Stefan Kehrein for suggesting to work on such an exciting topic as the non-equilibrium Kondo problem. I appreciate a lot all long discussions we had about essential physics of the non-equilibrium systems as well as his patience in helping me to find some hidden mistakes of the tricky calculation I have performed. His advices were always in time and really valuable.

Prof. Dr. Thilo Kopp kindly agreed to co-report on this thesis.

Many thanks to all group members for their constant interest in my work.

I want to thank specially my great friend Eugene Gudzovsky and my brother Vladimir for reading the draft of my thesis and valuable comments on its content as well as its presentation.

I could not finish my work without constant support of my mother, my father and Olga.